LIÈGE université Library

https://lib.uliege.be

https://matheo.uliege.be

Master thesis : Design of a Blade - Hub Joint for a Built-Up Propeller

Auteur : Zar Ni,
Promoteur(s) : 14957; 14965
Faculté : Faculté des Sciences appliquées
Diplôme : Master : ingénieur civil mécanicien, à finalité spécialisée en "Advanced Ship Design"
Année académique : 2021-2022
URI/URL : http://hdl.handle.net/2268.2/16493

Avertissement à l'attention des usagers :

Tous les documents placés en accès ouvert sur le site le site MatheO sont protégés par le droit d'auteur. Conformément aux principes énoncés par la "Budapest Open Access Initiative"(BOAI, 2002), l'utilisateur du site peut lire, télécharger, copier, transmettre, imprimer, chercher ou faire un lien vers le texte intégral de ces documents, les disséquer pour les indexer, s'en servir de données pour un logiciel, ou s'en servir à toute autre fin légale (ou prévue par la réglementation relative au droit d'auteur). Toute utilisation du document à des fins commerciales est strictement interdite.

Par ailleurs, l'utilisateur s'engage à respecter les droits moraux de l'auteur, principalement le droit à l'intégrité de l'oeuvre et le droit de paternité et ce dans toute utilisation que l'utilisateur entreprend. Ainsi, à titre d'exemple, lorsqu'il reproduira un document par extrait ou dans son intégralité, l'utilisateur citera de manière complète les sources telles que mentionnées ci-dessus. Toute utilisation non explicitement autorisée ci-avant (telle que par exemple, la modification du document ou son résumé) nécessite l'autorisation préalable et expresse des auteurs ou de leurs ayants droit.

With the support of the Erasmus+ Programme of the European Union

Design of a Blade – Hub Joint for a Built-Up Propeller

Submitted on 01st August, 2022

by

NI Zar | Erich-Schlesinger-Str. 19 | 18059 Rostock | zar.ni@uni-rostock.de

Student ID No.: 221 200 002

First Reviewer:

Prof. Dr.-Eng. Patrick Kaeding

Chair of Ship Structures

University of Rostock

Albert-Einstein-Str. 2

18059 Rostock

Germany

Second Reviewer:

Dipl.-Ing. Jörn Klüss

Head of Design Department

Mecklenburger Metallguss GmbH

Teterower Str. 1

17192 Waren

Germany

EMship+ Advanced Design

Master Thesis

[This page is intentionally left blank]

ABSTRACT

With the enormous demands and busy schedules of water transportation by the sea-going vessels, the propulsion system and components are taking part in one of significant roles. In order to navigate the ship into the water, the marine propellers are crucial to be efficiently and safely designed. Typically there are two types of propellers: fixed pitch propeller (FPP) and controllable pitch propeller (CPP), depending on application and mission. Unlike CPP, a built-up propeller does not include a hydraulic system to control the pitch of the blades but each blade can be replaced in the case of damage.

This thesis is specifically focused on the design of the blade and hub joint for a built-up propeller. Additionally, it is intended for the application of ice class for the ship operating in the Baltic Sea with the ice strengthening materials. There are some obvious benefits of using built-up propellers. It is a comparatively much simpler and faster change of blades than conventional mono-block propellers without the need for dry docking and dismounting facilities if the blades are necessary to be repaired and replaced.

For the blade-hub joint design, there are some possible configurations having their own benefits and drawbacks. But finally bolted joint design was selected in the aspects of flexible manufacturing capabilities, easy to mount or dismount the blade on the hub with less effort, with the least impact on vessel operation. Blades are mounted on the hub and the hub assembly is connected to the propeller shaft. There are some available shaft connection methods. Considering the design aspects to support the structure of the hollow hub, and with experiences and suggestions from (MMG personal communication), shrink fit or keyless fitting was chosen.

A detailed 3D of the built-up propeller assembly was modelled in Rhino. Also, Siemens NX was used for blade fillet and detailed bolt threads modelling. Blade-hub assembly design was developed complying with GL and Finnish-Swedish Ice Class Rules. The special bolts to connect the blade and hub were designed according to VDI2230, DIN EN ISO 3506-1 and ANSI/ASME B1 standards. Analytical strength calculations for the bolted joint have been performed and the results were compared to Ansys structural analysis for different load cases and FE models to get a safe and efficient design.

Keywords: built-up propeller, ice class, ice strengthening, blade-hub joint, bolted joint, shrink fit or keyless fitting

[This page is intentionally left blank]

CONTENT

ABSTRACT ii
LIST OF FIGURES vii
LIST OF TABLES x
DECLARATION OF AUTHORSHIP xiii
NOMENCLATURE xv
1. INTRODUCTION 1
1.1 Outlines and Scope of the Topic 2
1.2 Motivation of Study 4
1.3 Literature Review 5
1.4 Approach and Methodology 9
1.5 Basics and Introduction to Marine Propeller Design 10
1.6 Propeller Geometry, Parameters and Definitions 12
2. CLASSIFICATION RULES FOR SHAFTING & PROPELLER 13
2.1 Shafting: Diameter, Connection Methods 14
2.1.1 Shaft Design *14*
2.1.2 Simplified Shafting Diameter *14*
2.2 Propeller: Blade Thickness, Fitting of Propeller to the Shaft 15
2.2.1 Design and Materials for Propeller *15*
2.2.2 Criteria for Propeller Blade Dimensions *16*
2.2.3 Blade Thickness and Calculation *16*
2.2.4 Fitting of Propeller Blades to the Hub *17*
2.3 Ice Class Rules 17
2.3.1 Ice Classes *18*
2.3.2 Ice Loads *19*
2.3.3 Ice Conditions for Design *20*
3. PRE-STUDY 21
3.1 Built-Up Propellers (General Design Hub, Blade, Joint Hub-Blade) 21
3.2 Different Design Layouts (Comparison, Assessment, Conclusion) 22
3.3 Bolted Joint (Standards, Analytical & FEM Methods) 24

3.3.1 Manufacturing Tolerances *25*

3.4 Materials with Respect to Application in Seawater, Strength, Ice Loading 26

3.5 Tightening Methods of the Bolted Joint 26

3.6 Bolt Securing/Locking 27

4. PRE-DESIGN OF A BUILT-UP PROPELLER 27

4.1 Input Data: Blade Design, Shaft, Power Output, Ice Loads 27

4.1.1 Propeller Shaft Diameter (without Ice Class) *28*

4.1.2 Propeller Shaft Diameter (ice class, IA Super) *29*

4.1.3 Principle Dimensions of the Hub (Ice Class) *31*

4.1.4 Blade Flange Dimensions *33*

4.1.5 Bolted joint design and dimensions *34*

4.1.6 3D Modelling of the blade bolts *41*

4.2 Hub Body and 3D Modeling of the Built-Up Propeller 42

4.3 Summary for the Preselection of Materials, Strength, Density and Weight of Built-up Propeller Assembly 42

4.4 Strength Calculations 43

4.4.1 The Blade Forces or Ice Loads *44*

4.4.2 Centrifugal Force Acting on a Single Blade *45*

4.5 Issues of an Optimized Manufacturing / Machining 46

5. DETAILED DESIGN AND ANALYSIS OF THE JOINT BETWEEN HUB AND BLADE 47

5.1 Analytical Approach 47

5.2 FE Simulation 55

5.2.1 Simplification of FE Models *55*

5.2.2 Input for Material Specifications *56*

5.2.3 Contact Definitions of the Components in FE Model *56*

5.2.4 Constraint and Boundary Conditions *57*

5.2.5 Load Case Definitions and Direction of Load Applications *58*

5.2.6 Mesh Studies *59*

5.2.7 Analysis of Model Class 3 at Different Load Cases *69*

5.2.7.1 Analysis of Model Class 3 with Load Case 1 ..... *69*

5.2.7.2 Analysis of Model Class 3 with Load Case 2 ..... *73*

5.2.7.3 Analysis of Model Class 3 with Load Case 3 ..... *76*

5.2.7.4 Analysis of Model Class 3 with Load Case 4 ..... *78*

5.2.7.5 Analysis of Model Class 3 with Load Case 5 ..... *81*

5.2.7.6 Analysis of Model Class 3 with Imported Hydrodynamic Pressure Load Acting around the Blade *85*

5.2.7.7 Analysis of Model Class 3 with Ultimate Blade Failure Load *88*

5.2.8 Sub-modelling Techniques for the Bolted Joint *92*

5.3 Comparison of Analytical and FE Results for a critical bolt 98

5.4 Issues Regarding to Corrosion Fatigue 99

5.5 Project Template for Analytical / Simulation Model 99

6. DISCUSSION 100

6.1 Strength Pyramid of Propulsion Components regarding to the Safety of Operation 100

6.2 Influence of the Different Ice Classes according to the Classification Rules on the Joint of Hub-Blade 101

7. CONCLUSION 102

8. FUTURE ASPECTS AND PROPOSALS FOR FURTHER INVESTIGATIONS 103

9. ACKNOWLEDGEMENTS 105

10. REFERENCES 106

APPENDICES 109

LIST OF FIGURES

Figure 1. A propeller diameter and pitch 11
Figure 2. Propeller rake and skew 12
Figure 3. A propeller geometry 13
Figure 4. Propulsion machinery in ice and ice-propeller interaction 18
Figure 5. Resultant backward blade force direction taken perpendicular to the chord line at radius 0.7R. At the leading edge, ice contact pressure is indicated with small arrows. 20
Figure 6. A typical built-up propeller of Wärtsilä 22
Figure 7. Bolted joint connection of MAN built-up propeller 23
Figure 8. CoB connection of Teignbridge built-up propeller 23
Figure 9. Reference diagram for ISO external thread dimensioning 35
Figure 10. Dimensions of blade bolts (All dimensions are in millimeter.) 38
Figure 11. 3D model of blade bolts 41
Figure 12. 3D model of built-up propeller assembly 42
Figure 13. Direction and application of load case 1, and fixed supports on blade model in Ansys 58
Figure 14. Direction and application of blade failure load, and fixed supports on blade model in Ansys 59
Figure 15. Maximum von Mises stresses and deformations at different element sizes (global mesh) 60
Figure 16. Maximum total deformation of a blade at LC1 for 100 mm mesh 61
Figure 17. Maximum von Mises stress of a blade at LC1 for 100 mm mesh 61
Figure 18. Maximum total deformation of a blade at LC1 for 50 mm mesh 62
Figure 19. Maximum von Mises stress of a blade at LC1 for 50 mm mesh 62
Figure 20. The cut profile of the blade at LC1 for 100 mm mesh with maximum von Mises stress 62
Figure 21. The cut profile of the blade at LC1 for 50 mm mesh with maximum von Mises stress 63
Figure 22. Maximum total deformation of a blade due to blade failure load 63
Figure 23. Maximum von Mises stress of a blade at pressure side due to blade failure load 64
Figure 24. Maximum von Mises stress of a blade at suction side due to blade failure load 64
Figure 25. Maximum von Mises stresses and deformations at different element sizes (bolt mesh) 65

Figure 26. Application of preload and fixed supports on bolt model in Ansys 66
Figure 27. Maximum total deformation of a bolt at preload for 30 mm mesh..... 66
Figure 28. Maximum von Mises stress of a bolt at preload for 30 mm mesh..... 67
Figure 29. Maximum total deformation of a bolt at preload for 15 mm mesh..... 67
Figure 30. Maximum von Mises stress of a bolt at preload for 15 mm mesh..... 68
Figure 31. Maximum total deformation of a bolt at preload for 5 mm mesh..... 68
Figure 32. Maximum von Mises stress of a bolt at preload for 5 mm mesh..... 69
Figure 33. Application of loadings and fixed supports for load case 1 of class 3 model..... 70
Figure 34. Maximum von Mises stress in load case 1 with R5 fillet bolts 70
Figure 35. Maximum total deformation in load case 1 with R10 fillet bolts 71
Figure 36. Maximum von Mises stress in load case 1 with R10 fillet bolts 71
Figure 37. Maximum von Mises stress in load case 1 with R10 fillet bolts seeing at the bolts' view 72
Figure 38. Maximum von Mises stress in load case 1 with R10 fillet bolts seeing at critical bolt's section view..... 72
Figure 39. Application of loadings and fixed supports for load case 2 of class 3 model..... 73
Figure 40. Maximum total deformation in load case 2 74
Figure 41. Maximum von Mises stress in load case 2 74
Figure 42. Maximum von Mises stress in load case 2 seeing at the bolts' view..... 75
Figure 43. Maximum von Mises stress in load case 2 seeing at critical bolt's section view... 75
Figure 44. Application of loadings and fixed supports for load case 3 of class 3 model..... 76
Figure 45. Maximum total deformation in load case 3 76
Figure 46. Maximum von Mises stress in load case 3 77
Figure 47. Maximum von Mises stress in load case 3 seeing at the bolts' view..... 77
Figure 48. Maximum von Mises stress in load case 3 seeing at critical bolt's section view... 78
Figure 49. Application of loadings and fixed supports for load case 4 of class 3 model..... 79
Figure 50. Maximum total deformation in load case 4 79
Figure 51. Maximum von Mises stress in load case 4 80
Figure 52. Maximum von Mises stress in load case 4 seeing at the bolts' view..... 80
Figure 53. Maximum von Mises stress in load case 4 seeing at critical bolt's section view... 81
Figure 54. Application of loadings and fixed supports for load case 5 of class 3 model..... 82
Figure 55. Maximum total deformation in load case 5 82
Figure 56. Maximum von Mises stress in load case 5 83
Figure 57. Maximum von Mises stress in load case 5 seeing at the bolts view..... 83

Figure 58. Maximum von Mises stress in load case 5 seeing at critical bolt's section view ... 84
Figure 59. Application of loadings with hydrodynamic pressure load and fixed supports 85
Figure 60. Imported hydrodynamic pressure load on the suction side of the blade 86
Figure 61. Imported hydrodynamic pressure load on the pressure side of the blade 86
Figure 62. Maximum total deformation in imported hydrodynamic pressure load 87
Figure 63. Maximum von Mises stress in imported hydrodynamic pressure load 87
Figure 64. Maximum von Mises stress at the bolts with imported hydrodynamic pressure load 88
Figure 65. Application of loadings with blade failure load and fixed supports 89
Figure 66. Maximum total deformation in blade failure load 89
Figure 67. Maximum von Mises stress in blade failure load 90
Figure 68. Maximum von Mises stress at the bolts with blade failure load 90
Figure 69. Maximum von Mises stress at the bolts of blade's suction side with blade failure load 91
Figure 70. Maximum von Mises stress in blade failure load seeing at critical bolt's section view 91
Figure 71. Sub-modelling geometry for critical bolted joint part from load case 1 93
Figure 72. Imported cut boundary constraint for critical bolted joint part from load case 1 ... 94
Figure 73. Total deformation in sub-modelling for critical bolted joint part from load case 1 94
Figure 74. Von Mises stress results in the bolts of sub-modelling from load case 1 95
Figure 75. Sub-modelling geometry for critical bolted joint part from blade failure load 96
Figure 76. Imported cut boundary constraint for critical joint part from blade failure load 96
Figure 77. Von Mises stress results in the bolts of sub-modelling from blade failure load 97
Figure 78. Strength pyramid for a built-up propeller assembly 101

LIST OF TABLES

Table 1. Material properties for propeller 15
Table 2. Definition of loads for design process 19
Table 3. Loaded areas and load cases on the blade 19
Table 4. Types of operation for different ice classes 20
Table 5. Thickness of design ice blocks for different ice classes 21
Table 6. Comparison of two possible connections for blade and hub 22
Table 7. Comparison of bolt specifications 24
Table 8. Propeller input data 27
Table 9. Minimun shaft diameter 29
Table 10. Minimun propeller shaft diameter (Ice classes) 31
Table 11. Dimensions of the hub 32
Table 12. Tapered shaft diameter 33
Table 13. Blade flange thickness 33
Table 14. Nominal diameter of blade retaining bolt 35
Table 15. Blade retaining bolts dimensions 37
Table 16. Clamped load or preload at the bolt shank 40
Table 17. Tightening torque of the bolt 41
Table 18. Materials, strength, densities of propeller components 43
Table 19. Weight of built-up propeller assembly 43
Table 20. Calculations of blade forces on propeller 45
Table 21. Forces on the blade due to ice loads 45
Table 22. Centrifugal force on a blade 46
Table 23. Stresses on one bolt for different load cases 49
Table 24. Von Mises stresses for a bolt at different load cases 51
Table 25. Total strain on a bolt 52
Table 26. Total deformation on a bolt's shank 52
Table 27. Compressive stresses at bolt head flange bearing area 53
Table 28. Thread shear stresses at bolt external threaded area 54
Table 29. Thread shear stresses at internal threaded area of hub 54
Table 30. FE model scheme 56
Table 31. Material specifications input to Ansys 56
Table 32. Contact definitions of Ansys 57

Table 33. Global mesh study for a blade with flange..... 60
Table 34. Mesh study for blade bolt..... 65
Table 35. Results comparison of R5 and R10 fillet bolts..... 72
Table 36. Summary of analysis results for ice load cases 1-5..... 84

[This page is intentionally left blank]

DECLARATION OF AUTHORSHIP

I, Zar Ni, declare that this thesis and the work presented in it are my own and have been generated by me as the result of my own original research.

Where I have consulted the published work of others, this is always clearly attributed.

Where I have quoted from the work of others, the source is always given. With the exception of such quotations, this thesis is entirely my own work.

I have acknowledged all main sources of help.

Where the thesis is based on work done by myself jointly with others, I have made clear exactly what was done by others and what I have contributed myself.

This thesis contains no material that has been submitted previously, in whole or in part, for the award of any other academic degree or diploma.

I cede the copyright of the thesis in favour of the University of Rostock.

Date: Signature

August 01, 2022

[This page is intentionally left blank]

NOMENCLATURE

BJ	Bolted joint connection
BUP	Built-up propeller
BV	Bureau Veritas
CoB	Clamp on blade
CFD	Computational fluid dynamics
CPP	Controllable pitch propeller
Cu3	Nickel aluminum bronze copper alloy
Cu4	Nickel manganese bronze copper alloy
DNV	Det Norske Veritas
EAR	Expanded area ratio
FEA	Finite element analysis
FEM	Finite element method
FoS	Factor of safety
FPP	Fixed pitch propeller
GL	Germanischer Lloyd
ISO	International standard organization
LC	Load case
Le	Length of engagement of bolt's thread
MBJ	Muiti-bolted joint
MCR	Maximum continuous rating
MMG	Mecklenburger Metallguss GmbH
NURBS	Non-uniform rational basis spline
PCD	Pitch circle diameter
P/D	Pitch diameter ratio
SBJ	Single bolted joint
TTJ	Tapped through joint
3D	Three-dimension model

1. INTRODUCTION

The conventional marine propeller is still the standard propulsion mechanism for ships and marine vehicles. Ensuring proper propulsion efficiency, the propellers generate enough thrust to propel the ship at the desired speed. Necessary design considerations should be made when designing a suitable propeller that matches the main engine power output, shaft speed, ship size and ship operating speed. **[1]**

It was also noted (Martinez, 1995-2022) that a screw or blade propeller makes a relative motion, pushing the surrounding fluid back along the axis. Then a pressure difference is created between the front and rear surfaces of the airfoil-shaped blades. It can create a driving force that is transmitted from the blades to the shaft and ultimately to the hull of the ship. **[2]**

Depending on the applications and missions, propeller designs, materials and efficiencies are different. For the various types of ships, the propulsion system integration can be found as fixed pitch propellers majorly installed in inland and sea-going vessels, built-up propellers commonly fitted on the offshore patrol vessels, ice breakers and some other cargo and container ships navigating in the icy water and in areas where increased risk of propeller damage, and controllable pitch propellers can be seen in some navy vessels and other sea-going cargo ships, water jet propulsion, azimuth or azipod propulsors installed on cruise and passenger vessels, Voith-Schneider propulsion, pump jet propulsion used in shallow water and inland vessels. **[25]** Additionally, the propulsion systems can be with a single screw, twin screw, triple screw and propellers with four shaft lines. Marine propellers can be made of sea water corrosion resistant and ductile materials such as a copper alloy including nickel aluminium bronze (Cu3) and manganese bronze (Cu4) with higher strength for navy ships and stainless steel propellers for ice class and higher polar ice class applications.

1.1 Outlines and Scope of the Topic

The scope of the context is composed of the following sections.

The introduction section is about the basics of marine propellers. It includes terms and definitions relating to propeller geometry, and the fundamental concepts of a mechanical propeller.

The applications of the classification rules section include ice class rules for shafting and propeller designs. (Mecklenburger Metallguss GmbH-MMG, personal communication) suggested and provided a propeller blade geometry with the corresponding blade thicknesses at different blade radius positions complying with ice class IA super. After that, the blade flange was designed accordingly to match with propeller hub diameter and length dimensioned for ice class. In this study, the propeller and the shaft were connected by means of keyless fitting. Minimum shaft diameter was calculated applying classification rules including ice class rules. Then the tapered solid shaft was developed to fit in the hub. For the ice strengthening designs of propeller and shaft, classification rules have been applied.

The pre-study section includes studies about built-up propeller joint design. Basically, there are fixed pitch and variable pitch propellers. The general design of the built-up propeller is similar to a variable pitch propeller regardless of the hydraulic system to alter the pitch. The hub diameter of the built-up propeller is typically bigger than a normal mono-block cast propeller since the blades are fitted separately onto the hub. The strength of the blade-hub joint is important to withstand the loads when the blade crushes the obstacles in water or hits the ice blocks during vessel operation. In this context, the bolted joint was picked based on the efficient replacement of blades with the least interrupting the operation of the ship, and with fewer efforts to replace the damaged blades. The propeller materials were selected complying with the ice class rules and with respect to corrosion resistance against the seawater. After the blades are installed on the hub, the securing procedures for the bolts are mandatory. The bolts can be locked with the locking plates or caps.

The pre-design section is concerned with the preliminary design of a built-up propeller. In order to develop the blade-hub joint design, some input data of the built-up propeller were required. Those included blade design and geometry, type of connection with the propeller shaft, the power output of main engines, ice class and ice loads considered for the design. The

bolted joint configuration between blade and hub was decided based on objectives of design convenience and flexibility for manufacturing, installation and operational points of view. According to class rules, Ni-Al bronze was selected as the propeller blade and hub material, and martensitic forged steel was taken as the shaft material for pre-selection. For the special bolts of blade-hub joint, martensitic C3 grade, class 80 was considered to have enough ice strengthening. The built-up propeller in this thesis was mostly designed by Rhino V7 and integrated and plugged in with Siemens NX for the blade fillet and the external threads of blade-fitted bolts to have design flexibility and convenience. After developing the 3D modelling of propeller design, the analytical strength calculations of the bolted joint design were performed. During the installation of shrink fit connection of shaft to hub and blade fitting, there would be some possible minor deformations at the hub and to be able to fit the blade to hub perfectly, and it should have enough facilities for machining perhaps for the blade flange. The manufacturing tolerances for the propeller shall comply with the specified tolerance class (ISO 484) as mentioned in classification rules.

The detailed design of the joint section includes the design of the connection between hub and blade. According to the bolt sizing calculations following the rules and manufacturing standards, 10 bolts were fitted on the blade flange near the blade fillet for each blade with the appropriate layout as per the 3D modelling shown in the later section. In the analytical analysis, some design assumptions and simplifications were made to be able to estimate the strength of the bolted joint and the bolt at the concerned point. During calculations, it was necessary to evaluate the external loads acting on the propeller and the initial load applied on the bolt. These included blade failure load for designing input as a separate case, blade forces or ice loads in 5 different cases, a centrifugal force due to blade rotation, and the bolt preloads. For the bolt, considering equivalent stress and deformation at the junction between the connection of blade flange and hub were estimated. Besides, the stresses at the bearing area under bolt flange, thread shear stresses at bolt thread and hub thread regions were predicted.

For the FE analysis and simulations, the global mesh study for the blade was firstly investigated. Then the refined meshes (local and specified concerned area in the model) were also studied. According to VDI2230 part 2, FE model class-3 (having equivalent volume body and without threads in the bolts) **[13]** was taken into account for analysis. The processes included analysis of model class 3 with different load cases, blade failure load and with refined mesh at the bolt. In the FEA scheme, detailed results were provided for the whole FE

model defined. The related concerned results of the strength and deformation were compared to analytical calculations.

The discussion section includes the design outputs and a comparison of analytical and numerical FE analysis results. In this section, the blade-hub joint layout was configured based on the strength pyramid of propulsion components for operational safety. The future aspects and proposals for further investigations and developments are also discussed.

1.2 Motivation of Study

Since the propeller stands as one of the main components in a ship propulsion system, it is important to care about the blade design, efficient capabilities in the aspects of installation, operation and manufacturing, maintenance and repair flexibilities for the vast amount of merchant and commercial sea-going vessels. For ships which have a tendency of propeller blade damage in frequent operational conditions, the blades should be repaired or replaced with fewer efforts and without much delay in the ship's operation.

The possible configurations of the previous and existing designs of the various propeller manufacturers have been reviewed for the built-up propeller. And the conceptual design was introduced and developed in this study. Unlike conventional fixed pitch propellers (FPPs), there is an additional connection between blade and hub. This joint design was the main focus of this thesis.

In this scenario propellers with built-up configuration can be used often in shipping route areas with multi-year ice conditions. Especially for the types of offshore patrol vessels and ice breakers which navigate on icy routes, built-up propellers are mainly applicable. The advantage of a built-up propeller consists of a comparable simple and fast change of the blade. In case of larger damages, the mono-block cast propellers or FPPs have to be repaired with bigger efforts such as docking, dismounting etc. or must be completely changed and this can significantly affect the operational costs and schedules of the vessel.

However built-up propellers offer the feasibility to change only the damaged blades in afloat condition by a diver with onboard tools and devices. Different design layouts are available for the built-up propeller depending on the type of applications and purposes.

Based on those design layouts, there are different advantages and drawbacks under the aspects of design, machining and operation. In this thesis, the bolted joint design is chosen.

In order to investigate whether it will be a safe and efficient design, strength calculations are required. In this study, the optimal bolted joint configuration is taken for design development with analytical calculations and a finite element approach with the aid of Ansys workbench structural analysis. FEA is developed and performed to get more detailed results of the design. Different FE model classes are feasible from simplified models to detailed models with different computational efforts for more realistic outcomes.

Applicable materials for the built-up propeller components are selected with respect to strength and ice class loads complying with the classification rules. The results are discussed upon design calculations, analytical strength results and FEA analysis.

1.3 Literature Review

For the literature review, basically, there were two parts in the study. The first part was about designing the connection joint between the blade and hub of the propeller and the second part was concerned with the strength analysis of that joint. The design part consisted of the selection of the type of joint, the material selection of the components, and the dimensioning of the parts. In the analysis part, the strength and deformation of the joint and components around the joint were investigated.

It could be noticed that many research works have been done for the propeller blade strength and design, as well as the control system and pitch mechanism of CPP but there was comparatively less focus on blade-hub joint design and analysis of the built-up propeller.

It was also noted (Wärtsilä, 2022) that built-up propellers are typically installed on icebreakers and offshore patrol vessels that operate in ice-affected waters or in areas where the risk of propeller damage is high. The limited blade replacement duration allows the ship to maintain its schedule, which is useful for ships with fixed operating schedules such as cruise ships and ferries. These built-up propellers are suitable for heavy loads and/or high ship speeds. Large size stainless steel fixed pitch propellers are also possible. **[32]**

It was also noted (MAN, 2022) that the hub and blade designs are with a small hub to propeller diameter ratio to reduce weight, reduce inertia and improve efficiency. The number of blades starts from 2 to 7 for the propellers. The blades, propellers, hub and shaft are designed strictly according to the principle of pyramidal force and meet the requirements of the extreme class to the highest classes of polar ice. Standard blade and hub materials are Ni-Al bronze and stainless steel. **[3]**

Research has been developed and the designs of the joint between the propeller blade and hub are also described in the class rules including ice class rules.

It was also noted (DNV-RU-SHIP Pt.4 Ch.5, 2021) that the fitting of propeller blades to the hub by means of bolted joints. Regulations for a built-up propeller are not specifically prescribed in DNV but they can be referred from the controllable pitch propellers (CPP) application in the propeller section. Without a pitch control mechanism, the CPPs behave as built-up propellers. The pretension stress in the minimum section of the blade bolts shall be in the range of 50-70% of the yield strength of the bolt material or a maximum of 56% of the tensile strength, whichever is less. Any permissible working conditions shall not be leading to the yielding of bolt material.

It was also noted (GL **[16]**, 2016) that the propellers and hubs shall be made of seawater-resistant cast copper alloy or cast steel alloy with a tensile strength of 440 N/mm^2 or higher. The type of joint between blade and hub is also bolted connection and the blade mounting bolts are designed to resist forces safely when plastic deformation occurs at 0.35 R due to the force acting at 0.9 R of the blade. On this occasion, the bolt material has a safety margin of 1.5 with respect to the yield point. The blade retaining bolts are tightened in a controlled manner so that the initial bolt tension is approximately 60-70 % of the yield strength. The shank of the blade bolts can be reduced to a minimum diameter of 0.9 times the root diameter of the threaded part. The blade bolts shall be secured against unintentional loosening.

For the Built-up propellers and controllable pitch propellers, it was also noted (BV **[18]**, 2022) that the studs are to be tightened in a controlled way such that the tension on the studs is approximately 60-70% of the yield strength. The shank of studs can be designed with a minimum diameter equal to 0.9 times the root diameter of the thread. The studs are to be properly secured against accidental loosening. The thickness of the flange shall not be less than one-tenth of the diameter of the blade flange.

Ice class rules and the use of different ice classes and ice thicknesses are also stated (Finnish-Swedish ice class rules, 2016). These regulations may apply to open-type propellers with an adjustable or fixed pitch for ice classes IA Super, IA, IB and IC. These rules shall then be referred to for the built-up propeller in this study. The design loads on the blades are the maximum forces (ice loads or blade forces) experienced by the propeller during the lifetime of a ship. These loads can bend the blades back and forth when the propeller mills an ice block and the ship is moving ahead. Materials exposed to seawater temperatures should be made of steel or other ductile materials. This applies to the propeller shaft, blade bolts, CP mechanisms, shaft bolts and so on. Regarding the design principle, the strength of the propulsion line is calculated based on the concept of pyramid strength. This means that the loss of a propeller blade will not cause significant damage to other propeller shaft line components.

There are various researches conducted for the mechanical bolted joint analysis and those were referred to and applied in the analysis of built-up propeller joint with simplifications.

It was also noted (VDI2230 part 1, 2015 and part 2, 2014) about the systematic calculations of the bolted joints in single joint and multi-joint layouts.

In VDI2230 part 1, the calculation of the single bolted joint (SBJ) is based on the elastic behaviour of the joint near the axis of the bolt. In the case of assembly and service, this region has a considerable impact on the deformation due to the loading of the bolt. The forces and axial deformations in the SBJ can be described by a simple mechanical spring model. In this model, the bolt and the clamped parts are treated as tension and compression springs with elastic resiliences. During the assembly of the joint, an assembly preload is generated, which creates a clamp load at the interface. An axial workload, introduced via the clamped parts and acts on the bolt, is proportionally transmitted through the clamped region of the interface as well as through the bolt. The forces and displacements occur in the bolted joint (BJ). The calculation of a BJ is based on the external workload acting on the joint. This workload and the resulting elastic deformations of the components produce an axial workload, a transverse load, a bending moment and in some cases a torque at the individual bolt point. In special cases, a “pure” working moment, i. e. operating moment in the absence of force, acts at the bolt point. Only simple symmetrical and relatively stiff joints can be performed by a simple analysis of the workload.

In VDI2230 part 2, it applies to high-strength steel bolted joints with screw threads, in other words, to strength grades of 8.8 to 12.9 (carbon steel) or class 70 and 80 (stainless steel) with a frictional transmission of the workload which basically acts on the clamped components or on the structure. Describing the behaviour of loads and deformations in multi-bolted joints (MBJs) is mathematically difficult. As a rule, when multiple statically indeterminate systems are present, their analytical solution requires simplified assumptions about the systems. While the SBJs only focus the clamped area and bearing areas on the component side, MBJs shall include the deformation behaviour of the entire structure and the interaction of all of the bolts. VDI2230 part 2 also considers the FEM method for detail analysis.

It was also noted (DIN EN ISO 3506-1, 2020) that applcation of standards **[14]** includes the mechanical properties of corrosion-resistant stainless steel fasteners. It also consists of chemical compositions, corrosion resistance, and mechanical and physical properties for austenitic and martensitic stainless steel bolts, screws and studs with specified grades and property classes according to ISO 3506-1:2020.

It was also stated (MechaniCalc Inc., 2014-2022) that among other common joining methods including riveting, welding, press fits, pins, keys, and adhesives, the bolted joint is the most common connection method. The main components of a bolted connection include the threaded bolt and the clamped parts which are connected together. A bolted joint works by creating an initial clamping force ("preload") in the joint by screwing the bolt into a nut or into the clamped component. This preload secures for the clamped parts to remain in contact and in compression throughout the service life of the connection. The use of washers in the joint can minimize the embedment of the bolt head and nut into the clamped parts, and make tightening easier. Bolt holes may have sharp edges and washers shall protect the fillet under the bolt head from scratching as it is a critical area of failure. The washer distributes the preload and applied force over a larger area, both on the head of the bolt and on the surface of the clamped parts and reduces bearing stresses preventing damage to the surface of the clamped parts. The stresses in the bolt shall include preload stress, tensile stress, shear stress, and bending stress. An equivalent von Mises stress can then be established in which a load factor is utilized for the tensile, bending and shear stress but not for the preload stress.

1.4 Approach and Methodology

In order to reach the goal of this study, there were some steps prepared in advance and done in the analysis. They are summarized as follows:

1. Defining the operational area of the ship (ice class)
2. Suitable joint type selection for blade-hub
3. Material selections for the design
4. Calculations of joint design and component dimensioning
5. 3D modelling for visualization and FEA
6. Analytical strength and deformation calculations for the joint
7. FE model and layouts, classes
8. FEA mesh study (global and refined)
9. Contact definitions of the FE model
10. FEA for different classes with load cases, Fex
11. FEA and joint design modification (if any)
12. Discussions on FEA outcomes
13. Result comparisons with feasible analytical calculation results
14. Suggestions for further design improvements

As a first approach, the operational environment and application were defined for the design. The application was intended for ships which may have frequent propeller blade damage by the ice blocks during operation and blades can be replaced easily. Thus the built-up propeller type is relevant and the design was considered up to the ice class (IA super).

In the built-up propeller, it was necessary to consider the appropriate type of joint between blade and hub based on design objectives. There are some possible joint configurations but the bolted joint was chosen in this study for the ease of installation and dismounting for blade repair or replacement.

To be able to withstand the seawater corrosion and navigate in icy areas, the materials were required to select correctly. Sea water corrosion resistance with high strength forged steel was used for the shafting, copper alloy material was considered for the propeller and hub to have corrosion resistance, ductility and strength. And for the blade bolts, high strength stainless

steel grade was selected to have higher mechanical strength (details in later section) and corrosion resistance.

The joint design was composed of components including blade flange, hub and bolts. The calculations have been done to get the minimum thickness of the blade flange, the diameter and length of the hub and the size of the bolts, applying the classification society rules.

After defining the dimensions of the respective components, the 3D modelling of the built-up propeller assembly was developed using Rhinoceros software. The blade root fillet around the flange and the threads in the bolts were modelled in Siemens NX to get better modelling accuracy and resolution. For finite element analysis, the simplified FE models have been prepared from the complete 3D assembly model.

The simplified analytical strength of the bolted joint especially at the bolt shank, threaded part, and clamped parts were calculated referring MechaniCalc, Inc. (2014-2022) **[20]**.

In the FEA section, the analysis layouts and FE model classes have been pre-defined. These layouts included applying different load cases on the respective model classes. Then the mesh studies were done for the blade and for the bolt to save computational time. During analysis, the appropriate contact definitions (bonded, frictional, etc.) have been chosen for the joint design. For the loadings, there were preloads applied on the bolts, centrifugal force due to shaft rotation, different ice loads and blade failure loads acting on the blade according to ice class rules, and a hydrodynamic pressure field around the pressure and suction sides of the blade. Deformations were noted and stresses have been investigated and compared with allowable yield strength of the materials after the FE analysis. To improve local stress distribution in some areas of the joint, necessary design modifications have been made for the joint design and performed the analysis again. FEA results have been compared with analytical strength calculations. Discussions were made for the further design improvements.

1.5 Basics and Introduction to Marine Propeller Design

The main components of a marine propeller assembly are the blade, hub, cap on the hub, and propeller shaft. The propeller geometry comprises a set of parameters. These include diameter, blade tip, leading edge and trailing edge, expanded area ratio (EAR), pitch, rake

angle, skew angle and chord. EAR is noted as the ratio of total expanded blade area to the disc area at the nominal diameter of that propeller. **[3]** The other related terms for a propeller can be noted as a number of blades, left-handed or right-handed type, single screw, twin screw, triple screw or propellers in four shaft line configurations.

Generally, it is less likely to extend the propeller tip under the hull baseline in many merchant vessels so as not to get blade damages in case of grounding. During installation, a propeller is fully submerged in water but it should not be fitted very close to the hull which can result in noise and vibration effects.

The size of a propeller is normally defined by the diameter (D). This parameter is crucial to determine the power capacity that a propeller can deliver and absorb. A greater diameter in relation to blade number is normally proportional to higher propeller efficiency.

When the propeller rotates in one turn, the axial movement for this rotation is the pitch. The propeller shaft torque is converted to the thrust force by pitch mechanism and deflecting the water to the aft of the propeller. The pitch can be adjustable at the blades radially and affect the axial movements in variable pitch propellers whereas in fixed pitch and built-up propellers the pitch is unchangeable.

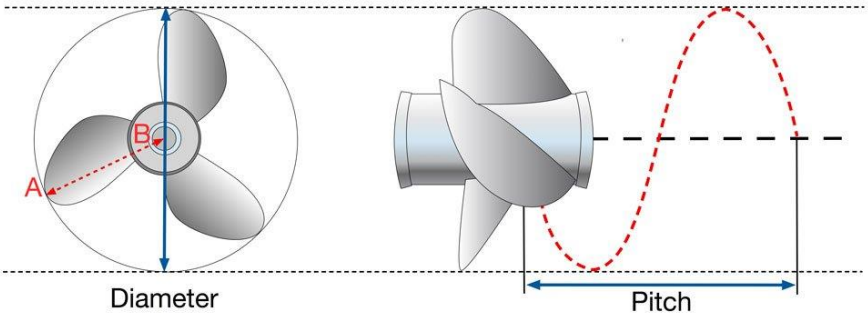

Figure 1. A propeller diameter and pitch

[33]

The ratio of propeller pitch to diameter is called pitch diameter ratio (P/D) which is used as a parameter in estimating the propeller efficiency.

The blades and hub are cast in a single block for solid propeller and fitted separately for CPP or BUP. The number of blades installed on a propeller varies from two to seven and sometimes eight blades can be seen in the submarines for the reasons of reduction in noise and vibration effects.

1.6 Propeller Geometry, Parameters and Definitions

When a propeller a viewed from the side, and at one blade the rake angle is measured between a line drawn perpendicular to the hub or shaft centre line and the leading edge line at the respective blade radius. The positive rake angle is towards the aft of the hub end and the negative rake angle is towards the forward hub end.

When a propeller is viewed from the aft of the ship, at one blade the skew angle is measured between a line drawn perpendicular to the shaft centre line and the mid-chord line at the respective blade radius. At a mid-chord line of certain blade section, aft skew is measured towards the left-hand side of perpendicular line whereas forward skew is towards the right-hand side.

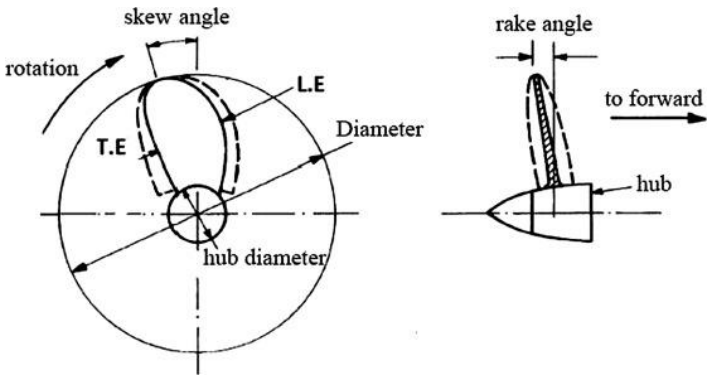

Figure 2. Propeller rake and skew

[34]

The propeller hub is the solid component typically in a cylindrical shape on which blades are cast and are connected with a propeller shaft. To get a higher thrust, the hub is typically shaped in a conical or cylindrical form. The ratio of propeller diameter to hub diameter also influenses the propeller efficiency. However, the smaller hub has less strength than the bigger one and there is a compromise between strength and size.

There are two faces on the blade. The high-pressure side of the blade is known as the face that pushes water for the vessel to have forward motion and the low pressure or suction side of the blade is called the back of the propeller blade.

A twisted blade has two edges. One edge which cuts the fluid when the propeller rotates is the leading edge whereas the other edge of the blade away from and follows the leading edge rotation is the trailing edge.

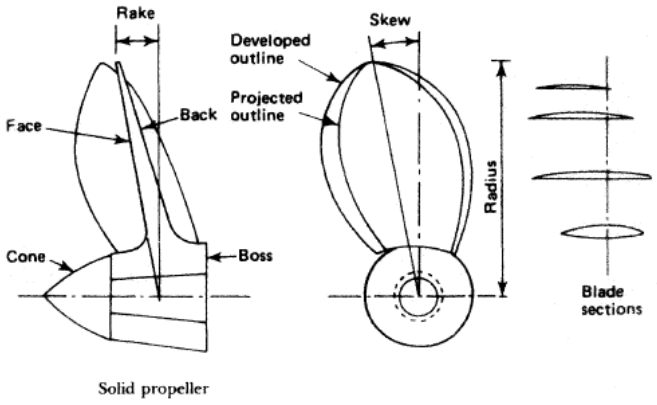

Figure 3. A propeller geometry

[35]

The optimum diameter of a propeller is estimated by a calculation based on a Troost series as: **[4]**

$$D = \frac{15.24\ x\ P_s^{0.2}}{n^{0.6}} \quad (1)$$

Where,

D is the diameter in metres,

P_s the shaft power in kW,

In this study, power output is 19500 kW and propeller speed is 133 rpm, the propeller diameter was decided to have 6 m.

2. CLASSIFICATION RULES FOR SHAFTING & PROPELLER

In general, the built-up propeller assembly is composed of propeller and shafting. In order to design these components, classification rules have been applied to get the optimum principle

dimensions and to be able to use the appropriate materials for the desired missions. References and comparisons were made among DNV, GL, BV and Finnish-Swedish Ice class rules and the required criteria were fulfiled for the shafting & propeller design calculations.

2.1 Shafting: Diameter, Connection Methods

The simplified shaft diameter formulae and the detailed shaft calculation method for marine applications can be found in the classification rules.

According to the class rules, the shaft line is composed of shafts, rigid couplings, shaft bearings and shaft seals. The possible methods of connection for propeller shaft rigid couplings and the propeller hub can be noted as flange couplings, shrink-fit couplings, keyed connections, clamp couplings, splines, etc. **[5]**

2.1.1 Shaft Design

The shafting shall be designed to withstand all relevant load conditions including rated power and reversing loads. For low cycle fatigue criteria of (10^3 to 10^4 cycles), the major load conditions due to load variations from zero to full load, clutching-in shock loads, and reversing torques are considered. A higher number of cycles (~10^5 cycles) can be applied for short-range ferries as a special case. Due to rotating bending and torsional vibration, high cycle fatigue of (>>$3 \cdot 10^6$ cycles) is used. For ice class vessels and icebreakers with ice shock loads, (10^6 to 10^7 cycles) is applicable. **[5]**

2.1.2 Simplified Shafting Diameter

In the classification rules for shafting, the simplified methodology of minimum shaft diameter evaluation for different design features has the following assumptions. **[5]**

1. Material yield strength is limited to 70% of tensile strength for calculation purposes only.
2. The value of application factors is less than or equal to 1.4 for ice-class notations.

3. In all operating conditions, vibratory torque shall be less than or equal to 35% of maximum continuous torque.
4. Inner diameter is less than or equal to half of the outer diameter in a hollow shaft. However inner diameter is less than or equal to 77% of the outer diameter for the oil distribution shaft with a longitudinal slot in a CPP system.
5. Corrosion protection shall be equipped.

2.2 Propeller: Blade Thickness, Fitting of Propeller to the Shaft

2.2.1 Design and Materials for Propeller

Propeller materials shall meet the requirements of the class rules. The material combination shall be carried out in such a way as to minimize galvanic corrosion. The hub, conical bores, blade and fillets surfaces shall be smoothly finished. The available materials and their mechanical properties for propellers in DNV rules are tabulated below. **[6]**

Table 1. Material properties for propeller

Material **[6]**	Material constant, U_1 [N/mm^2]	Material constant, U_2 [-]	Minimum yield strength [N/mm^2]	Minimum tensile strength [N/mm^2]
Mn-Bronze, CU1 (high tensile brass)	55	0.15	175	440
Mn-Ni-Bronze, CU2 (high tensile brass)	55	0.15	175	440
Ni-Al-Bronze, CU3	80	0.18	245	590
Ni-Mn-Bronze, CU4	75	0.18	275	630
Martensitic stainless steel (12Cr 1Ni)	60	0.20	440	590
Martensitic stainless steel (13Cr 4Ni)	65	0.20	550	750
Martensitic stainless steel (16Cr 5Ni)	70	0.20	540	760

Austenitic stainless steel (19Cr 11Ni)	55	0.23	180	440

In this study, the materials for propeller and hub were considered to be Ni-Al-bronze, Cu3. The minimum tensile strength and yield strength were taken as 590 MPa and 270 MPa respectively (MMG, personal communication).

2.2.2 Criteria for Propeller Blade Dimensions

The following load criteria shall be considered for blade dimensioning: **[6]**

a) Due to variation of propeller rotational load in normal, ahead operation, high cycle dynamic stresses as ($> 10^8$ cycles).

b) low cycle dynamic stresses as ($< 10^6$ cycles) due to variations of propeller load in a seaway, starting and stopping, reversing, manoeuvres, redundant ice shock loads etc. It is also taken into account when dynamic stresses are not overwhelmed by high cycle load variations.

Moreover, the propeller blades shall be designed with the minimum safety factors as mentioned in the class rules. The safety factors reflect the desired inaccuracies in the approaches used to predict calculations of loads and stresses, as well as the influence of acceptable material defects. If the detailed stress distribution are documented by an advanced computational CFD method together with reliable measurements and FE analysis, lower safety factors can be accepted with special considerations. Blade root fillet shall be developed to sustain a safety factor required for the root section. **[6]**

2.2.3 Blade Thickness and Calculation

The blade thicknesses of controllable pitch propellers (similarly in built-up propellers) are determined at radii 0.35 R and 0.6 R. The blade thicknesses evaluated according to the class rules represent the lowest satisfactory values for the finish-machined propellers. **[6]**

2.2.4 Fitting of Propeller Blades to the Hub

Practically there are some existing possible methods of connection of propeller blades to the hub for controllable pitch propellers and built-up propellers. However, only one method is highlighted in the class rules. This is the bolted joint connection method.

The other norms of fitting methods are treated and managed on a case-by-case basis with approval from the classification society. The pretension in the minimum section of blade bolts shall be ranging from 50% to 70% of yield strength or a maximum of 56% of the tensile strength of that material, whichever is less according to DNV rules. Furthermore, adequate pretension is necessary for required safety factors in the following conditions: **[6]**

1. sufficient frictional forces prevent sliding of the propeller flange
2. the bolts preserve a prestress maintaining surface pressure between mating surfaces in all allowable operational situations
3. Any permissible working state shall not lead to the yielding of bolt materials.

According to GL rules, the blade retaining bolts shall be tightened in a controlled manner so that the initial tension is about 60 to 70 % of the bolt's yield strength. The bolt's shank may be reduced to a minimum diameter of 0.9 times the threaded part's root diameter. Blade bolts shall also be assured against unintended loosening. **[6]**

In the later design calculation sections of this thesis, it was decided to follow GL rules for the shaft diameter estimation and preload criteria of the blade bolts. The blade force calculations and applications followed the Finnish-Swedish Ice Class rules.

2.3 Ice Class Rules

Since the built-up propeller in this focus of the study was to be applicable for ice class, the ice class rules have also complied. The propeller in this focus was neither to use for the vessel in ice-breaking works nor on the ice breakers so the polar ice classes were not considered. It was only intended to operate in basic ice and northern Baltic ice regions.

2.3.1 Ice Classes

Following the Finnish-Swedish Ice Classes Rules, the definitions of ice classes are mentioned by: **[10]**

1. ice class IA Super: ships with structure, engine output and other characteristics typically capable of navigating in harsh ice conditions without icebreaker assistance
2. ice class IA: ships with structure, engine output and other characteristics generally capable of navigating in difficult ice conditions, with icebreakers assistance when necessary
3. ice class IB: ships with structure, engine output and other characteristics commonly capable of navigating in moderate ice conditions, with icebreaker assistance when necessary
4. ice class IC: ships with structure, engine output and other characteristics capable of navigating in light ice conditions, with icebreaker assistance when necessary
5. ice class II: ships with a steel hull and are structurally fit for navigation in the open sea but not being strengthened for ice navigation. Besides from their own propulsion machinery, they are capable of operating in very light ice conditions
6. ice class III: ships which are not complying with ice classes with reference to paragraphs 1-5

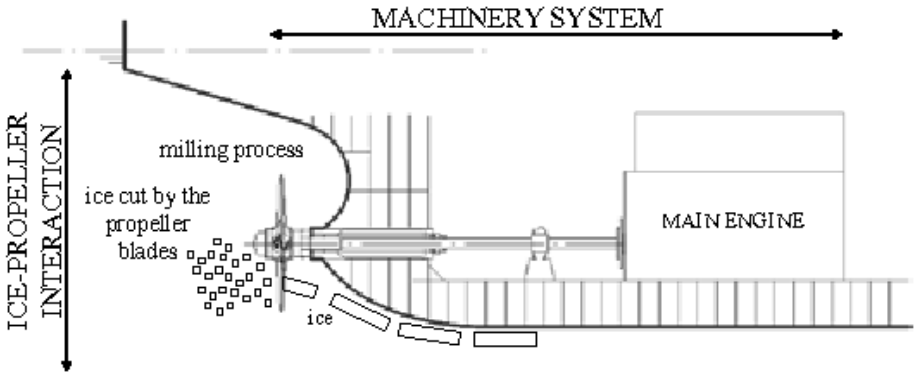

Figure 4. Propulsion machinery in ice and ice-propeller interaction

[36]

2.3.2 Ice Loads

Definitions of ice loads and use of them in the designing process of propellers are summarized in the following table.

Table 2. Definition of loads for design process

	Definition **[10]**	Use of loads in design process
F_b	A propeller blade's maximum lifetime backward force results from ice and propeller interaction, including hydrodynamic loads on that blade. The force direction is perpendicular to the 0.7R chord line.	As a design force for propeller blade strength calculation.
F_f	A propeller blade's maximum lifetime forward force results from ice and propeller interaction, including hydrodynamic loads on that blade. The force direction is perpendicular to the 0.7R chord line.	As a design force for propeller blade strength calculation.
F_{ex}	Ultimate blade load causes plastic bending at blade and blade loss. The force required to induce total blade failure so that in the blade root area a plastic hinge emerges. The force is exerted on a 0.8R blade radius. At 0.8R, the spindle arm is 2/3 of the distance between the blade spin axis and the leading or trailing edge (whichever is the greater).	Blade failure load is utilised in the design and sizing of blade bolts, pitch control mechanism, propeller shaft, shaft bearing and thrust bearing. The objective is to ensure not to happen any damage to other components due to total blade failure.

The loaded areas on the blade for the load cases are also summarized in the following table.

Table 3. Loaded areas and load cases on the blade

Load case **[10]**	Force	Loaded area for Right-handed propeller blade seen from behind
LC1	F_b	At the blade back (suction side) a uniform pressure is applied to an area from the leading edge to 0.2 times the chord length and from 0.6R to the tip.
LC2	50 % of F_b	At the blade back (suction side) a uniform pressure is applied on the blade tip area outside 0.9R radius.

LC3	F_f	At the blade face (pressure side) a uniform pressure is applied to an area from the leading edge to 0.2 times the chord length and from 0.6R to the tip.
LC4	50% of F_f	At the blade face (pressure side) a uniform pressure is applied on the blade tip area outside 0.9R radius.
LC5	60% of F_f or F_b, whichever is greater	At the blade face (pressure side) a uniform pressure is applied to an area from the leading edge to 0.2 times the chord length and from 0.6R to the tip.

LC5 is required to implement only for FPP and BUP.

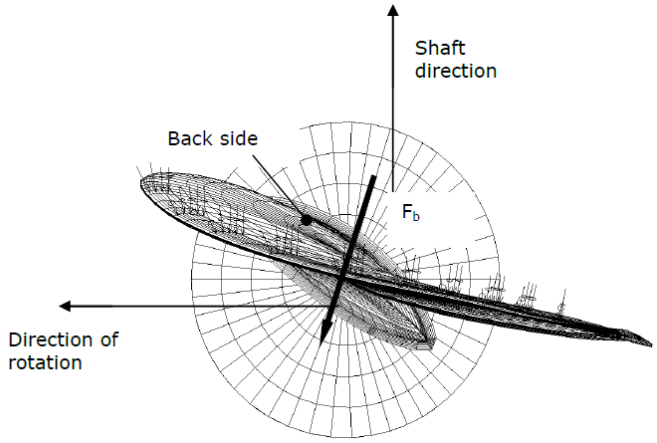

Figure 5. Resultant backward blade force direction taken perpendicular to the chord line at radius 0.7R. At the leading edge, ice contact pressure is indicated with small arrows.

Available from **[10]**

2.3.3 Ice Conditions for Design

Different types of operations are tabulated to predict the ice loads on the propeller for various ice classes. Besides maximum ice block thickness shall also be determined to estimate design ice loads. The respective details are summarized in the following tables. **[10]**

Table 4. Types of operation for different ice classes

Ice class **[10]**	Ship's operation
IA Super	Operation in ice channels and in level ice

	The ship may proceed by ramming
IA, IB, IC	Operation in ice channels

Table 5. Thickness of design ice blocks for different ice classes

[10]	IA Super	IA	IB	IC
Thickness of the design maxi-mum ice block entering the propeller (H_{ice})	1.75 m	1.5 m	1.2 m	1 m

3. PRE-STUDY

3.1 Built-Up Propellers (General Design Hub, Blade, Joint Hub-Blade)

In the BUPs the hub and the propeller blades are individually cast. The materials can be used either the same or different types for the blade and the hub. As the blades cannot change the pitch, they are already oriented at the desired pitch before fitting to the hub.

According to DNV rules, the propeller hub shall be able to withstand the static loads against yield strength with a safety factor. When a propeller blade is subjected to maximum hydrodynamic load, the safety factor of 2.0 should comply with load transmission. **[6]**

The outer surface of the propeller hub is exposed to seawater and the inner portion should be waterproofed.

The propeller blades are separately fitted onto the hub by means of appropriate methods. Bolted connection is a common type.

The propeller blades shall be designed to fulfil the required minimum safety factors as per class rules. The safety factors should also meet the manufacturing tolerance class I or S according to ISO484. **[6]**

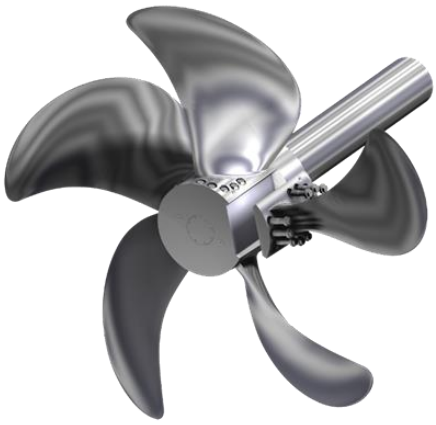

Figure 6. A typical built-up propeller of Wärtsilä

[37]

3.2 Different Design Layouts (Comparison, Assessment, Conclusion)

Some design layouts of blade and hub joint can be categorized as:

1. Bolted Joint Type
2. Clamp on Blade, CoB (developed by Teignbridge Co., UK)
3. Fixed Pitch Adjustable (FP-A) Type (developed by West Mekan Produksjon AS, Norway)
4. Form Fit or Interlock or Modular Type (applicable for small boats)

Among these configurations, the most possible and closely matched methods were extracted to be bolted joints and clamped on blade types. Further comparison and assessment have been made for these methods as following.

Table 6. Comparison of two possible connections for blade and hub

S/N	Fitting	Components	Benefits	Drawbacks	Existing manufacturers
1	Bolted type	blade, hub, bolts	1) easy to install and dismount the blades with the aid of appropriate tools e.g torque wrench 2) without the need for dry docking and blades can be with the least interruption of vessel operational schedule		MAN, Wartsila, GE, Kongsberg/ Rolls-Royce,

			3) this method is presented in the class rules		
2	Clamp on Blade (CoB)	blade, hub, clamped pins	1) easy to install and dismount the blades with the aid of appropriate tools 2) according to the manufacturer, it is possible to carry the blades up to 1.20m in diameter and hub components by a diver	1) small size propellers up to 5.5 m are applicable and for superyachts 3) need more research for ice class applications 4) propeller components are fully CNC machined	Teignbridge Co. (UK)

Figure 7. Bolted joint connection of MAN built-up propeller

[38]

Figure 8. CoB connection of Teignbridge built-up propeller

[39]

According to comparison and assessment, the bolted connection was selected for the blade and hub joint in this thesis.

3.3 Bolted Joint (Standards, Analytical & FEM Methods)

After the bolted joint layout was selected, it was necessary to design the bolts for the connection of the propeller blade and hub. The bolts were designed according to DIN EN ISO 3506-1 standards referring to the required strength classes and mechanical properties, and VDI2230 standards for some design calculations. The required bolt size was calculated applying the class rules.

From DIN EN ISO 3506-1 standard, initially, the strength classes and mechanical properties for the bolt were preliminarily extracted among available classes to have enough strength, to be practical application and be compatible with the 6-meter diameter propeller in this study.

Table 7. Comparison of bolt specifications

Material and grade	Strength class	Tensile strength	0.2% yield point
Austenitic A4, A5	80	800	600
Martensitic C3	80	800	640

Since the bolts are important parts in the bolted joint design, they should have enough strength to withstand the loads. The stainless steel materials of austenitic and martensitic grades from Table 7 had the same tensile strength whereas the martensitic steel had higher yield point. In addition, the given mechanical properties for martensitic steel can be better met for bolts in bigger size. The hardening process for required strength of austenitic steel is limited in bolt size (limited material sheet from the outer surface). After a comparison between these two materials, martensitic C3 class (80) material was considered in order to provide higher yield strength and to be compatible for bigger bolts.

Since the blade was fitted to the hub with more than one bolt, the bolted joint layout was a multi-bolted joint (MBJ) and the bolts were screwed to the hub without nuts and it is a tapped-through joint (TTJ). For the analytical calculation of the bolted joint, simplifications

and some assumptions have been made due to the complex propeller geometry. VDI2230 part 2, provides some analytical calculation methods for mechanical bolted joints namely rigid body mechanics and elastomechanics. However, these methods are not directly compatible with the bolted joint of the built-up propeller. Thus simplifications were made and using the concepts of load distribution on the bolts and taking the critically loaded bolt, stresses and deformations were estimated. The detailed calculations were included in the following sections.

Since the analytical calculations could not provide very detailed results of stresses and deformations at every single point on the bolted joint layout, FEA was performed with the aid of Ansys commercial software. According to VDI2230 part 2, there are four classes of FE models as below: **[13]**

1. Neither the interface nor the bolt itself is considered in model class I. The component solely is modelled.
2. The bolt is illustrated as a line element in model class II for FE calculation. It is represented as a tension member, beam or spring element.
3. The bolt is described as an equivalent volume body and is modelled without a thread in model class III.
4. The bolt is extensively modelled including the thread and the contact conditions for all contact surfaces in model class IV.

The model class 3 was developed in the later section of FEM part to have a compromise between detailed results and computational time.

3.3.1 Manufacturing Tolerances

In order to improve the fitting of the bolted joint and propeller components and to accept a certain amount of dimensioning error without affecting the proper functioning of the parts, manufacturing tolerances shall be considered. The applicable standards are to be used for the manufacturing of the propeller components and the bolted joint.

3.4 Materials with Respect to Application in Seawater, Strength, Ice Loading

According to GL ice class rules and Finnish-Swedish ice class rules, the materials for the propellers and propeller components shall meet the following specifications and criteria.

Steel or another ductile material shall fulfil as materials when exposed to sea water temperature. The material elongation of parts exposed to seawater, such as propeller blades and propeller hubs, should be at least 15% in a specimen and the gauge length which is five times the diameter. A Charpy V impact test shall be performed on materials other than bronze and austenitic steel. An average impact energy value of 20 J from three tests must be obtained at -10 ºC. This involves the propeller shaft, shaft bolts, blade bolts, CP mechanisms etc. It is not applicable to bearings and gear teeth which are surface-hardened components. The nodular cast iron with ferrite structure may be used for appropriate parts other than bolts. Nodular cast iron shall have average impact energy as a minimum of 10 J at -10 ºC. **[10]**

The chemical composition of the selected material for propeller blade, blade flange and hub can be noted as:

CU3 (Nickle-Aluminium Bronze) which is derived from 77-82% copper, 7-11% aluminium, 3-6% nickel, 0.5-4% of manganese, tin, lead, zinc and iron. These alloys have a tensile strength of minimum 590 N/mm^2. **[11]**

3.5 Tightening Methods of the Bolted Joint

The tightening procedure for the bolted joint has been carried out by the use of a special torque wrench. Additionally, the hydraulic torque device is feasible especailly for this size of blade bolts to be tightened. The required tightening torque values for the blade bolts were calculated according to the formulation from VDI2230 part 1 and cross-checked with the general tightening torque formula for the bolts. Detailed calculations are mentioned hereafter.

3.6 Bolt Securing/Locking

After tightening the bolts to the specified torque values by the hydraulic torque tool, the bolts are required to be secured. The final torque has been applied and in order not to loosen the bolts in the case when shock loads are acted during vessel operation, the bolt heads are required to be locked. There are some available methods for securing of the bolts including use of locking wire, tap washers, locking plates/caps, and creating high friction on the bearing surface of the bolt. However the compatible method for the bolted joint of the built-up propeller shall be by means of locking plates welded to the blade flange part or by the use of customized bolt locking cap or device.

4. PRE-DESIGN OF A BUILT-UP PROPELLER

In this section, in order to develop a 3D design model of the built-up propeller, calculations have been performed according to the class rules for propeller shaft dimensioning (with and without ice class), blade root fillet, blade flange thickness, hub dimensioning (with ice class), blade bolt sizing (with ice class).

4.1 Input Data: Blade Design, Shaft, Power Output, Ice Loads

To be able to calculate the principal dimensions for the propeller shaft, hub and blade bolts, (MMG, personal communication) provided the propeller input data as tabulated.

Table 8. Propeller input data

Description	Value	Unit
Selected ice class	IA Super	
Power output at MCR	19500	kW
Propeller speed at MCR	133	RPM

Propeller speed in ice	133	RPM
Propeller thrust at MCR	1112	kN
Propeller Diameter	6000	mm
Blade number, *z*	5	
Expanded area ratio, *EAR*	0.581	
Blade root section outside fillet radius, *r*	852	mm
Chord length of blade root section, *c*	849	mm
Thickness of blade root section, *t*	328	mm
Pitch at section *0.7R*, $P_{0.7}$	6724	mm
Proof yield strength	270	MPa
Ultimate tensile strength	590	MPa
Design draft	8300	mm

4.1.1 Propeller Shaft Diameter (without Ice Class)

Applying GL rules, the minimum propeller shaft diameter (without ice class) was estimated using the following formulation. **[16]**

$$d \geq F.\ k.\ \sqrt[3]{\frac{P_w}{n.\left[1-\left(\frac{d_i}{d_o}\right)^4\right]}}.C_w \qquad (2)$$

Where

d : minimum required outer shaft diameter [mm]

d_o : actual outer shaft diameter [mm]

d_i : actual diameter of shaft bore [mm], (it is taken as 0 for solid shaft in this study)

P_w : rated power of propulsion motor [kW]

n : shaft speed at rated power [min^{-1}]

F : factor for type of propulsion installation [-]

: propeller shaft = 100, for all types of propulsion

C_w : material factor [-]

$$\frac{560}{R_m + 160} \tag{3}$$

R_m : specified minimum tensile strength of shaft material (taken as 590 MPa in this study)

Table 9. Minimun shaft diameter

Parameters	Value	Unit
F	100	
k	1.22	
n	133	min^{-1}
P_w	19500	kW
$1-(d_i/d_a)^4$	1.00	
R_m	590	MPa
C_w	0.75	
d	583.62	mm
d_i	0	mm

After calculation, the minimum propeller shaft diameter (without ice class) was obtained as 584 mm.

4.1.2 Propeller Shaft Diameter (ice class, IA Super)

Applying GL and Finnish-Swedish Ice Class Rules, the minimum propeller shaft diameter (ice class) was estimated using the following formulations. **[16]**

$$d_{ps} = 140. \sqrt[6]{\left(F_{ex}.S_{Fex}.\frac{D}{\sigma_{yield}}\right)^2} + 5.6\,.\left(\frac{Q_r.S_Q}{\sigma_{yield}}\right)^2 . \sqrt[3]{\frac{1}{1-\left(\frac{d_i}{d_{ps}}\right)^4}^2} \tag{4}$$

In this formulation, the blade failure load is introduced to design the shaft for ice class.

$$F_{ex} = \frac{300 \,.\, c \,.\, t^2 . \sigma_{ref}}{0.8 \;.D - 2 \,.\, r} \tag{5}$$

$$\sigma_{ref} = 0.6 \,.\, \sigma_{0.2} + 0.4 \,\sigma_u \tag{6}$$

Where

d_{ps} : minimum required outer propeller shaft diameter [mm]

F_{ex} : ultimate blade load resulting in plastic bending deformation of the blade [kN]

Blade failure load, F_{ex} can be calculated using Eq. 5. MMG provided the numerical value of F_{ex} which was more accurate and in detailed result obtained from a separate FE analysis. Thus it was considered for further design calculations.

S_{Fex} : safety factor for loads resulting from loss of the propeller blade (Fex) through plastic bending (S_{Fex} shall be greater than 1.0 against yielding)

D : Propeller diameter [m]

σ_{yield} : yield strength of propeller shaft [MPa]

Q_r : maximum response torque along the propeller shaft line [kN-m]

Considering there were very less transmission losses from the engine to the propeller shaft, the delivered power at the propeller was taken as propulsion engine power and the torque was calculated as:

$$P_w = 2\pi \; n \; Q_r \tag{7}$$

S_Q : safety factor against yielding

d_i : inner shaft diameter (it is taken as 0 for solid shaft)

c : chord length of blade root section [m]

t : thickness of blade root section [m]

r : blade root section outside fillet radius [m]

σ_{ref} : reference stress [MPa]

$\sigma_{0.2}$: proof yield strength of propeller blade [MPa]

σ_u : ultimate tensile strength of blade material [MPa]

Table 10. Minimun propeller shaft diameter (Ice classes)

Parameters	Value	Unit
c	849	mm
t	328	mm
r	852	mm
σ_u	590	N/mm²
$\sigma_{0.2}$	270	N/mm²
σ_{ref}	398	N/mm²
D	6000	mm
S_Q	1.3	
S_{Fex}	1.1	
Rule based, $F_{ex,r}$	3522.56	kN
Numerical/FE, $F_{ex,n}$ (given by MMG)	3926	kN
σ_{yield}	290	N/mm²
P	19500	kW
n	2.217	rps
Qr	1400	kNm
$1-(di/dps)^4$	1	
$d_{PS,r}$ (calculated propeller shaft diameter using $F_{ex,r}$)	607	mm
$d_{PS,n}$ (calculated propeller shaft diameter using $F_{ex,n}$)	629	mm
d_{PS}	650	mm

After calculation, the minimum propeller shaft diameter (ice classes) was taken as 650 mm. The shaft diameter was increased a little bit more with respect to the keyless fitting of propeller material to have larger contact surface area. This value is used for further calculations.

4.1.3 Principle Dimensions of the Hub (Ice Class)

For the calculations of the hub design in ice class, mainly the hub diameter and hub length or the tapered shaft length were estimated.

According to Wärtsilä, a typical hub diameter to propeller diameter ratio for ice class or very high-loaded propellers may vary from 0.25 to 0.38 or higher. **[40]**

In this study, the ratio of hub diameter to propeller diameter was considered as 0.25.

After the hub diameter was calculated, the taper length of the shaft for keyless fitting or the hub length was estimated.

It was also noted (boatdiesel.com/Forums, 2022) that in general a tapered hub length is estimated to be 3 times the shaft diameter. In order to locate the blade bolts properly on the blade flange and with the developed 3D geometry, hub length was taken as 3 times the propeller shaft diameter as for pre-design. Additionally in order to reduce the shear stress acting on the bolted joint in case of shock loads and to secure the fitting of blade flange and hub, two shear pins with 100 mm diameter size, (MMG, personal communication) suggested based on similar designs of CPPs, were included on the hub surface for each blade. At the blade root, fillet radius can be normally chosen as one-third of blade thickness at root section. With respect to the available design, (MMG, personal communication) suggested the fillet radius as 100 mm. The strength of that blade fillet radius would be further investigated with FE analysis in the next section. The dimensions of the hub were tabulated as:

Table 11. Dimensions of the hub

Parameters	Value	Unit
hub diameter, *d*	1500	mm
hub length	1950	mm

Since the propeller and shaft were connected by keyless fitting, the shaft was tapered at the other end of the hub with the taper ratio. Referring the class rules, the taper ratio for the keyless fitting was considered as 1:20 in this study. Tapered shaft diameter at the other end of the hub was calculated as:

$$taper\ ratio\ = outer\ diameter - \frac{tapered\ diameter}{tapered\ length} \tag{8}$$

Table 12. Tapered shaft diameter

Parameters	Value	Unit
shaft taper ratio	0.05	
tapered length	1950	mm
taper diameter, d_{taper}	553	mm

From the calculation, the tapered shaft diameter was taken as 553 mm.

4.1.4 Blade Flange Dimensions

The outer shape of the hub was considered to be a cylindrical body and the inner bore of the hub was attached to the tapered shaft. The blade was fitted to the hub with the flange and the length of the blade flange was taken 100 mm less than the hub length at each end as a pre-design. There were five blades in this built-up propeller assembly and the width of the blade flange was occupied as one-fifth portion on the outer surface of the hub. Hereafter the detailed dimensions were developed in a 3D model using Rhino software.

Applying the BV rules the effective thickness of the blade flange was calculated. For Built-up propellers and controllable pitch propellers, it was also noted (Bureau Veritas **[18]**, 2022) that the thickness of the blade flange shall not be less than 1/10 of the diameter of that flange. In the pre-design of the 3D model, the blade flange was not circular in shape and it was in a rectangular geometry. The reason why the rectangular shape was considered was that it had more area at the flange than the circular shape having higher strength and stiffer blade root when the applied loads were exerted. So the minimum flange diameter was estimated by measuring the minor length of the flange in 3D. The effective thickness of the blade flange was tabulated.

Table 13. Blade flange thickness

Parameters	Value	Unit
minimum flange diameter from 3D model	760	mm
minimum flange thickness as per BV rules	76	mm
Existing effective flange thickness measured from 3D model	89	mm

The effective thickness of the blade flange in the developed 3D was designed as 89 mm. The actual strength of the blade flange at the joint area was analyzed in detail in the FEA section.

4.1.5 Bolted joint design and dimensions

Since the bolted joint type was selected for the blade and hub connection, applying GL rules the size and principle dimensions of blade retaining bolts for ice class were calculated as in Eq. 9. The blade failure load was taken into account in the formulation. **[16]**

$$d_{bb} = 41 \cdot \sqrt{\frac{F_{ex} \cdot S_{Fex} \cdot (0.8D - d) \cdot \alpha_A}{\sigma_{yield} \cdot z_{bb} \cdot PCD}} \quad (9)$$

Where

d_{bb} : minimum diameter of blade retaining bolt [mm]

z_{bb} : number of bolts (as for pre-design, 10 bolts are considered for each blade)

PCD : pitch circle diameter of the bolt holes [m], (as for pre-design in 3D, approximately 900 mm was set)

d : hub diameter [m]

α_A : bolt tightening factor

For tightening with a torque wrench the tightening factor is usually taken as 1.6. **[41]**

It was also noted (VDI2230 part 1, 2015) that tightening factor range from 1.6 to 2 is also compatible for torque-controlled tightening with a torque wrench.

In Eq. 9, the higher the tightening factor value, the bigger the bolt size. So for safety reasons, a tightening factor value of 1.7 was selected:

σ_{yield} : yield strength of bolt material [MPa]

Table 14. Nominal diameter of blade retaining bolt

Parameters	Value	Unit
PCD	900	mm
z_{bb}	10	
α_A	1.7	
σ_{yield}	640	MPa
d	1500	mm
Applying rule based F_{ex}, d_{bb}	79.65	mm
Applying FE based F_{ex}, d_{bb}	84.09	mm
Selected size M85 x 4, d_{bb}	85	mm

After calculation, the blade bolt was selected to be M85 with 85 mm nominal diameter referring to external metric ISO thread and ANSI/ASME B1.13M-1995. **[42]**

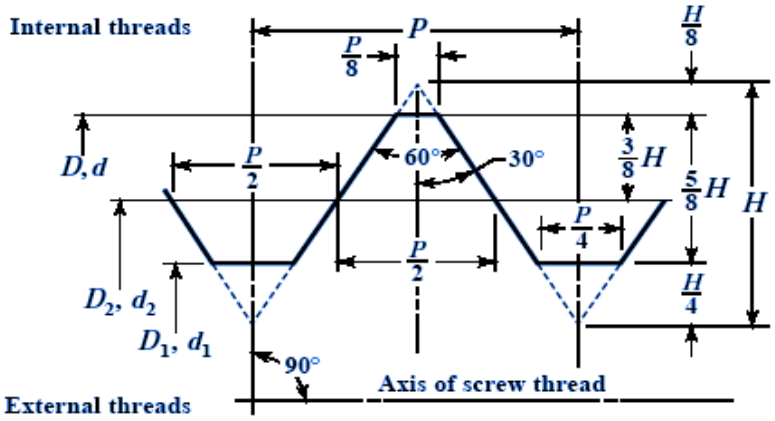

Figure 9. Reference diagram for ISO external thread dimensioning

[43]

where $H = 0.866025\ P$, **[42]**

The other principle parameters for the bolts were further defined. (MMG, personal communication) suggested the pitch of the thread as 4 mm referring to standard for fine thread (DIN 13-2 or international standard). Following ISO external metric thread standard, the value H, pitch diameter and core diameter were calculated.

The bolt's hole diameter was taken and considered as close-fit series. **[44]**

The thread height could be known as half of the difference between nominal diameter and core diameter.

Then the minimum thread engagement length was calculated as per Eqs. 10-12. **[45]**

$$L_e = \frac{(D-0.938194)^2}{D - 0.64952\ x\ p} \quad (10)$$

$$J = \frac{\text{Tensile strength of bolt}}{\text{Tensile strength of nut (hub in this case)}} \quad (11)$$

$$L_{e1} = L_e\ .J \quad (12)$$

In case of the nut and bolt had the same material property then the minimum thread engagement length (*Le*) could be found by using Eq. 10.
In case of the nut and bolt had different materials and the value of J from Eq. 11 was more than 1, then it would be necessary to use Eq. 12 for calculating the minimum thread engagement length (*Le1*).

Where,
L_e , L_{e1} – required minimum thread engagement length
D – Basic diameter of bolt

As a pre-design, the bolt head was considered to be a hexagonal flange bolt. The height of the head and flange was set at 85 mm to be in line with M85 size and the flange height was one-third of that size. The effective head diameter was the same as the M85 size. The head flange diameter was set as one and half times of effective head diameter.

According to the 3D geometry of the blade flange, the lengths of the bolts differed. The difference was at the shank length. There were two shank lengths for the bolts the long shank bolts at the middle of the blade flange and the short shank near the edge of the blade flange. To define the dimensions of the shank lengths, (MMG, personal communication) suggestions were followed.

Referring to the standards of DIN EN ISO 4014 (Hexagon head bolts) and DIN EN ISO 4762 (Hexagon socket head cap bolts), the ratio of shank length to bolt length of approximately

0.38 to 0.40 for hexagon head bolts and approximately 0.30 to 0.32 for hexagon socket head cap bolts were considered. (MMG, personal communication) suggested that these ratios for the bigger thread sizes were also referable as guidance. (MMG, personal communication) suggested using a ratio of approximately 0.4 for sufficient wall thickness at the blade flange, and a lower ratio but not less than 0.32 at smaller wall thickness.

It was also noted (GL **[16]**, 2016) that shank diameter can also be reduced to a minimum of 0.9 times of root diameter of the threaded part in pre-design so that the stress on threads can be reduced in case of shock loads.

The fillet was at the connection between the bolt head flange and shank to reduce the stress. The reducer transition part was included between the shank and threaded parts to avoid an abrupt change in diameters.

The principal dimensions of the blade retaining bolts were tabulated.

Table 15. Blade retaining bolts dimensions

Parameters	Value	Unit
nominal dia.	85	mm
Pitch, *p*	4	mm
H	3.464	mm
Pitch diameter	82.342	mm
core dia.	80.61	mm
Hole diameter	87	mm
thread height	2.165	mm
TPI	6.35	
L_e	85.70	mm
J	1.33	
L_{e1}	114.26	mm
Taken L_{e1}	120.00	mm
Bolt Head	Hexagonal Flange or collar bolt	
head+collar height	85	mm
head diameter	98.15	mm
effective head diameter	85	mm
collar/flange height	28.33	mm
collar/flange diameter	127.5	mm
Preload (initial tension)	384	N/mm²
Long shank length	90	mm

Short shank length	70	mm
reduced shank diameter	72.55	mm
shank diameter, taken	75	mm
fillet at Shank and collar	5	mm
height of tapered core	10	mm
Total long shank bolt length, *L*	220	mm
Total short shank bolt length, *L*	200	mm
shank length/bolt length	0.41	
shank length/bolt length	0.35	

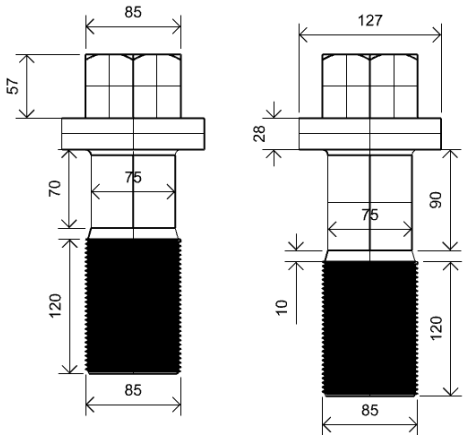

Figure 10. Dimensions of blade bolts (All dimensions are in millimeter.)

The bolt preload ensures the clamped parts stay connected during operation. Insufficient preload can cause the bolts to loosen and leading to the failure of the joint assembly. Tightening of bolts produces tensile loads in the bolts and the bolt preload is also called bolt pretension. **[19]**

In this study, the initial pretension of the bolt was taken as 60% of the yield strength of the bolt complying with the class rules.

The total loads acting on the bolt were initial pretension and external loads. The clamped load at the joint components or preload applied at the bolt shank was calculated as: **[19]**

$$P = \frac{1}{FoS}\left(\sigma_y . \frac{\pi}{4} D^2\right) - F \qquad (13)$$

Where

P : bolt preload [N]

FoS : factor of safety taken into account in the case of total load acting on a bolt

σ_y : yield strength of bolt material [MPa], for initial pretension 60% of the yield strength of the bolt was considered

D : major diameter of the bolt [mm], shank diameter was taken

F : external load applied on the bolt [N]

For the bolt preload calculations, the external loads acting on the propeller assembly and bolted joint were taken as the centrifugal force (also refer to subsubsection *4.4.2*) due to propeller rotation acting on the 10 bolts for each blade and the designed blade failure load acting on the 5 bolts. The blade failure load, which could be regarded as the worst-case load in the design, was applied at the pressure side of the blade and considering 5 bolts at the suction side were not be loaded.

In order to calculate the tightening torque values for the bolts, the formulation from VDI2230 part 1 **[12]** was applied and crossed checked with the general tightening formula in the Ansys presentation. **[19]**

Tightening torque as per VDI2230 part 1 was expressed as:

$$M_A = F_{Mzul}[0.16 \,.\, p + 0.58 \,.\, d_2 . \mu_{Gmin} + \frac{D_{Km}}{2} . \mu_{Kmin}] \quad (14)$$

Where

M_A : Tightening torque for the bolt [N-m]

F_{Mzul} : bolt preload [kN]

p : pitch of bolt thread [mm]

d_2 : pitch diameter [mm]

μ_{Gmin} : coefficient of friction in the thread, (MMG, personal communication) suggested that 0.15 was taken

μ_{Kmin} : coefficient of friction in the head bearing area, (MMG, personal communication) suggested that 0.22 was taken

D_{Km} : effective diameter for the friction moment at the bolt head [mm]

General Tightening torque formula was noted as:

$$T = K . D . P \quad (15)$$

Where

T : Tightening torque at the bolt [N-m]

K : nut factor [taken as 0.2 for steel bolts with no plating or plain (dry) finish]

D : major diameter of the bolt [mm]

P : bolt preload [kN]

The preload and tightening torque of the blade retaining bolts were tabulated.

Table 16. Clamped load or preload at the bolt shank

Parameters	Value	Unit
longer shank area	4417.86	mm²
shorter shank area	4417.86	mm²
safety factor for bolt	1.30	
external load on a bolt, *F1*	785.20	kN
external load on a bolt, *F2*	2.45	kN
Preload at short shank, *P* or F_{Mzul}	517.32	kN
Preload at long shank, *P* or F_{Mzul}	517.32	kN

Table 17. Tightening torque of the bolt

Parameters	Value	Unit
$\mu_{G\,min}$	0.15	
$\mu_{K\,min}$	0.22	
d2	82.342	mm
D_{Km}	85	mm
[According to VDI2230]		
short shank, M_A	8873.97	N-m
long shank, M_A	8873.97	N-m
[General tightening torque]		
short shank, M_A	8788.23	N-m
long shank, M_A	8788.23	N-m

4.1.6 3D Modelling of the blade bolts

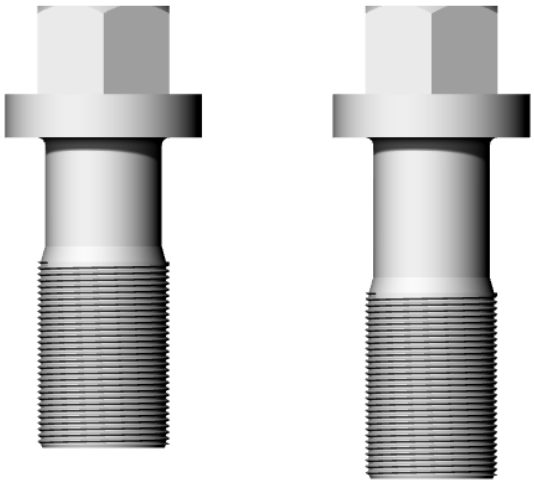

Figure 11. 3D model of blade bolts

4.2 Hub Body and 3D Modeling of the Built-Up Propeller

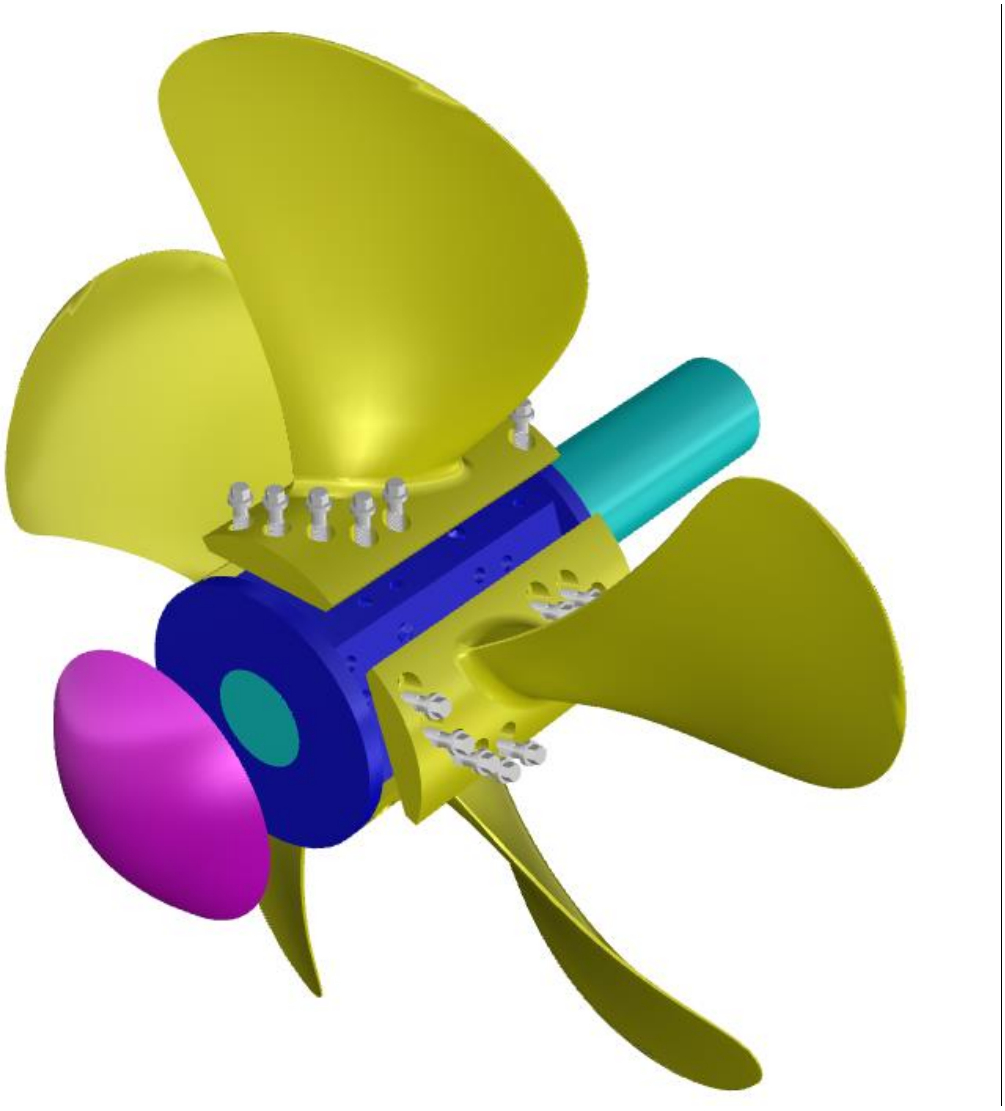

Figure 12. 3D model of built-up propeller assembly

The detailed design drawings of the built-up propeller assembly and components were also attached in the APPENDIX A1.

4.3 Summary for the Preselection of Materials, Strength, Density and Weight of Built-up Propeller Assembly

The preselection of materials, densities and weights of the built-up propeller assembly were tabulated.

Table 18. Materials, strength, densities of propeller components

Description	Material	Tensile strength [MPa]	Yield strength [MPa]	Densities [kg/m^3]
Blade	Ni-Al-bronze (Cu3)	590	270	7640
Hub	Ni-Al-bronze (Cu3)	590	270	7640
Propeller Shaft	Forged steel	590	290	7850
Blade retaining bolts	Martensitic stainless steel	800	640	7850

Table 19. Weight of built-up propeller assembly

Description	Value	Unit
Weight of one short shank bolt	13.43	kg
Weight of one long shank bolt	14.125	kg
Volume of BUP assembly (w/o shaft and end cap)	6.11	m^3
Weight of BUP assembly including bolts (w/o shaft shaft and end cap)	47369	kg

4.4 Strength Calculations

To perform the analytical calculations of the strength of the bolted joint for the built-up propeller, the externally applied loads with different load cases including ice loads according to ice class rules, the centrifugal force of the propeller, ultimate blade failure load and hydrodynamic pressure distribution around the blades were required to predetermine. Since the propeller rotation was 133 rpm and it was just a slow speed, the influence of centrifugal force acting on the joint would be comparatively small. However, it was included in the calculations to be a more realistic situation. The data regarding hydrodynamic pressure around the blades were obtained from the separate CFD analysis (MMG, personal communication) and it was taken into account in the detailed structural analysis by Ansys in the next section.

4.4.1 The Blade Forces or Ice Loads

The maximum blade force acting on the back or suction side of the blade for open propellers was formulated as: **[10]**

$$F_b = 23 . (n . D)^{0.7} . (\frac{EAR}{z})^{0.3} . D . H_{ice}^{1.4} \text{ , when D > D}_{\text{limit}} \quad (16)$$

$$D_{limit} = 0.85 . H_{ice}^{1.4} \quad (17)$$

The maximum blade force acting on the face or pressure side of the blade for open propellers was formulated as: **[10]**

$$F_f = 500 . (\frac{EAR}{z}) . D . \frac{1}{1-d/D} H_{ice} \text{ , when D > D}_{\text{limit}} \quad (18)$$

$$D_{limit} = \frac{2}{1 - d/D} H_{ice} \quad (19)$$

Where

F_b : Maximum backward blade force [kN]

F_f : Maximum forward blade force [kN]

n : nominal rotational speed of propeller at MCR in free running condition [rps]

D : propeller diameter [m]

D_{limit} : Limiting propeller diameter [m]

EAR : Expanded area ration of the propeller

H_{ice} : Design ice block thickness [m] according to Table 5

Thus the calculations of blade forces on propeller for IA Super were tabulated.

Table 20. Calculations of blade forces on propeller

Parameters	Value	Unit
EAR	0.581	
D	6	m
d	1.5	m
n	2.217	rps
z	5	
H_{ice}	1.75	m
Blade back, D_{limit}	1.861	m
F_b	969.1485	kN
Blade face, D_{limit}	4.667	m
F_f	813.4	kN

The different ice load cases according to ice class rules as mentioned in Table 3 were calculated. And the blade failure load from Table 10 was also summarized again.

Table 21. Forces on the blade due to ice loads

Load cases	Values	Unit
LC1	969.15	kN
LC2	484.57	kN
LC3	813.4	kN
LC4	406.7	kN
LC5	581.49	kN
F_{ex}	3926	kN

4.4.2 Centrifugal Force Acting on a Single Blade

The centrifugal force acting on a single blade due to propeller rotation was calculated as:

$$F_c = m \,.\, r \,.\, \omega^2 \tag{20}$$

Where

F_c : Centrifugal force on one blade [N]

m : mass of the blade with flange [kg]

r : perpendicular distance between centroid of blade and axis of propeller rotation [m]

ω : propeller speed [rps]

Table 22. Centrifugal force on a blade

Parameters	Value	Unit
density of blade	7640	kg/m^3
volume of blade with flange	0.5557	m^3
Mass of blade&flange	4245.40	kg
propeller speed	2.217	rps
distance, r	1.174	m
Centrifugal load, F_c	24.496	kN

Because of the lower propeller speed, the centrifugal force was comparatively not significant load.

4.5 Issues of an Optimized Manufacturing / Machining

The components of BUP assembly such as blade with flange, hub, blade bolts and propeller shaft shall be designed and manufactured complying with the manufacturing tolerances (ISO 484) for design flexibilities during the installation and assembly process.

For the shrink fit shaft connection to the propeller, it is necessary to ensure sufficient surface pressure between hub and shaft due to different temperature changes and the effect of thermal expansion of bronze hub and steel shaft.

During the installation of the propeller shaft into the hub, possible issues may arise causing deformation of the bore of the hub which can lead to some minor misalignments of the blade flange and hub. In this scenario, the machining of the blade flange under sufficient facilities to fit into the hub shall be fulfilled.

5. DETAILED DESIGN AND ANALYSIS OF THE JOINT BETWEEN HUB AND BLADE

In this section, the simplified analytical strength calculations of a bolted joint for a concerned single bolt and FE analysis using Ansys workbench for the different load cases were performed.

5.1 Analytical Approach

In principle, the loads acting on the propeller blade could be categorized as:

1. blade forces or ice loads
2. centrifugal load
3. hydrodynamic pressure around blade surfaces
4. ultimate blade failure load (considered as a separate and for design purpose)

To estimate the bolted joint strength, some simplifications and assumptions were made due to the complex geometry of the propeller. The assembly was simplified and considered as a cantilever beam with a fixed end plate joint. For calculations, there were 10 bolts on each blade flange and one single bolted joint was taken. The considered loads were preload on the bolt, blade force or ice loads, centrifugal load and blade failure load which were assumed to be equally distributed on each bolt. The directions of the load applications were according to ice class rules but were considered as simple distribution on the joint to calculate stresses on the bolt appropriately.

Thus the loads on the bolted joint were assumed and treated as:

1. shear force on bolt due to transverse loads on the blade such as blade forces and blade failure load
2. tension on bolt due to centrifugal load on the blade
3. tension on bolt due to transverse loads on the blade such as blade forces and blade failure load

Due to the blade loads, there may be bending moments at the blade. During installation there was no gap between the clamped parts (blade flange and hub) of the joint design. The gap might be possible by a bigger load but for simplification the gap was not considered and the bending moment for the bolt was omitted.

Therefore the stresses acting on the bolt could be summarized as:

1. initial pretension stress on the bolt
2. tensile stress on the bolt due to centrifugal load on the blade
3. tensile stress on the bolt due to transverse loads on the blade
4. shear stress on the bolt due to transverse loads on the blade

For simplification, the stresses on a bolt were estimated at the junction between the blade flange and the hub primarily at the shank. Due to the direction of the external loads and the positions of the bolts on the blade flange, the stress distribution on each bolt would not be the same. However, in these analytical calculations, it was considered the same for the bolt with either a long shank or short shank, and for the bolts at the same side of the force direction or at the opposite side for simplicity.

The pretension stress of the bolt was taken as 60% of the bolt's yield stress and it became 384 MPa. Then the stress in the clamped parts assembly could be regarded as the same in magnitude but it was compressive stress.

There were 10 bolts on a blade flange and the blade centrifugal force was assumed to be equally distributed on each bolt. Then the tensile stress on a bolt was taken as the ratio of one-tenth of centrifugal force to shank cross-sectional area.

For the transverse loads, ice loads and blade failure loads were applied on the pressure side of the blade in some load cases and on the suction side in the other cases. The assumption was made that although the simplified cantilever beam with fixed end by bolted joint, externally applied loads were simply transferred to the bolted joint without losses. So each time when the load was applied, it was assumed that the load was equally distributed only on 5 bolts whereas no load distribution on the other 5 bolts, except for the centrifugal load. So the tensile stress on a bolt was taken as the ratio of one-fifth of transverse load to shank cross-sectional area.

The shear forces due to transverse loads on the blade were assumed to be equally distributed over 10 bolts. Thus the shear stress on a bolt was taken as the ratio of one-tenth of transverse load to shank cross-sectional area.

Since there was no gasket or long spacer between the bolted joint i.e the clamped parts of blade flange and hub, the bending stress at the bolt was assumed negligible.

The different stresses on a bolt shank for different load cases were tabulated below.

Table 23. Stresses on one bolt for different load cases

Stresses	Value	Unit
Pre-tension stress on a bolt	384	N/mm²
Stress at clamped parts assembly	-384	N/mm²
Tensile stress on a bolt due to centrifugal loads on blade	0.554	N/mm²
Tensile stress on a bolt due to ice load case 1	43.874	N/mm²
Tensile stress on a bolt due to ice load case 2	21.937	N/mm²
Tensile stress on a bolt due to ice load case 3	36.823	N/mm²
Tensile stress on a bolt due to ice load case 4	18.412	N/mm²
Tensile stress on a bolt due to ice load case 5	26.324	N/mm²
Tensile stress on a bolt due to F_{ex}	177.73	N/mm²
Shear stress on a bolt due to ice load case 1	21.937	N/mm²
Shear stress on a bolt due to ice load case 2	10.969	N/mm²
Shear stress on a bolt due to ice load case 3	18.412	N/mm²
Shear stress on a bolt due to ice load case 4	9.206	N/mm²
Shear stress on a bolt due to ice load case 5	13.162	N/mm²
Shear stress on a bolt due to F_{ex}	88.866	N/mm²

Therefore the equivalent von Mises Stresses acting on the bolt was calculated using the following Eq. 21. Available from: **[20]**

$$\sigma_{VM} = \sqrt{[\sigma_{PL} + n(\sigma_t + \sigma_{bnd})]^2 + 3(n\,.\,\tau_{sh})^2} \tag{21}$$

Where

σ_{VM} : Equivalent von Mises stress [N/mm²]

σ_{PL} : pretension stress of the bolt [N/mm²]

n : load factor

σ_t : tensile stress [N/mm²]

σ_{bnd} : bending stress [N/mm²], it is omitted since there is no gap between clamped parts

τ_{sh} : shear stress [N/mm²]

As per Eq. 21, to calculate the von Mises stress, it was necessary to identify the value of the load factor. The load factor was important in determining equivalent stress on the bolted joint not to be beyond the yield strength. It was applied only at the stresses due to external loads and not at the pretension stress.

The total loads acting on the bolt could be defined as the combination of initial preload and some fraction of the externally applied loads which were contributed to the bolt. **[21]**

It could be expressed as:

$$F_{tot} = F_{PL} + n \,.\, F_{ext} \tag{22}$$

Then the load factor became:

$$n = \frac{F_{tot} - F_{PL}}{F_{ext}} \tag{23}$$

Where

n : load factor

F_{tot} : total load on one bolt [kN]

F_{PL} : preload on the bolt [kN]

F_{ext} : external loads acting on the bolt [kN]

The total loads on one bolt were assumed and considered as preload, one-tenth of centrifugal load, and one-fifth of blade failure load for the purpose of the design case. The external loads acting on the bolted joint were taken as centrifugal load and blade failure load.

The results of von Mises stresses for different load cases were tabulated.

Table 24. Von Mises stresses for a bolt at different load cases

Von Mises stress for different load cases	Value	Unit
Load factor, *n*	0.1994	
LC1	392.93	N/mm²
LC2	388.50	N/mm²
LC3	391.50	N/mm²
LC4	387.79	N/mm²
LC5	389.39	N/mm²
Fex	420.67	N/mm²

After getting equivalent stress on the bolt and considering the linear elastic behaviour of the material, Hook's law was applied to find the total deformation on the bolt shank due to those stresses.

$$\sigma = E \, . \, \varepsilon \tag{24}$$

where

σ : equivalent stress on the bolt

E : elastic or Young's modulus

ε : strain on the bolt

And the strain had the following relation:

$$\varepsilon = \frac{\Delta L}{L} \tag{25}$$

where

ΔL : deformation

L : length of the bolt shank

According to VDI2230 part 2, in order to reflect more realistic results, elastic resiliences for the bolt and clamped parts should be considered. It was also observed that those values were very small and had less influence on total deformation. The results of strain and deformation of the bolt were tabulated.

Table 25. Total strain on a bolt

Parameters	Value	Unit
Young's modulus of propeller , *E*	125000	MPa
Young's modulus of bolt , *E*	215000	MPa
Strain at *LC1*	0.00183	
Strain at *LC2*	0.00181	
Strain at *LC3*	0.00182	
Strain at *LC4*	0.00180	
Strain at *LC5*	0.00181	
Strain at F_{ex}	0.00196	

Table 26. Total deformation on a bolt's shank

Parameters	Value	Unit
Deformation on long shank bolt at LC1	0.1645	mm
Deformation on long shank bolt at LC2	0.1626	mm
Deformation on long shank bolt at LC3	0.1639	mm
Deformation on long shank bolt at LC4	0.1623	mm
Deformation on long shank bolt at LC5	0.1630	mm
Deformation on long shank bolt at F_{ex}	0.1761	mm
Deformation on short shank bolt at LC1	0.1279	mm
Deformation on short shank bolt at LC2	0.1265	mm
Deformation on short shank bolt at LC3	0.1275	mm

Deformation on short shank bolt at LC4	0.1263	mm
Deformation on short shank bolt at LC5	0.1268	mm
Deformation on short shank bolt at F_{ex}	0.1370	mm

Then the compressive stresses at the bearing area under the bolt flange due to centrifugal and transverse loads on the blade were calculated by the ratio of respective loads over the bearing area of the bolt head flange bottom side. The bearing area was calculated as:

$$A_{be} = \frac{\pi}{4}(d_o^2 - d_h^2) \tag{26}$$

A_{be} : bearing area under bolt head flange

d_o : diameter of bolt head flange

d_h : hole diameter of a bolt

The results of compressive stress under bolt head flange at different load cases were tabulated.

Table 27. Compressive stresses at bolt head flange bearing area

Description	Value	Unit
bearing area	804.25	mm²
Stress at bolt bearing area for LC1	-244.05	N/mm²
Stress at bolt bearing area for LC2	-123.55	N/mm²
Stress at bolt bearing area for LC3	-205.32	N/mm²
Stress at bolt bearing area for LC4	-104.18	N/mm²
Stress at bolt bearing area for LC5	-147.65	N/mm²
Stress at bolt bearing area for F_{ex}	-979.36	N/mm²

Considering the geometry of the outer threaded part of the bolt was simplified as the cylindrical part and the total thread shear stresses at that threaded area due to preload, transverse and centrifugal loads were estimated by the ratio of respective loads over a cylindrical surface area of the threaded part. Similarly, the inner threaded part of the hub to fit the bolt was also simplified as the cylindrical part and the thread shear stresses were accordingly predicted.

Surface areas of the outer threaded part of the bolt and inner threaded part of the hub were expressed as: **[20]**

$$A_{bt} = \frac{5}{8}\pi d_p L_e \quad (27)$$

$$A_{ht} = \frac{3}{4}\pi d_p L_e \quad (28)$$

Where

d_p : pitch diameter of a bolt

L_e : engagement length of threaded part

The thread shear stresses at the external and internal threaded parts of the bolt and the hub were respectively tabulated.

Table 28. Thread shear stresses at bolt external threaded area

Description	Value	Unit
Tensile shear stress at *LC1*	36.78	N/mm²
Tensile shear stress at *LC2*	31.79	N/mm²
Tensile shear stress at *LC3*	35.18	N/mm²
Tensile shear stress at *LC4*	30.98	N/mm²
Tensile shear stress at *LC5*	32.78	N/mm²
Tensile shear stress at F_{ex}	67.26	N/mm²

Table 29. Thread shear stresses at internal threaded area of hub

Description	Value	Unit
Tensile shear stress at *LC1*	30.65	N/mm²
Tensile shear stress at *LC2*	26.49	N/mm²
Tensile shear stress at *LC3*	29.31	N/mm²
Tensile shear stress at *LC4*	25.82	N/mm²
Tensile shear stress at *LC5*	27.32	N/mm²
Tensile shear stress at F_{ex}	56.05	N/mm²

5.2 FE Simulation

In order to perform the detailed analysis for the bolted joint of the built-up propeller, the FEA was applied using the Ansys workbench. Some steps were prepared in advance before doing FEM. These include:

1. Defining and simplifying FE models
2. Input for Material specifications
3. Contact definitions of the components in the FE model
4. Constraint and boundary conditions
5. Load case definitions and direction of load applications
6. Mesh study including element types and sizes for global and specific components on the model
7. Analysis
8. Submodeling for refined mesh at specific and focusing part to get detailed results with efficient computational efforts

5.2.1 Simplification of FE Models

To be able to save computational efforts in the FEA, the whole geometry of the built-up propeller was not taken for the FE model. Initially, one single blade with a blade flange model was used for the global mesh study. The size of the bolt was much smaller compared to the propeller and hub then it was required to have fine mesh at the bolts than the blade and hub. A single short shank bolt was taken generally and modelled for mesh study of the bolts. As the propeller had 5 blades and there were 10 bolts for the blade-hub joint, 1 blade with 10 bolts, and half part of the hub were considered for the FE model. Due to the fact that the threaded portions of some bolts would be out of the geometry if one-fifth of the hub part was taken for the FE model. Additionally in this model, the threaded parts of the bolts were simplified as without threads according to the class 3 model of VDI2230 part 2. The class 4 model is a detailed model (which was not included in the analysis of this study) with threads at the bolts and other parts as a complete FE model which can provide more realistic and detailed results through analysis but the drawback is that it takes significantly high computation time for analysis due to very detailed thread geometries included in the modelling and it also takes

huge time of preparation e.g defining contact surfaces for the components in the model, meshes generation, etc.

For different simulations starting from mesh study to class 3 model, the layout summary of FE models was tabulated.

Table 30. FE model scheme

S/N	FE Model	Analysis	Loading	Boundary condition	Remark
1	Blade with flange	static, structural	blade force LC1	blade flange bottom fixed	global mesh study
2	Short shank bolt	static, structural	preload	threaded part surface is fixed, frictional support at head bearing surface	bolt mesh study
3	Class 3 model with blade and flange, bolts, part of hub	static, structural	preload, blade forces, centrifugal load, Fex	inner bore of hub is fixed as it is shrink fit shaft connection	bolted joint analysis

5.2.2 Input for Material Specifications

As for the input of material properties and specifications to the Ansys analysis, there were two types of materials predefined as nickel aluminium bronze (Cu3) for the blade and hub and martensitic stainless steel for the blade bolts. The specifications for Cu3 and martensitic steel were created in Ansys as shown in Table 31.

Table 31. Material specifications input to Ansys

Description	Ni-Al-bronze (Cu3)	Martensitic stainless steel
Density [kg/m^3]	7640	7850
Ultimate tensile strength [MPa]	590	800
Yield strength [MPa]	270	640
Young's modulus [GPa]	125	215
Poisson ratio	0.33	0.3

5.2.3 Contact Definitions of the Components in FE Model

When performing the analysis of the class 3 model consisting of blade, hub and bolts, there were contacts between the components and these should be defined appropriately and

manually to be realistic in the analysis. In Ansys, there are a couple of different types of contacts and in general, these can be summarized as in Table 32.

Table 32. Contact definitions of Ansys

Type of contact	Separation of target and contact components	Sliding of target and contact components
Bonded	Separation not possible	No sliding
Frictionless	Separation possible	Sliding without resistance
Frictional	Separation possible	Sliding with resistance
No separation	Separation not possible	Sliding without resistance
Rough	Separation possible	Sliding with much higher resistance or cannot slide

For the analysis of the class 3 FE model, the contacts between blade flange and hub were defined as frictional contact as these parts are joined by the bolts. The contacts between bolt threaded surface and hub threaded parts were defined as bonded contact without allowing separation and sliding to be realistic analysed. The contacts between bolt head flange's bearing surface and blade flange were defined as frictional contact.

5.2.4 Constraint and Boundary Conditions

During the analysis of the FE model of the blade with flange, the supports were fixed at the bottom of the blade flange considering the blade would be fixed at the hub, and also at the shell plane which was used to define the direction of the blade force.

For the analysis of the bolt model, the supports were fixed at the threaded surface and bolt head bearing area under the head flange.

In the analysis of the class 3 model with blade, hub and bolts, the supports were fixed at the inner bore of the hub's surface considering the hub would be fixed at the shaft, and also at the shell plane.

5.2.5 Load Case Definitions and Direction of Load Applications

In the analysis of the class 3 model, 5 load cases of ice loads, a centrifugal load of the blade, preload at the bolts, hydrodynamic pressure around the blade sides, and blade failure load were applied on a case by case basis.

The directions of resultant ice loads were defined perpendicular to the 0.7R chord line according to Finnish-Swedish ice class rules in which a shell plane was projected from that chord profile and created out of the geometry.

The direction of the resultant blade failure load was defined at the 0.8R chord line and the position was 75% of the distance from the leading edge. In this study, it was applied at the pressure side of the blade.

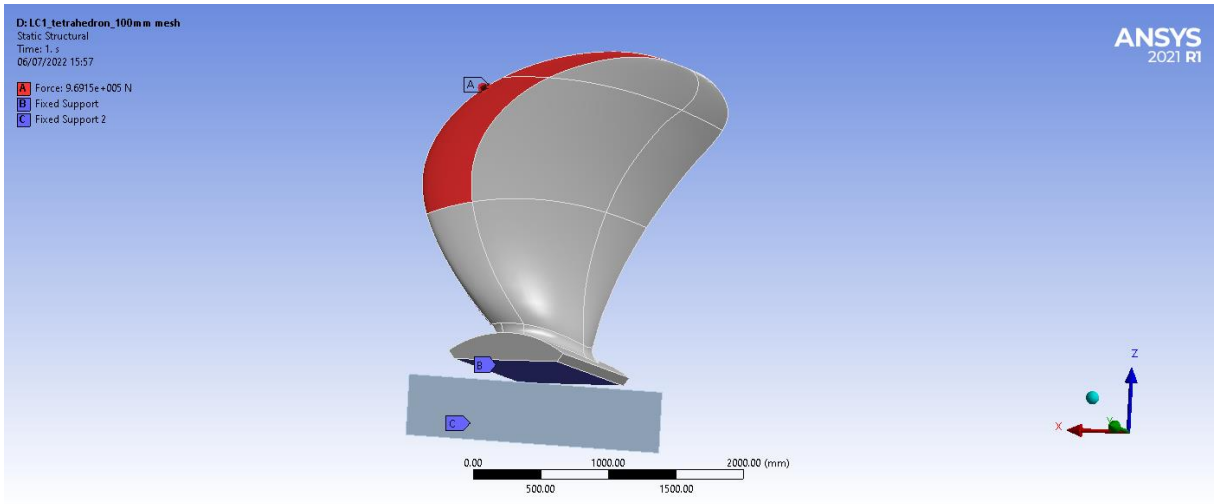

Figure 13. Direction and application of load case 1, and fixed supports on blade model in Ansys

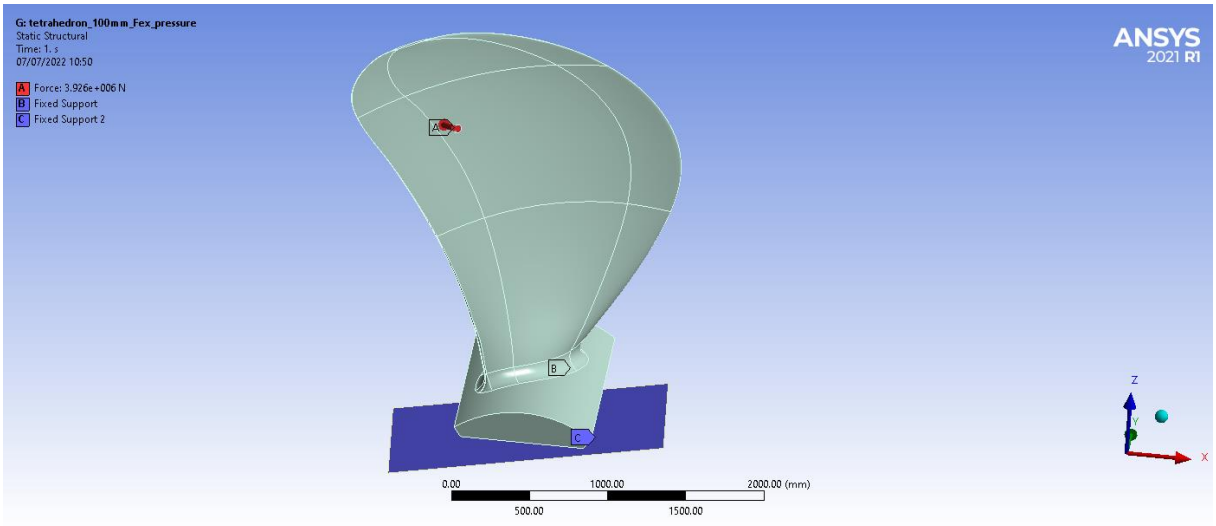

Figure 14. Direction and application of blade failure load, and fixed supports on blade model in Ansys

5.2.6 Mesh Studies

The mesh studies were performed for propeller, hub and blade bolts.

5.2.6.1 Mesh Studies for Propeller and Hub

Global mesh study for propeller and hub was preliminarily prepared with a blade with flange model. Different mesh sizes and mesh types were applied. For the coordinate system, the global coordinate was set as the same origin i.e at the shaft or hub centre against the blade profile centre when the 3D modelling was first developed. Only load case 1 of blade force was used as loading in this mesh study considering it has a higher value than other ice loads. Since the resultant blade force direction is perpendicular to the 0.7R chord line, a shell plane was projected from the 0.7R chord profile section and placed out of the geometry. This shell was then a fixed constraint not to influence the results during analysis. Element sizes starting from 500 mm to 20 mm sizes have been studied. For different mesh types, the suitable element types of the tetrahedron, hexahedron dominant with quads and tri elements, and hexahedron with all quad elements were studied particularly. However, due to the abrupt changes in the geometry of the blade flange, both hexahedron elements were not compatible for this FE model and meshes could not be generated until 18 mm in size. Only tetrahedron mesh was flexible for the model at every element size studied. Thus tetrahedron mesh with

quadratic element order or behaviour was selected in the analysis. The summary of the mesh study for tetrahedron elements was tabulated and plotted in the graphs.

Table 33. Global mesh study for a blade with flange

FE Model	BC	Method/Elem order	Elem size (mm)	Max. von Mises stress (MPa)	% diff.	Max. total deformation (mm)	% diff.	Solution time (s)
blade with flange	fixed at blade flange base and shell plane	Tetrahedrons/ quadratic	500	232.68	-	36.98	-	3
			450	229.18	1.5	37.46	1.32	3
			400	259.87	13.39.0	40.09	7.02	3
			350	252.85	2.7	41.76	4.15	3
			300	256.7	1.5	41.95	0.46	4
			250	245.6	4.3	42.77	1.94	4
			200	258.65	5.3	43.38	1.44	4
			150	257.1	0.6	43.66	0.63	4
			100	259.18	0.8	43.90	0.56	4
			50	276.81	6.8	44.10	0.46	14
			20	304.32	9.9	44.24	0.31	1797

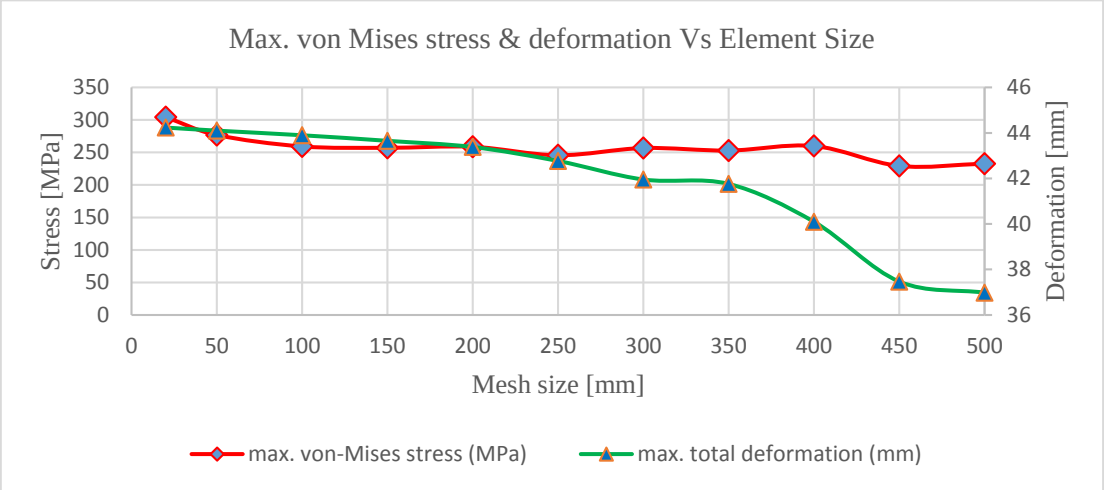

Figure 15. Maximum von Mises stresses and deformations at different element sizes (global mesh)

From the mesh studies, it could be noticed that the maximum deformations at different element sizes had very small variations and it was getting converged from 200 mm until 20 mm mesh. From element sizes 150 to 100 mm, it only had a 0.56% difference and from 100 to 50 mm, only a 0.46% difference. For maximum von Mises stresses, the values were fluctuating at the beginning of coarse meshes and getting converged from 200mm to 100 mm

meshes, then gradually increasing again at the smaller meshes. From element sizes from 150 to 100 mm, it only had a 0.81% difference and from 100 to 50 mm, it had a 6.8% difference. However, the computational time was increased when refining to 50mm just for the blade geometry and even much higher effort when going to 20mm size. Only the bolted joint is the concerning part in the analysis and a mesh size of 100 mm was taken for global mesh sizing.

The result figures of maximum von Mises stresses and total deformation from Ansys analysis were as follows.

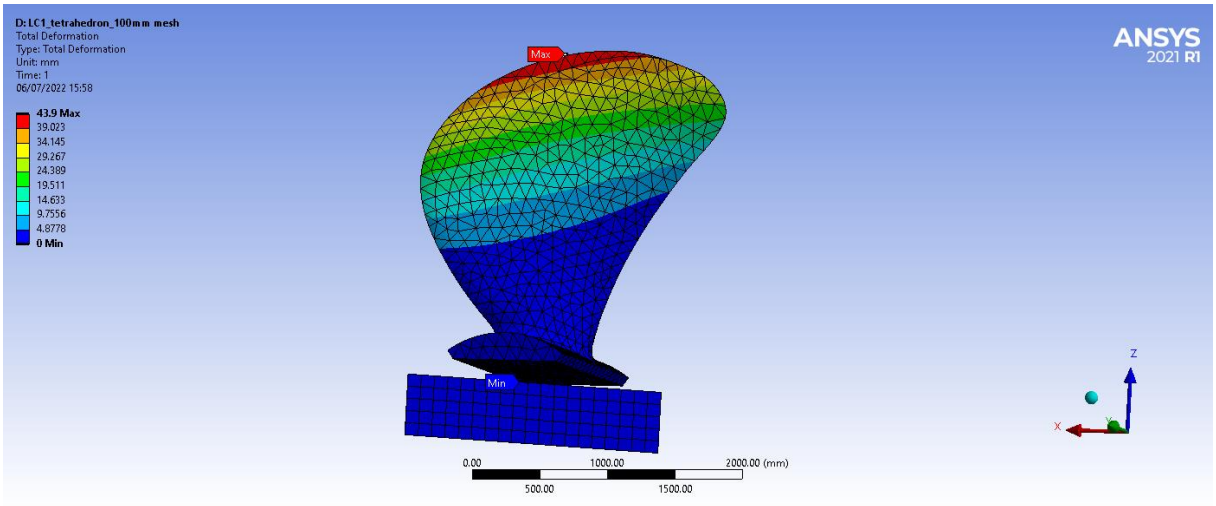

Figure 16. Maximum total deformation of a blade at LC1 for 100 mm mesh

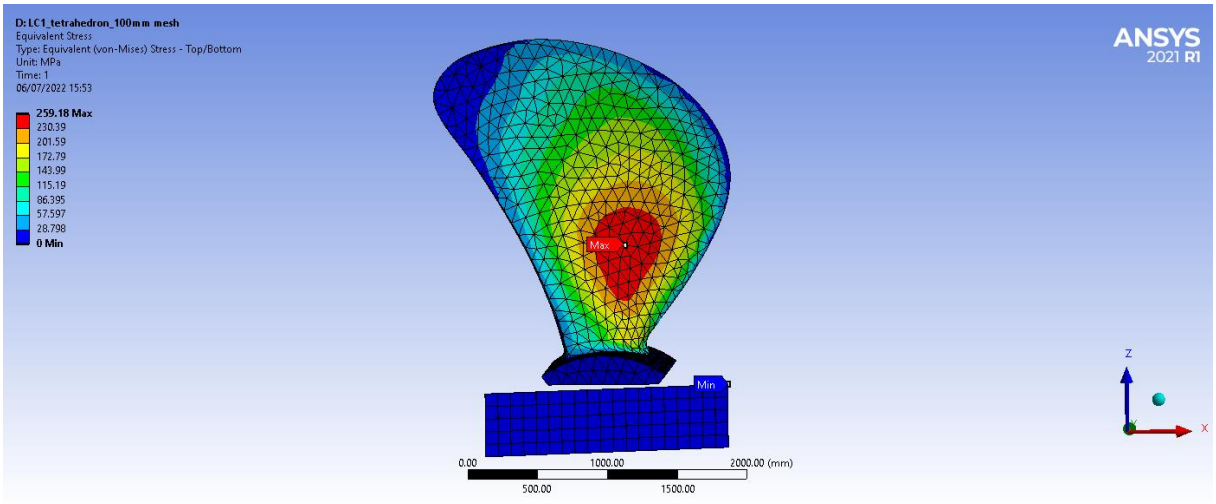

Figure 17. Maximum von Mises stress of a blade at LC1 for 100 mm mesh

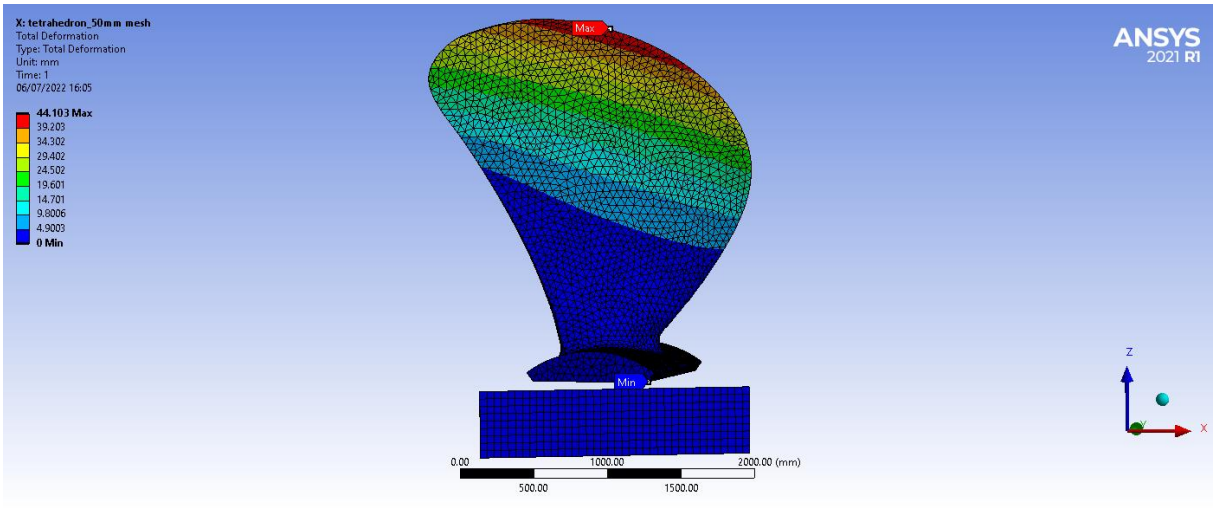

Figure 18. Maximum total deformation of a blade at LC1 for 50 mm mesh

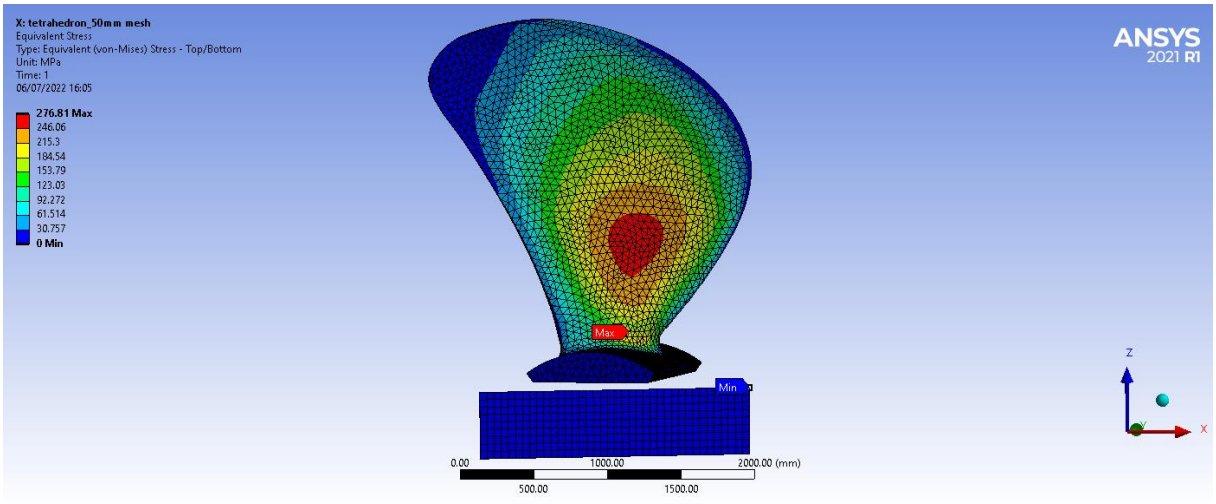

Figure 19. Maximum von Mises stress of a blade at LC1 for 50 mm mesh

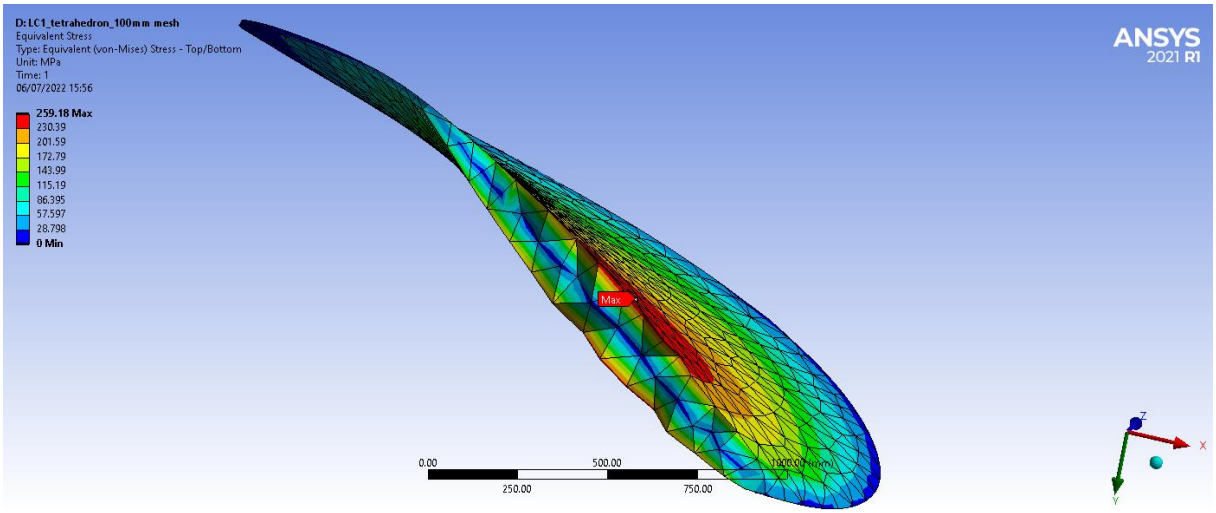

Figure 20. The cut profile of the blade at LC1 for 100 mm mesh with maximum von Mises stress

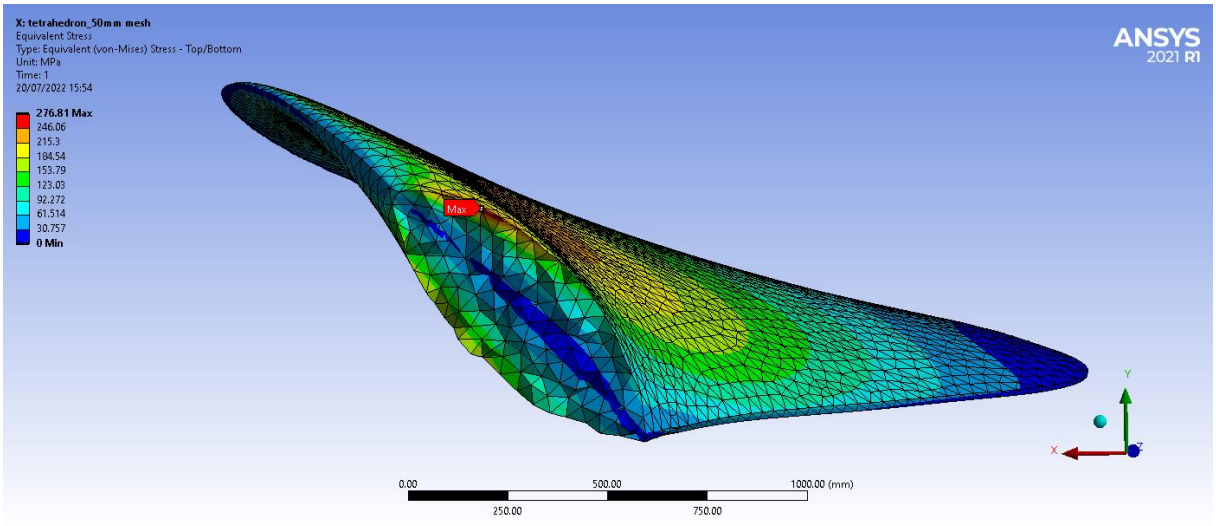

Figure 21. The cut profile of the blade at LC1 for 50 mm mesh with maximum von Mises stress

From the two blade profile cuts of 100 mm and 50 mm meshes, the maximum stress concentration at 50 mm mesh was slightly higher than the yield strength of the blade material. At the cut of 100 mm mesh, there were two elements. At 50 mm mesh, there were six elements and stress concentration was near the blade root. This increase in element numbers might cause an increase in stress concentration as in Figure 21. However, in this study, only the bolted joint is the main focus and the 100 mm element size was considered to be sufficient for the global mesh of the FE model to save computation effort.

The stress distribution and deformation of a blade profile were as per the following figures when blade failure load was applied.

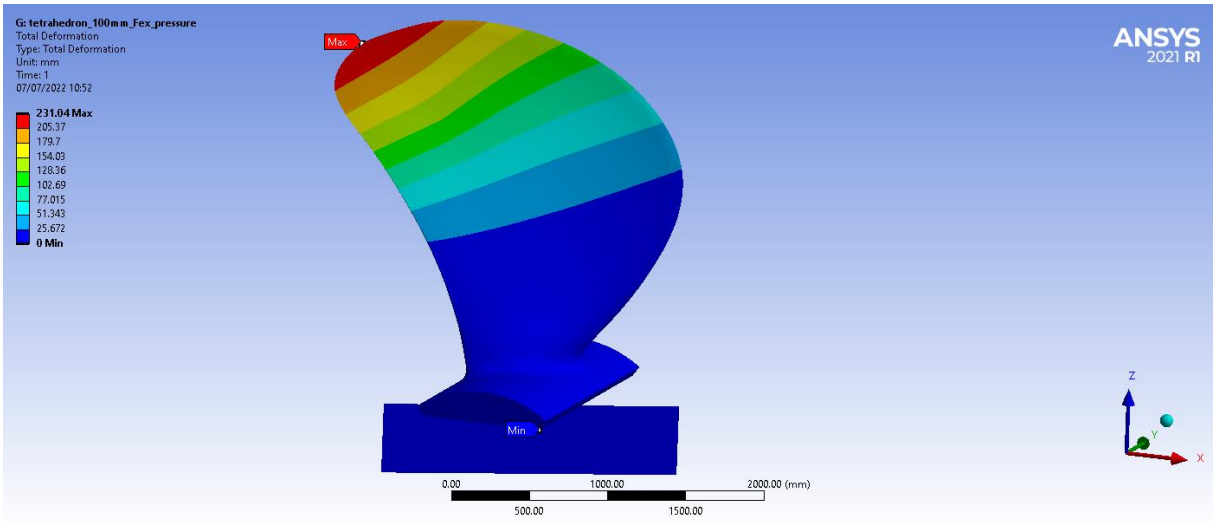

Figure 22. Maximum total deformation of a blade due to blade failure load

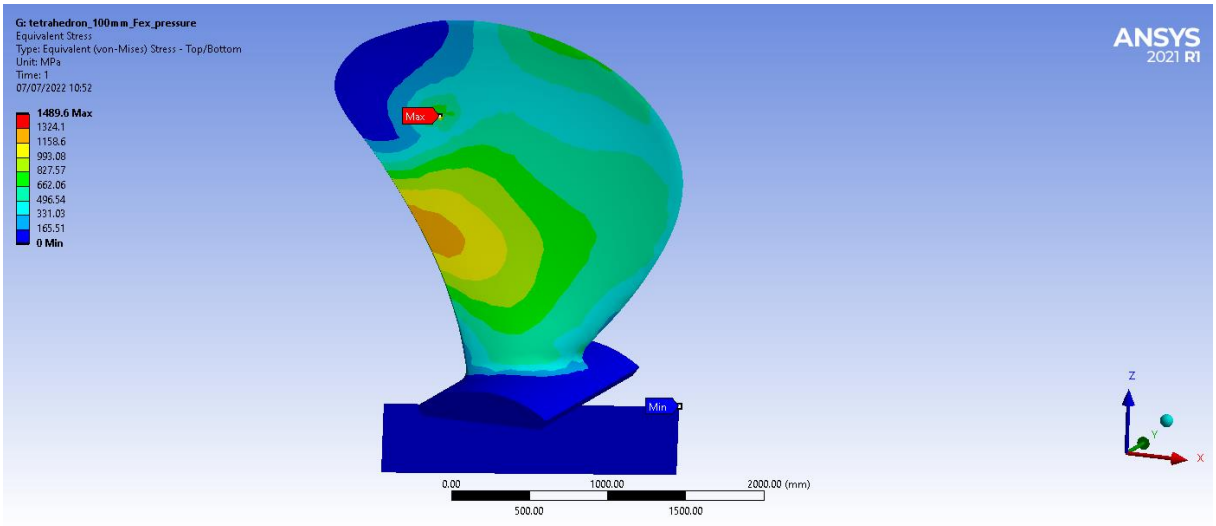

Figure 23. Maximum von Mises stress of a blade at pressure side due to blade failure load

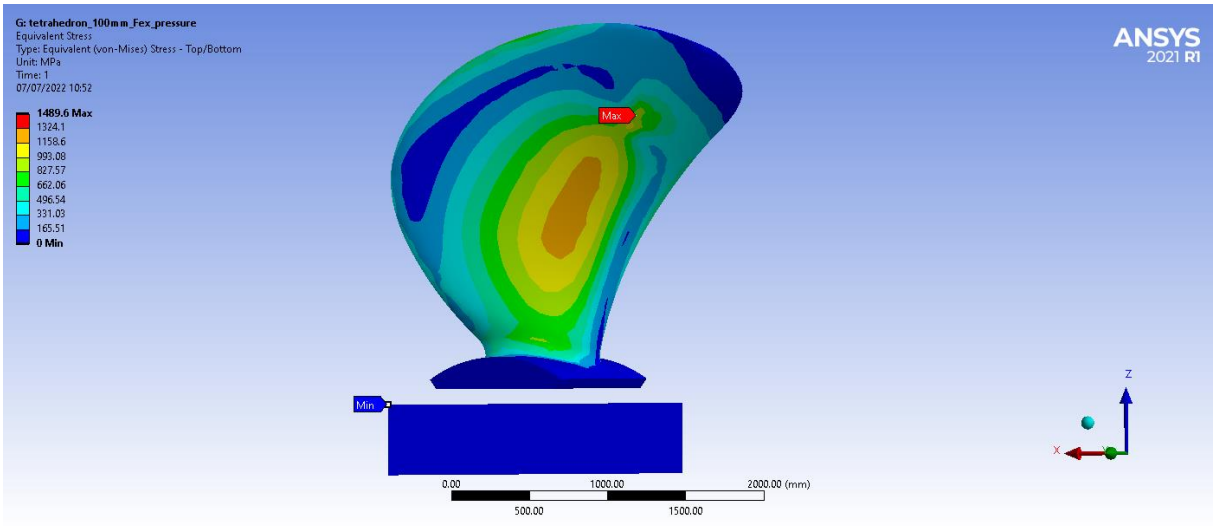

Figure 24. Maximum von Mises stress of a blade at suction side due to blade failure load

5.2.6.2 Mesh Study for Blade Bolts

The mesh study for the bolt was prepared with a short shank bolt model. Different mesh sizes and mesh types were applied. Only bolt preload was used as loading in this mesh study. Regarding to the element size of the bolt it was started with an applicable size with respect to the bolt dimension and geometry. Element sizes above 100 mm were too big and thus those starting from 100 mm to 5 mm sizes have been studied.

For different mesh types, tetrahedron, hexahedron dominant with quads and tri elements, and hexahedron with all quad elements were studied. However, both hexahedron elements were not compatible with coarse mesh for this bolt model. Hexahedron mesh should normally be possible but it was dependent on the geometry of the bolt. The element size must also reproduce the detailed geometry, otherwise it may not be feasible element type. Thus tetrahedron mesh was flexible for the bolt model at every element size studied. Tetrahedron mesh with quadratic element order was selected in the analysis. The summary of the mesh study for tetrahedron elements was tabulated and plotted in the graphs.

Table 34. Mesh study for blade bolt

FE Model	BC	Method/ Elem order	Elem size (mm)	Max. von Mises stress (MPa)	% diff.	Max. total deformation (mm)	% diff.	Solution time (s)
Bolt	fixed at thread and head flange	Tetrahedrons /quadratic	100	281.56	0	0.046	0	3
			50	269.42	4.3	0.041	12.48	3
			30	279.5	3.7	0.042	3.62	4
			15	243.91	12.7	0.038	8.92	5
			10	268.08	9.9	0.041	6.76	8
			5	297.87	11.1	0.043	5.3	96

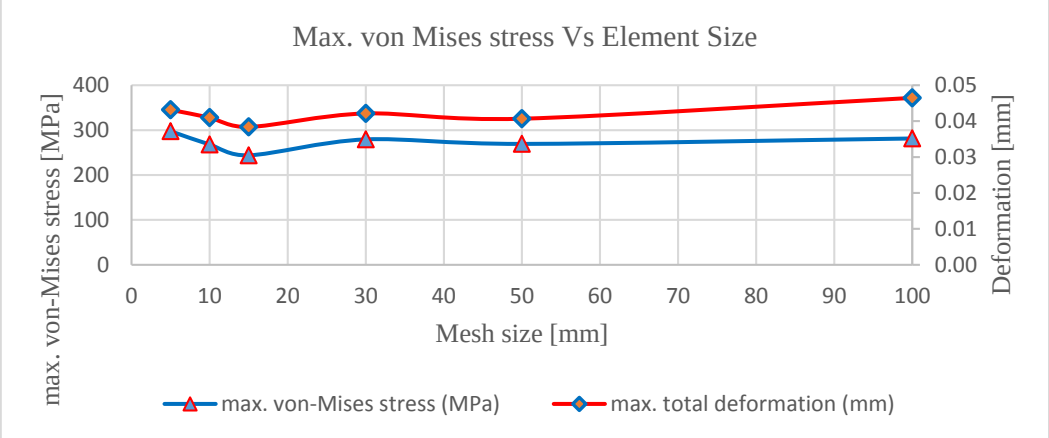

Figure 25. Maximum von Mises stresses and deformations at different element sizes (bolt mesh)

From the bolt mesh studies, it could be noticed that the maximum deformations at different element sizes had almost the same values. From element sizes 30 to 15 mm, it only had an 8.92% difference and from 15 to 10 mm, only a 6.76% difference. For maximum von Mises stresses, the values were converging at the beginning of coarse meshes and getting a bit

fluctuating from 50 mm until 5 mm meshes. From element sizes from 30 to 15 mm, it had a 12.73% difference, from 15 to 10 mm, it had a 9.91% difference, and from 10 to 5 mm, it had an 11.11% difference. However, the computational time was increased when refining to 10mm just for the bolt geometry and even much higher effort when going to 5 mm size. If the very refined mesh was used in the global model, it would be of much higher computation effort. Thus the mesh size of 15 mm for the bolt was taken in the preliminary analysis. For the critical stress concentrated part of the bolted joint, the sub-modelling techniques were prepared to get the detailed results in the last part of the analysis section.

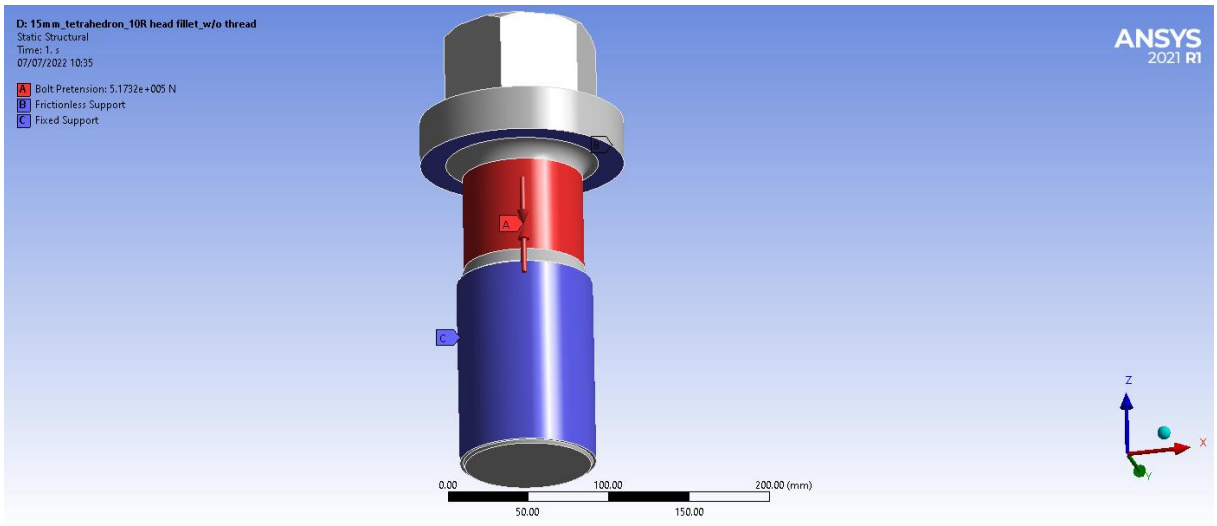

Figure 26. Application of preload and fixed supports on bolt model in Ansys

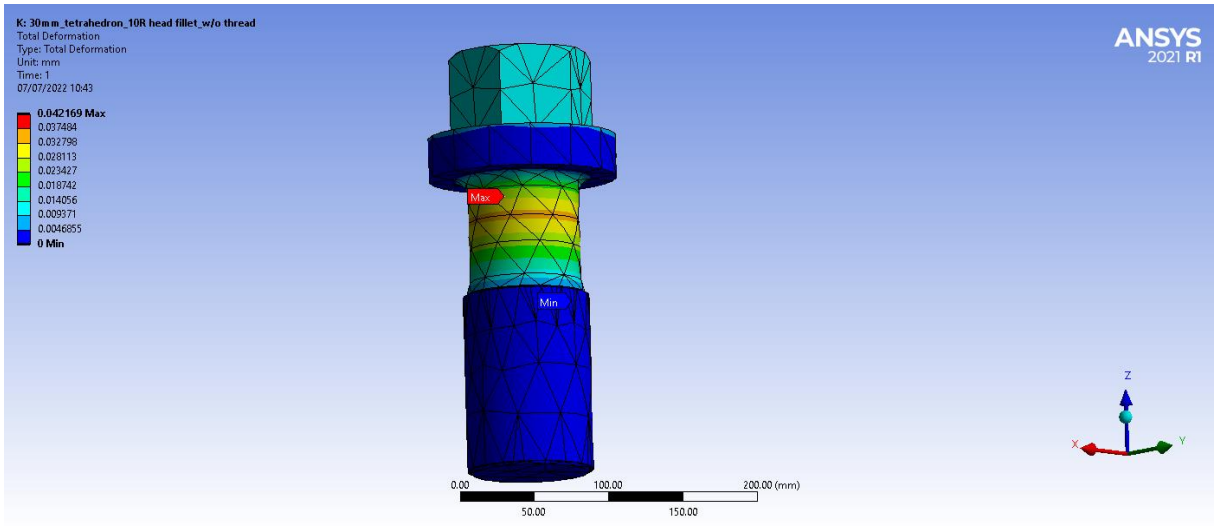

Figure 27. Maximum total deformation of a bolt at preload for 30 mm mesh

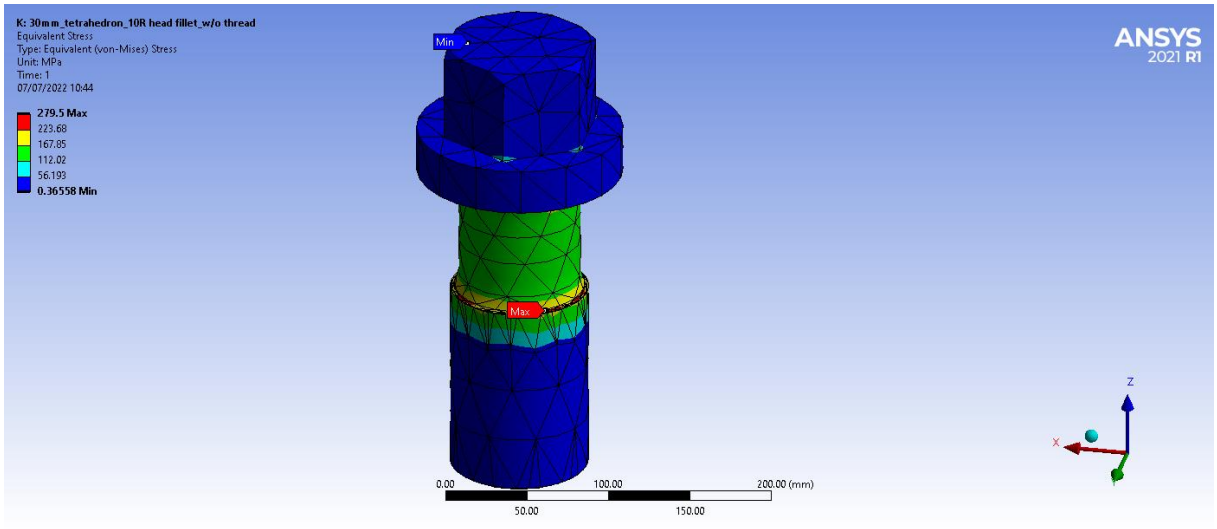

Figure 28. Maximum von Mises stress of a bolt at preload for 30 mm mesh

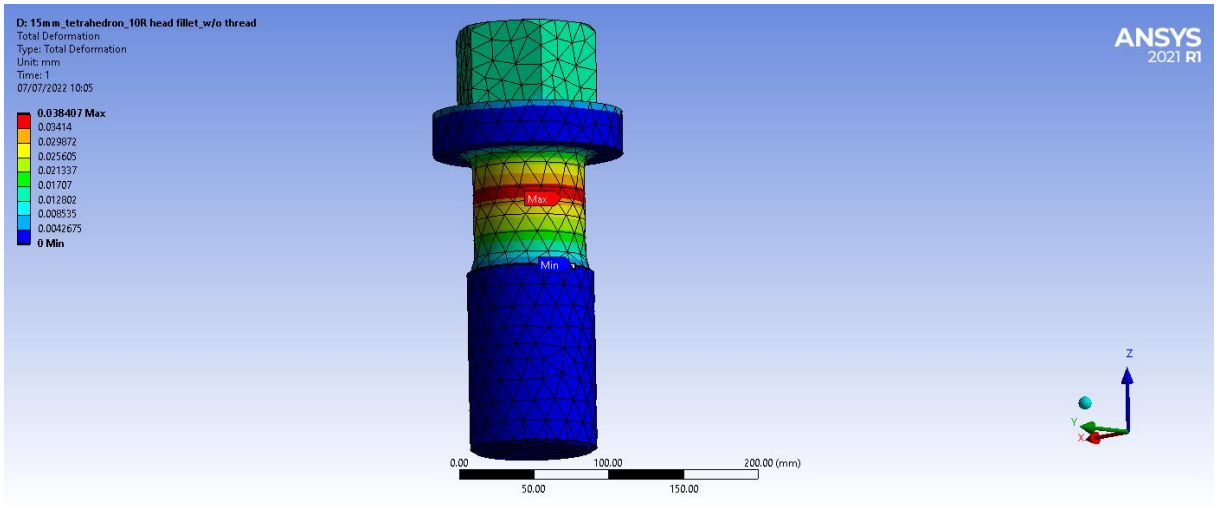

Figure 29. Maximum total deformation of a bolt at preload for 15 mm mesh

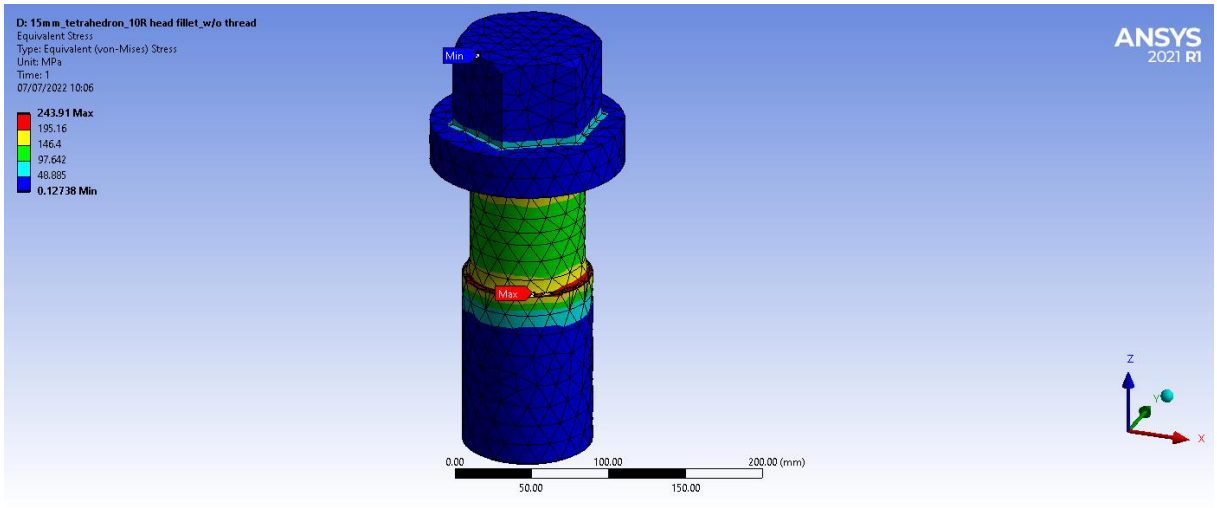

Figure 30. Maximum von Mises stress of a bolt at preload for 15 mm mesh

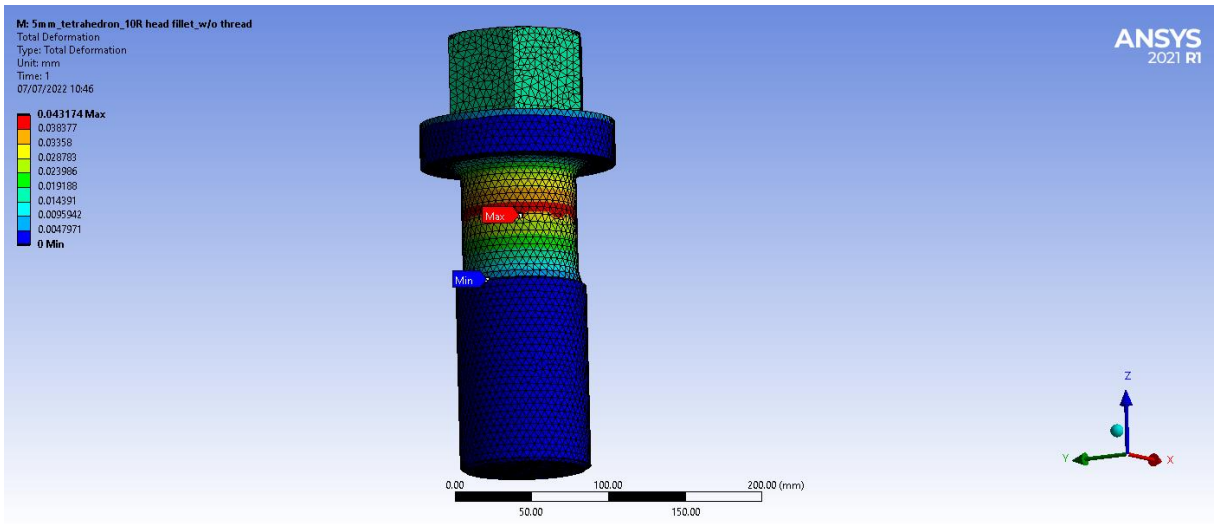

Figure 31. Maximum total deformation of a bolt at preload for 5 mm mesh

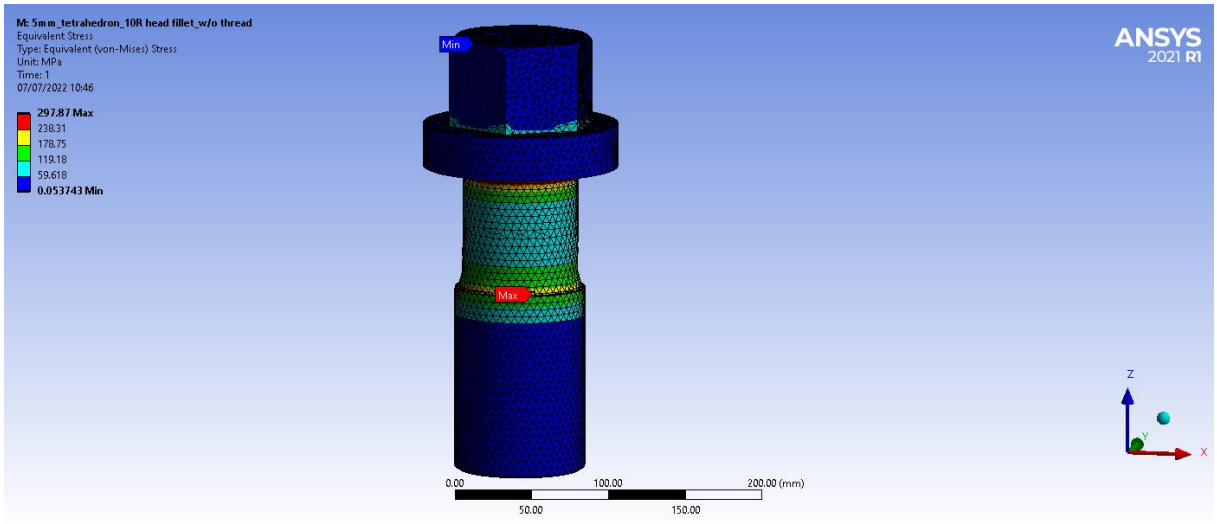

Figure 32. Maximum von Mises stress of a bolt at preload for 5 mm mesh

5.2.7 Analysis of Model Class 3 at Different Load Cases

The element size, type and order were selected after mesh studies. The global mesh size of 100 mm was set. Tetrahedron elements with 100 mm size and quadratic order were set for the blade with flange and hub. For the bolts tetrahedron elements with 15 mm size and quadratic order were set.

5.2.7.1 Analysis of Model Class 3 with Load Case 1

For the bolted joint, initially, the bolts having R5 fillet at the head flange and shank connection were included in the model and analyzed. The results were compared with the bolts having R10 fillets in the next analysis. It could be noticed that the maximum von Mises stress concentration at the bolt was reduced at the R10 fillet bolt.

In this analysis, FE model class 3 including two pins, fitted in between blade flange and hub, was used and the loadings of ice load case 1, preload on bolts and centrifugal blade force were applied. For boundary conditions, fixed supports at the inner bore of the hub and shell plane for blade force direction were used. For meshing, a global element size of 100 mm for blade and hub and 15 mm for bolts were used. For the load steps, 2 steps were defined as step 1 with only preloads on bolts and step 2 with complete loadings during analysis. The bolt preloads were defined as loading in step 1 and locking in step 2. Locking was after the final

tightening of the bolts by a torque wrench, they were locked having the same preloads to avoid loosening. The contacts between blade flange and hub, and also bolt head flange bearing area with blade flange were set as frictional contacts. The contacts between bolt threaded parts with hub were set as bonded contacts. The analysis results were investigated as per the following figures.

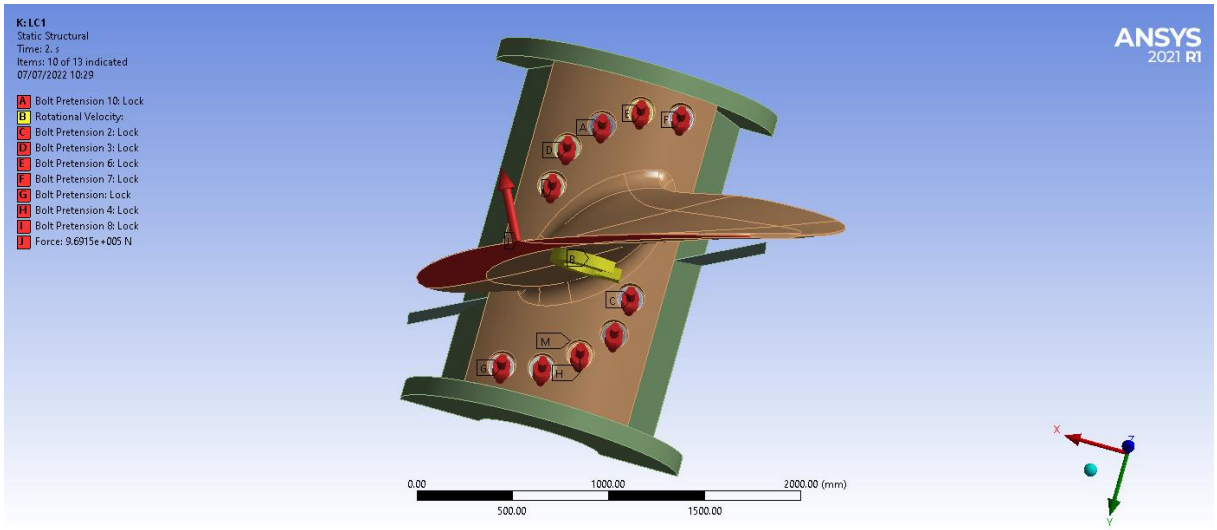

Figure 33. Application of loadings and fixed supports for load case 1 of class 3 model

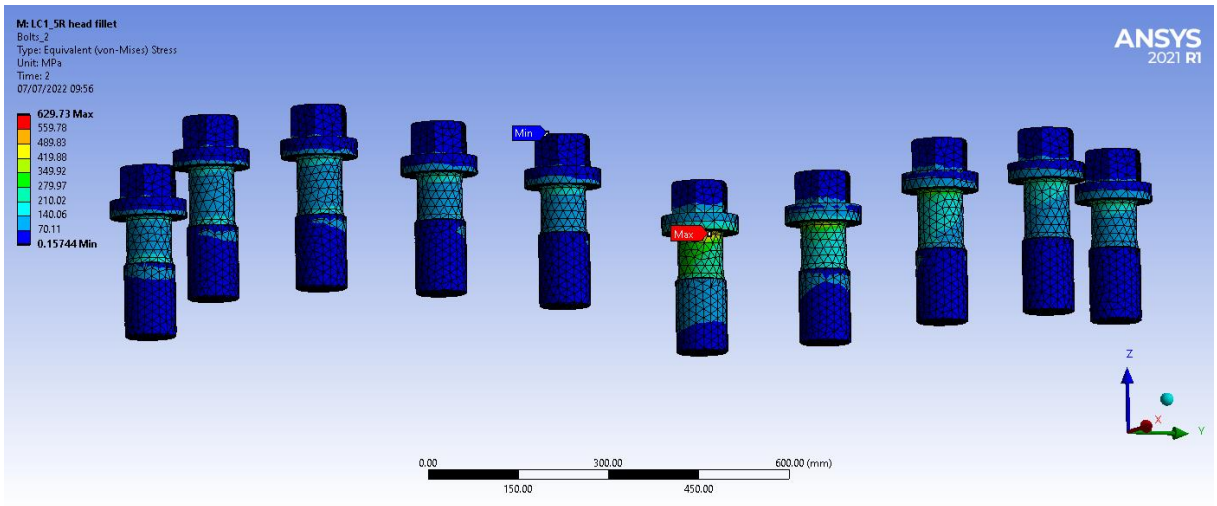

Figure 34. Maximum von Mises stress in load case 1 with R5 fillet bolts

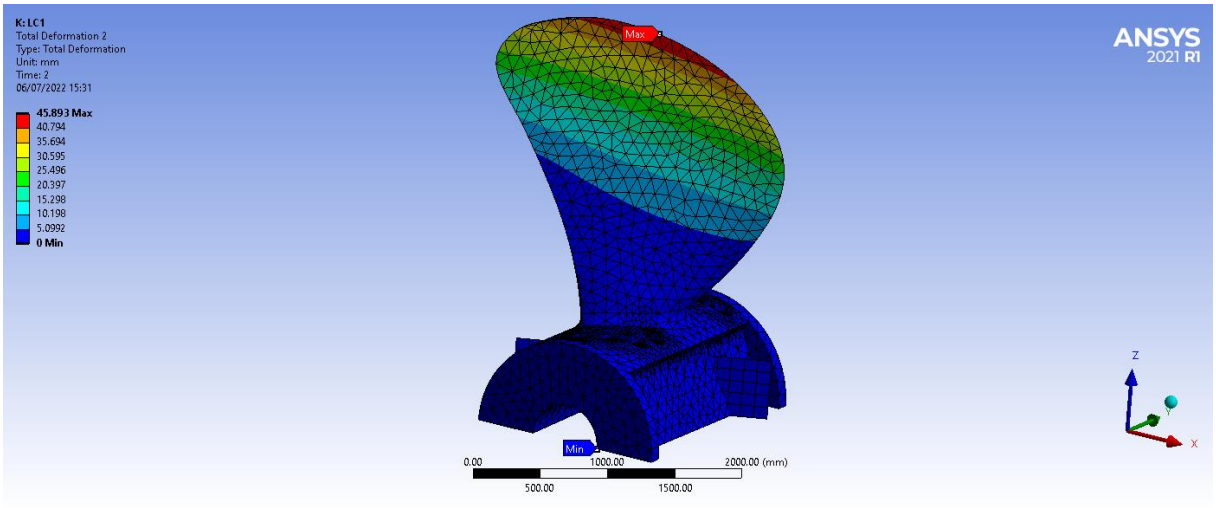

Figure 35. Maximum total deformation in load case 1 with R10 fillet bolts

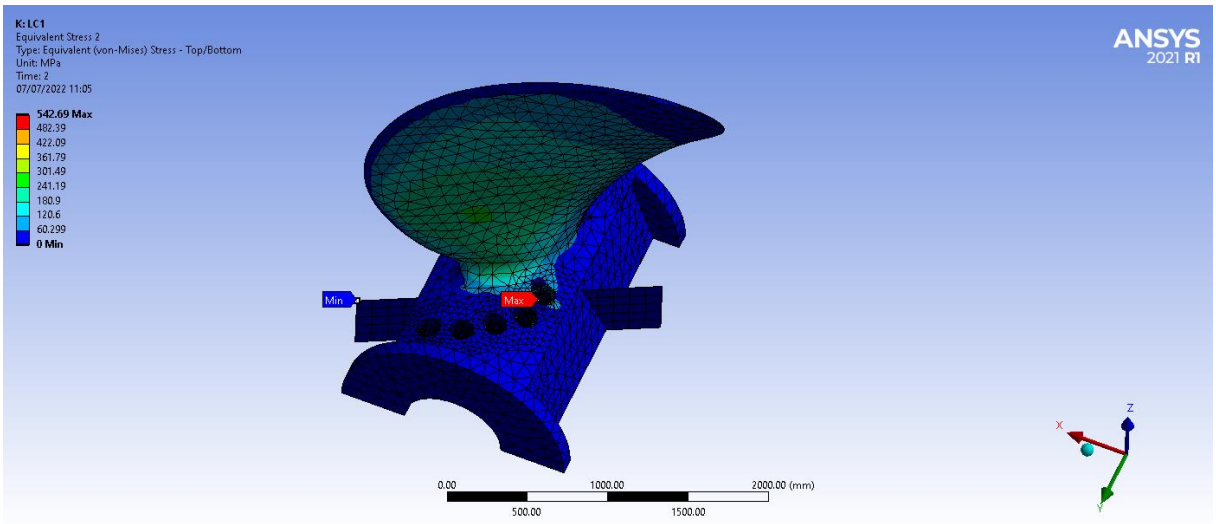

Figure 36. Maximum von Mises stress in load case 1 with R10 fillet bolts

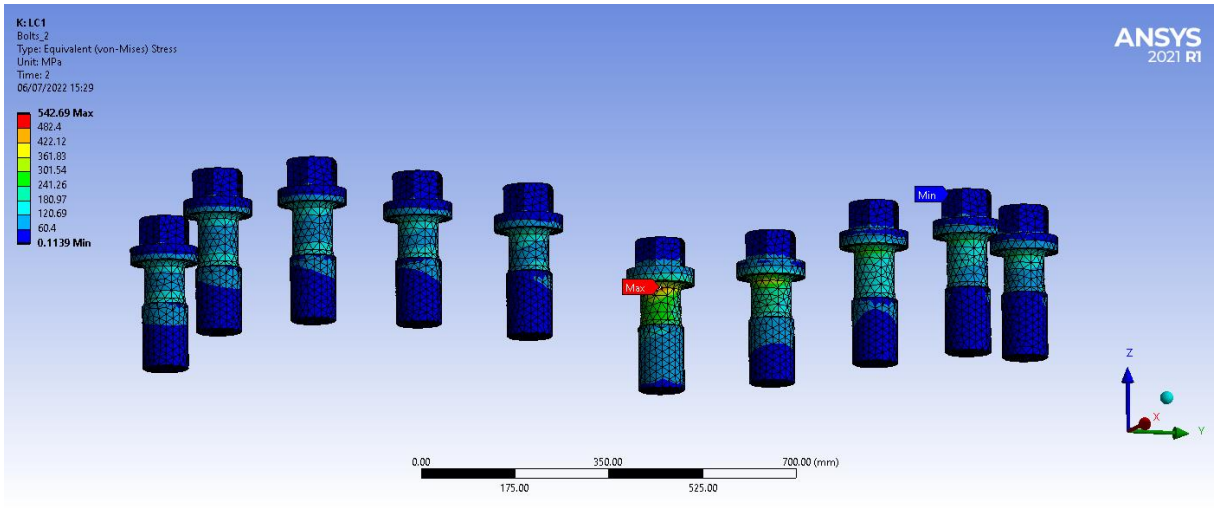

Figure 37. Maximum von Mises stress in load case 1 with R10 fillet bolts seeing at the bolts' view

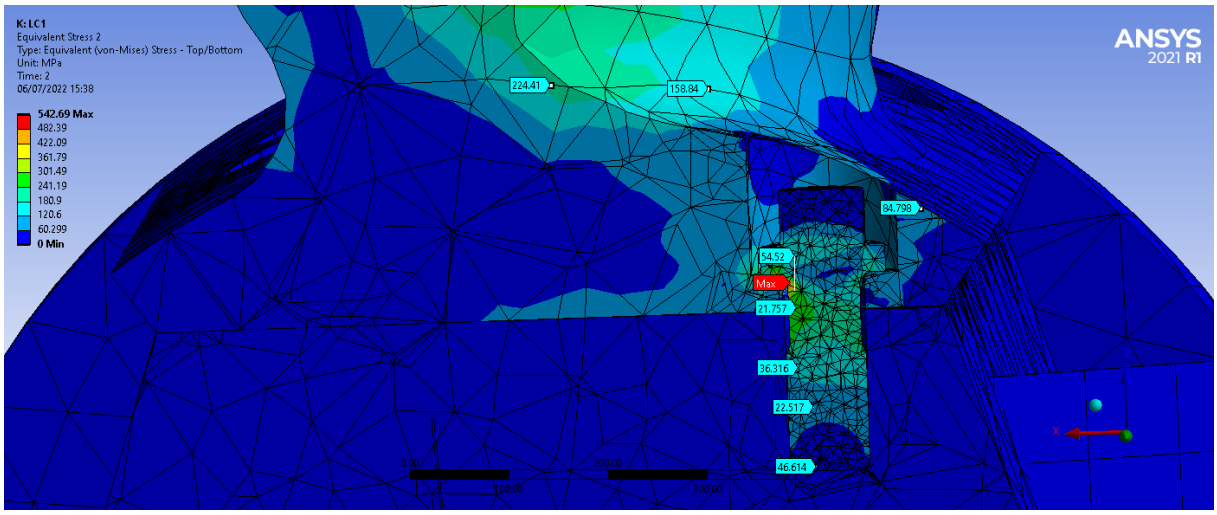

Figure 38. Maximum von Mises stress in load case 1 with R10 fillet bolts seeing at critical bolt's section view

Table 35. Results comparison of R5 and R10 fillet bolts

S/N	Analysis	Max. von Mises stress (MPa)	Max. total deformation (mm)	Max. stress region	Max. def. Region
1	Class 3 model with R5 head fillet bolts	629.73	45.851	around bolt fillet bet. shank and head flange	blade tip (middle)
2	Class 3 model with R10 head fillet bolts	542.69	45.893	around bolt fillet bet. shank and head flange	blade tip (middle)

From the analysis, using R5 and R10 fillet bolts, maximum total deformation results were almost the same but the maximum von Mises stress was reduced from 629.73 MPa to 542.69 MPa. In order to increase that fillet radius by more than R10, it was not appropriate for geometrical contact of the bolt to the blade flange. Additionally, the different type of elliptical fillet was also modelled and tested, and the stress was slightly reduced but not significant. That is why the bolt with the R10 fillet was continued in use for further analysis.

In load step 1 with only preloads, the maximum von Mises stress of 213.41 MPa was seen at the bolt and with a very small total deformation of 0.178 mm. It could be noticed that the influence of load step 1 when the bolted joint only had preloads was comparatively small. In load step 2 with complete loadings, the maximum deformation of 45.893 mm occurred at the blade tip and the maximum von Mises stress of 542.69 MPa was found at the bolt fillet between the head flange and shank. That bolt was in the first position from the trailing edge at the suction side of the blade. However, the critical stress at the bolt was less than the allowable yield strength of the bolt. The stresses at the blade, blade foot fillet and the hub were also lower than their respective yield strengths. For this load case, the bolted joints were safe.

5.2.7.2 Analysis of Model Class 3 with Load Case 2

In this analysis, ice load case 2, was applied and the analysis results were as per the following figures.

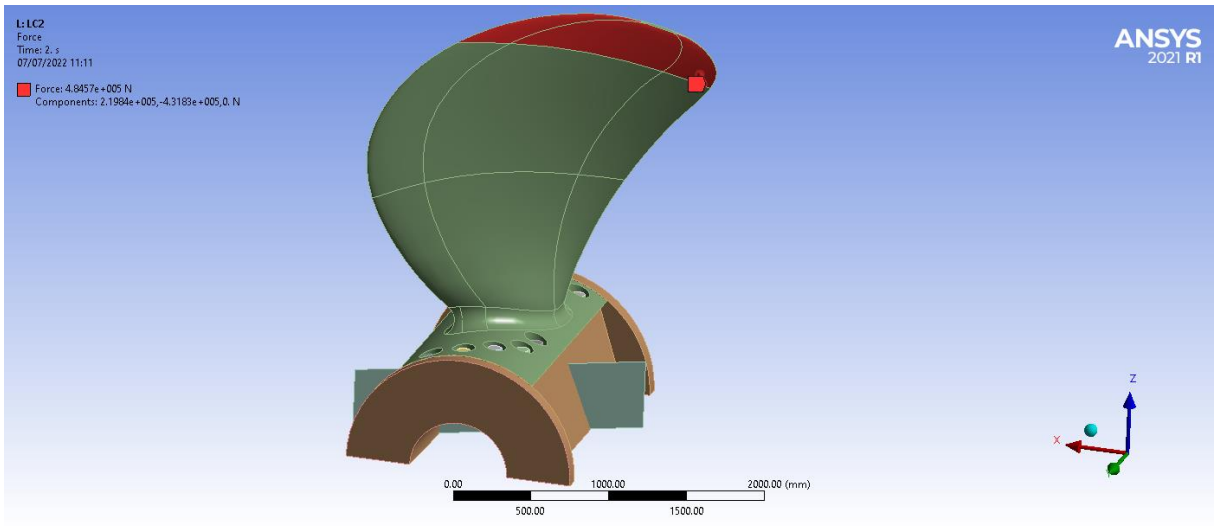

Figure 39. Application of loadings and fixed supports for load case 2 of class 3 model

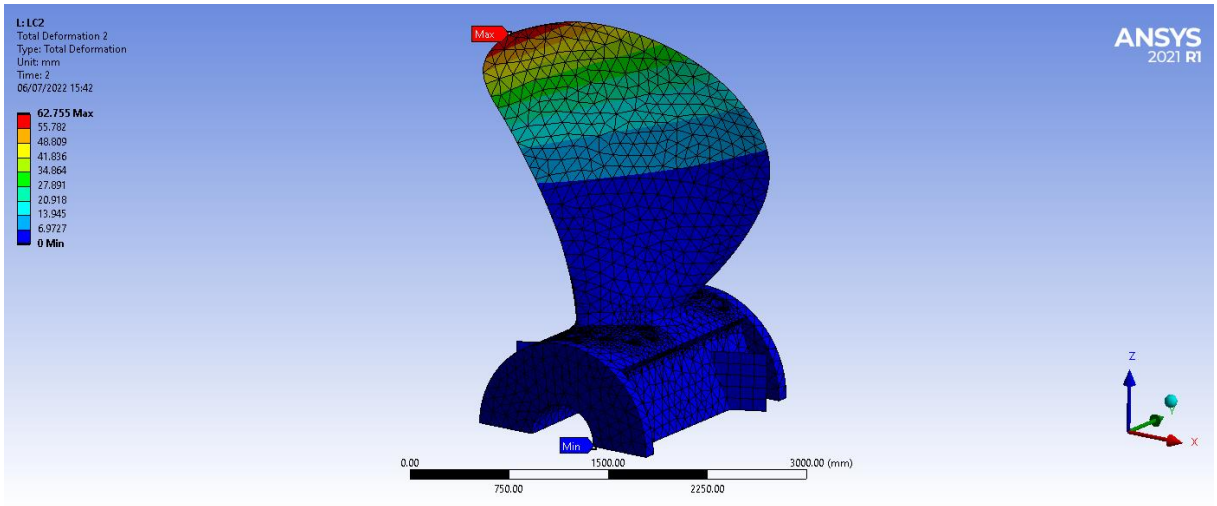

Figure 40. Maximum total deformation in load case 2

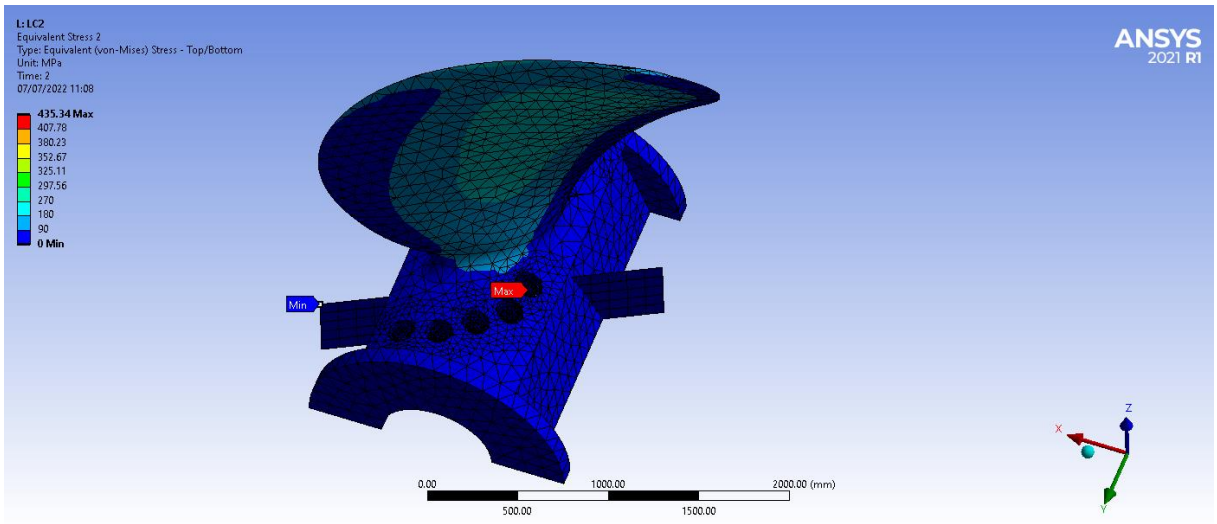

Figure 41. Maximum von Mises stress in load case 2

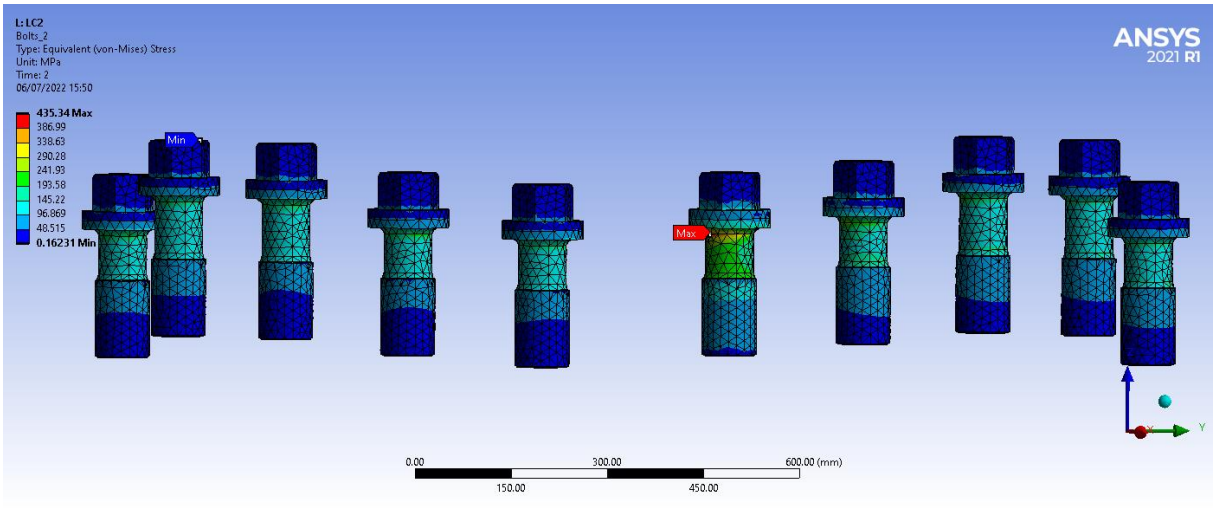

Figure 42. Maximum von Mises stress in load case 2 seeing at the bolts' view

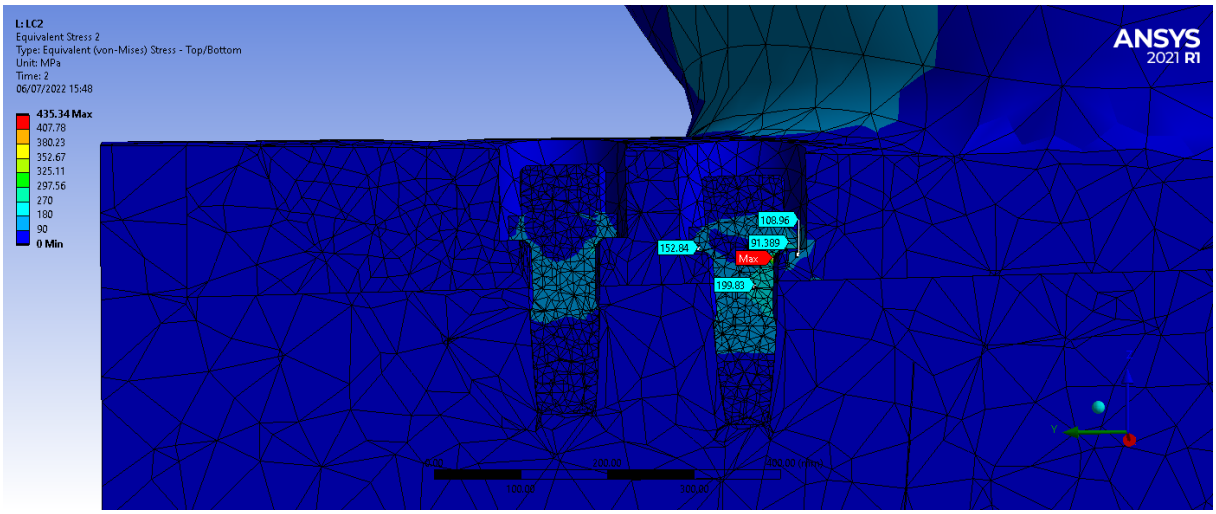

Figure 43. Maximum von Mises stress in load case 2 seeing at critical bolt's section view

From the analysis, the maximum deformation of 62.755 mm occurred at the blade tip and the maximum von Mises stress of 435.34 MPa was found at the bolt fillet between the head flange and shank. That bolt was also in the first position from the trailing edge at the suction side of the blade. However, the critical stress at the bolt was less than the allowable yield strength of the bolt. The stresses at the blade, blade foot fillet and the hub were also lower than their respective yield strengths. For this load case, the bolted joints were safe.

5.2.7.3 Analysis of Model Class 3 with Load Case 3

In this analysis, ice load case 3, was applied and the analysis results were as per the following figures.

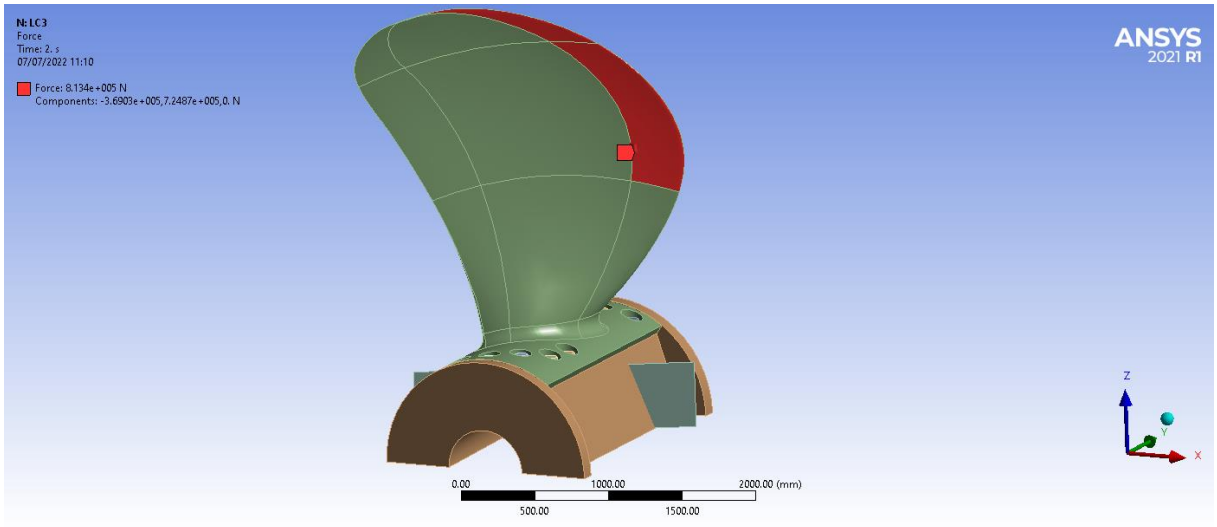

Figure 44. Application of loadings and fixed supports for load case 3 of class 3 model

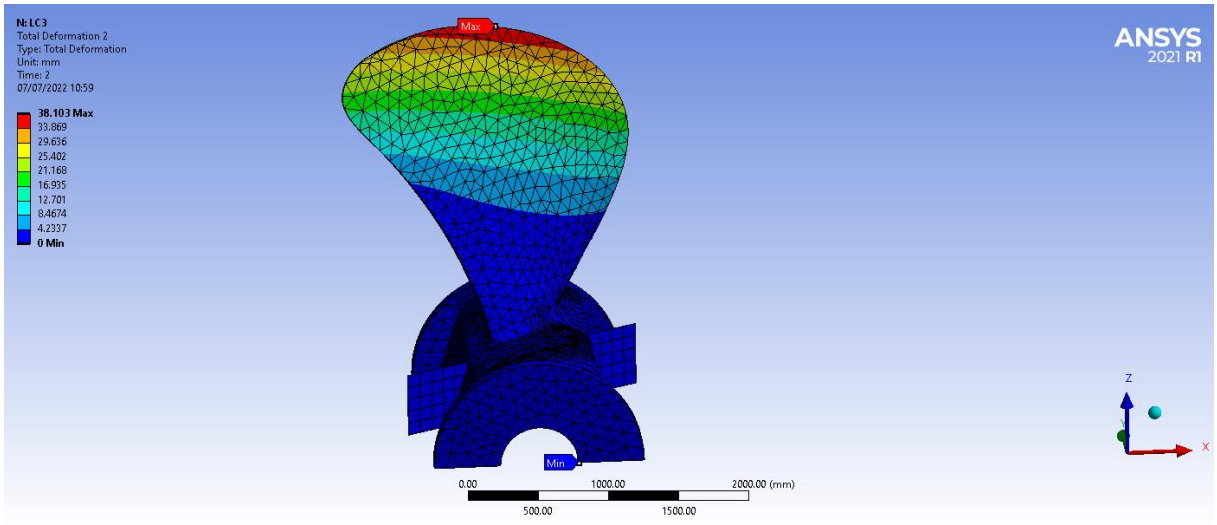

Figure 45. Maximum total deformation in load case 3

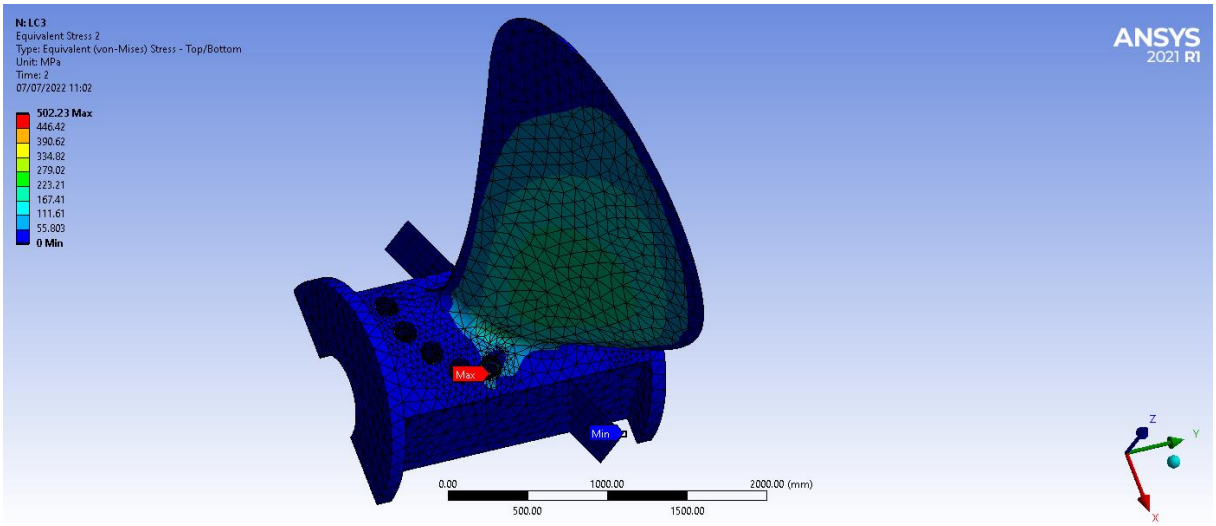

Figure 46. Maximum von Mises stress in load case 3

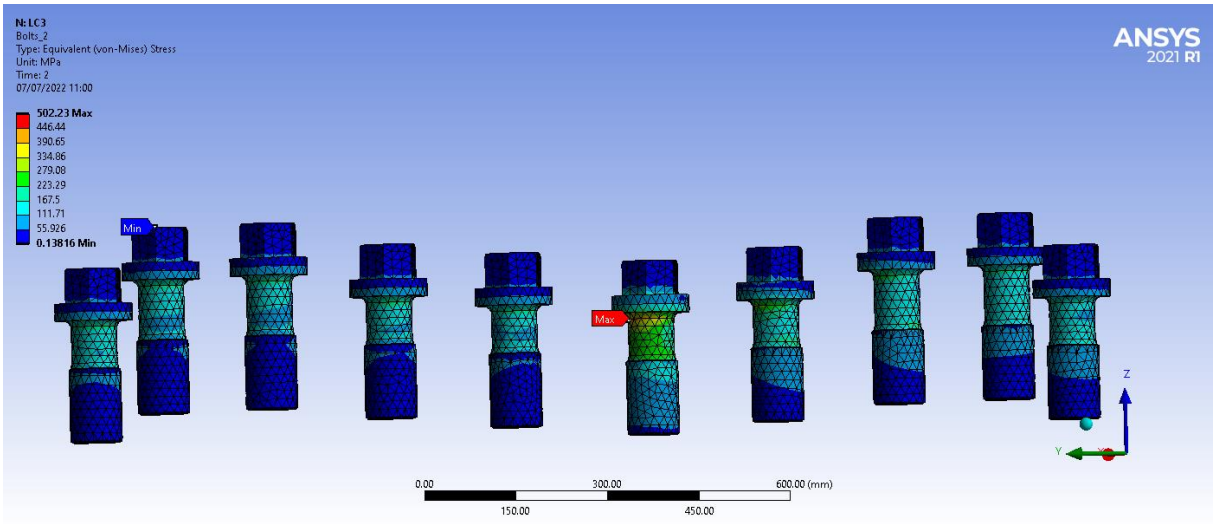

Figure 47. Maximum von Mises stress in load case 3 seeing at the bolts' view

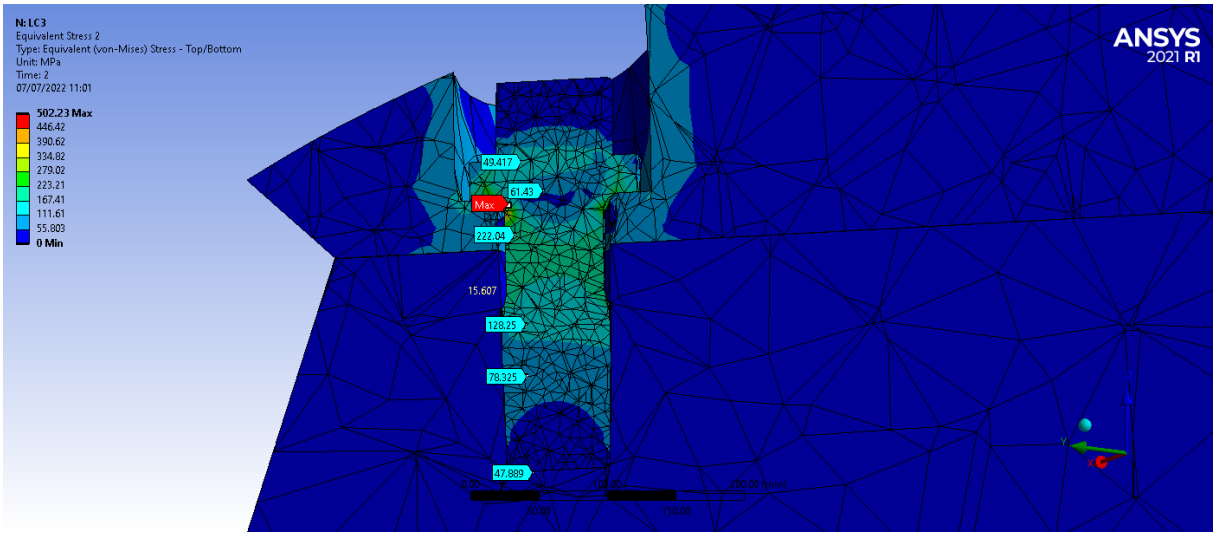

Figure 48. Maximum von Mises stress in load case 3 seeing at critical bolt's section view

From the analysis, the maximum deformation of 38.103 mm occurred at the blade tip and the maximum von Mises stress of 502.23 MPa was found at the bolt fillet between the head flange and shank. That bolt was in the first position from the leading edge at the pressure side of the blade. However, the critical stress at the bolt was less than the allowable yield strength of the bolt. The stresses at the blade, blade foot fillet and the hub were also lower than their respective yield strengths. For this load case, the bolted joints were safe.

5.2.7.4 Analysis of Model Class 3 with Load Case 4

In this analysis, ice load case 4, was applied and the analysis results were as per the following figures.

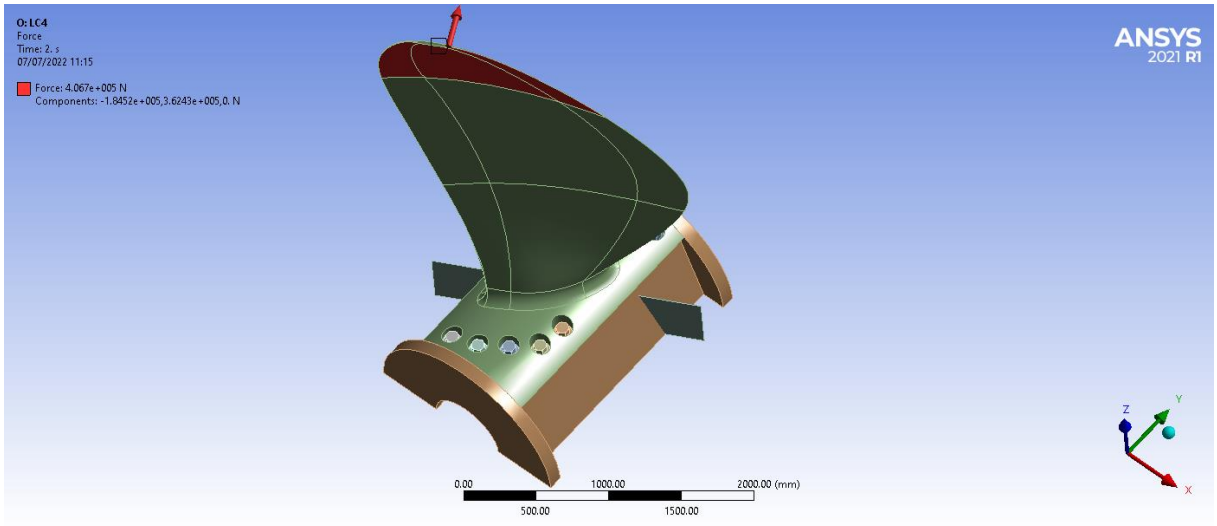

Figure 49. Application of loadings and fixed supports for load case 4 of class 3 model

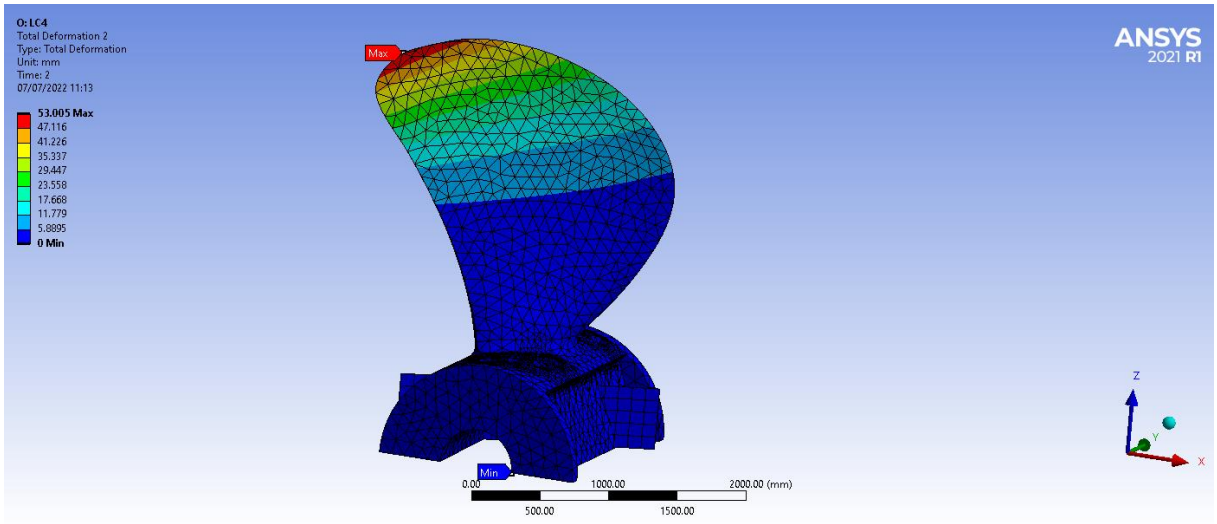

Figure 50. Maximum total deformation in load case 4

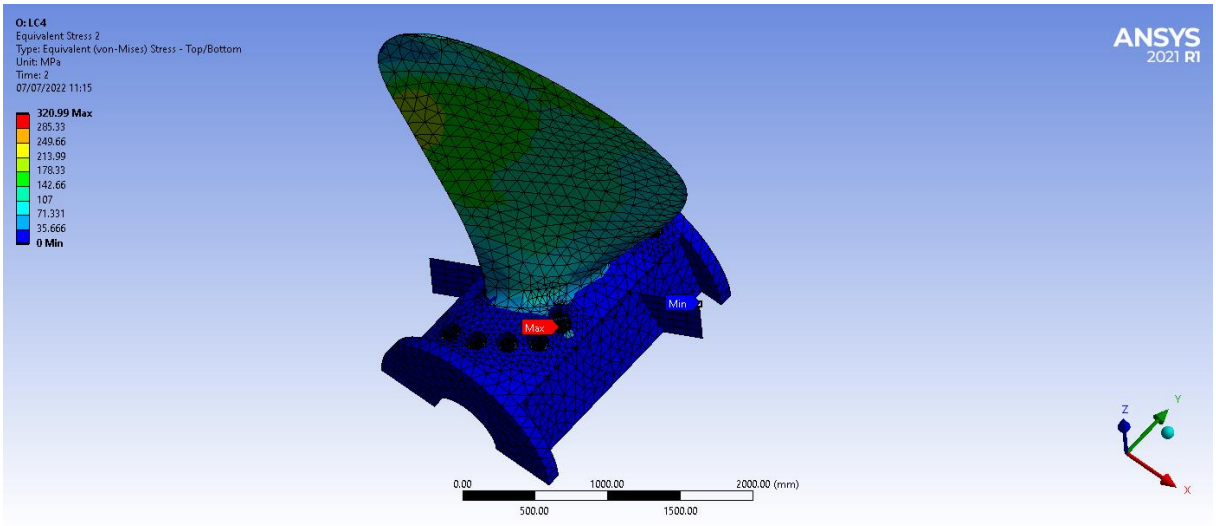

Figure 51. Maximum von Mises stress in load case 4

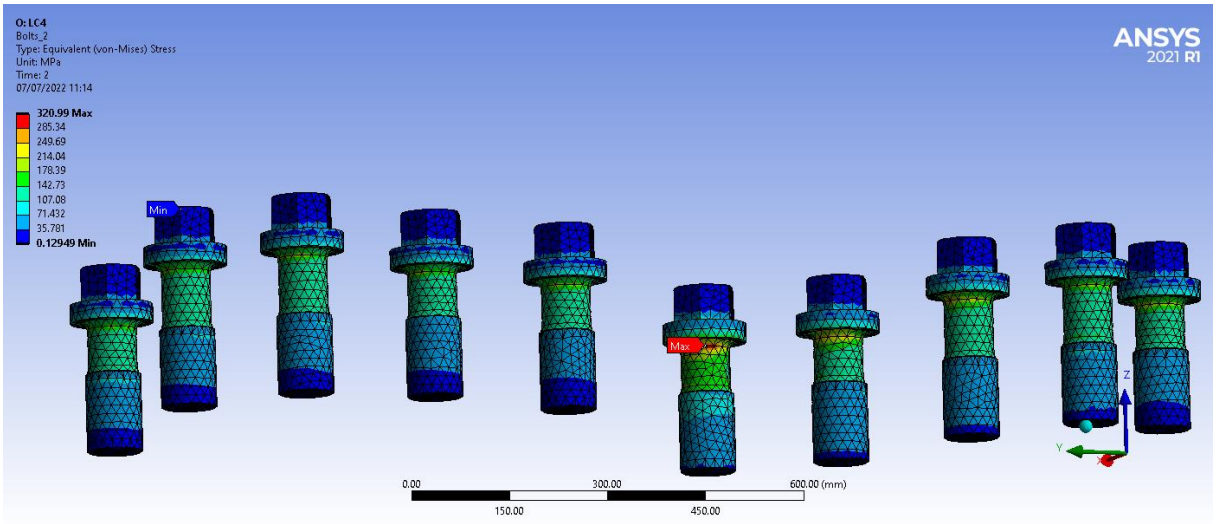

Figure 52. Maximum von Mises stress in load case 4 seeing at the bolts' view

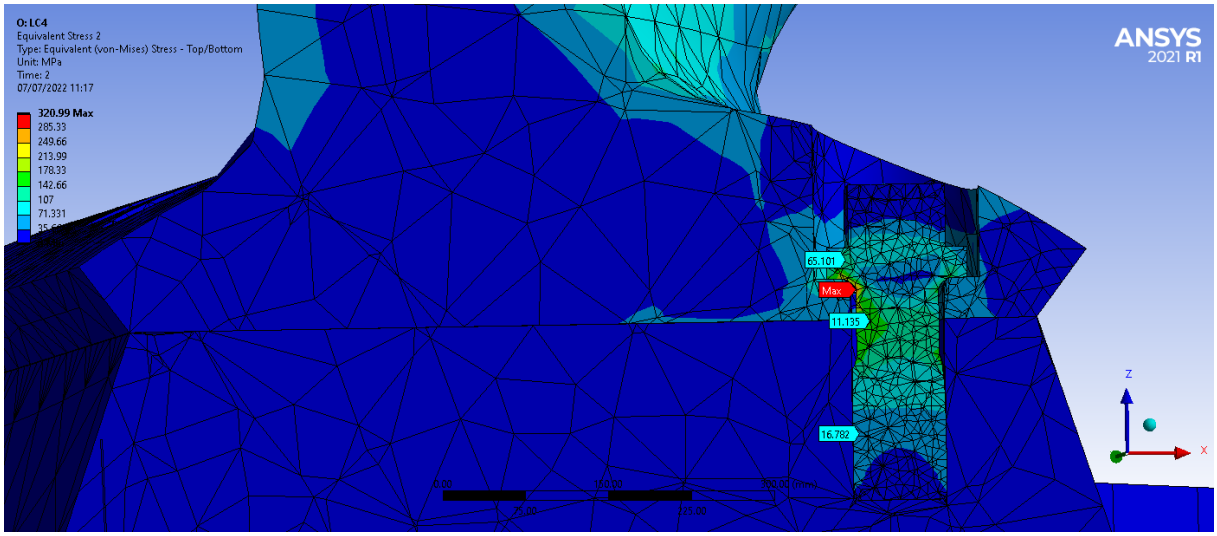

Figure 53. Maximum von Mises stress in load case 4 seeing at critical bolt's section view

From the analysis, the maximum deformation of 53 mm occurred at the blade tip and the maximum von Mises stress of 320.99 MPa was found at the bolt fillet between the head flange and shank. That bolt was also in the first position from the leading edge at the pressure side of the blade. However, the critical stress at the bolt was less than the allowable yield strength of the bolt. The stresses at the blade, blade foot fillet and the hub were also lower than their respective yield strengths. For this load case, the bolted joints were safe.

5.2.7.5 Analysis of Model Class 3 with Load Case 5

In this analysis, ice load case 5, was applied and the analysis results were as per the following figures.

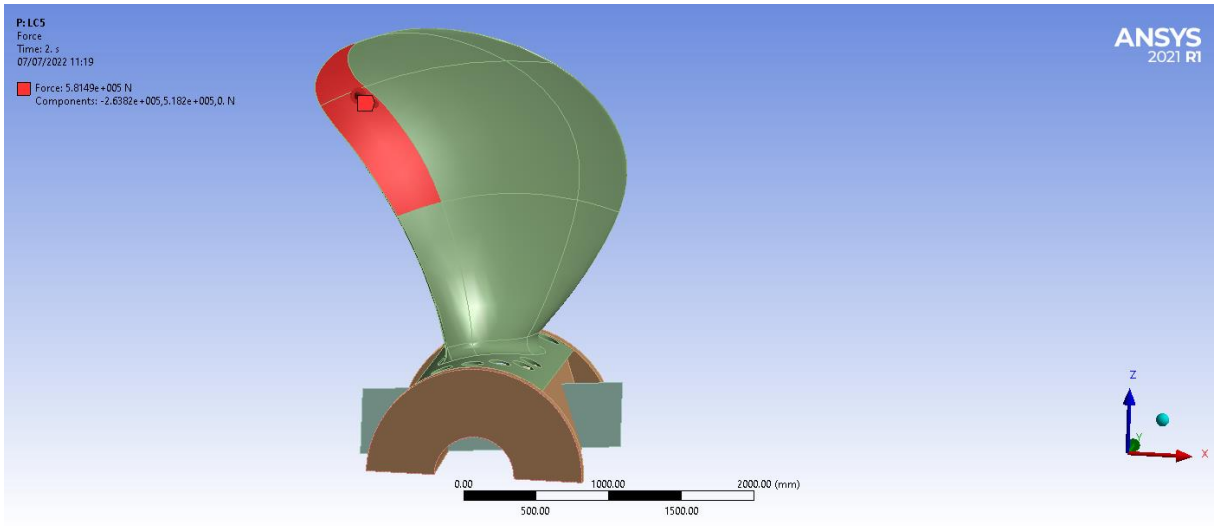

Figure 54. Application of loadings and fixed supports for load case 5 of class 3 model

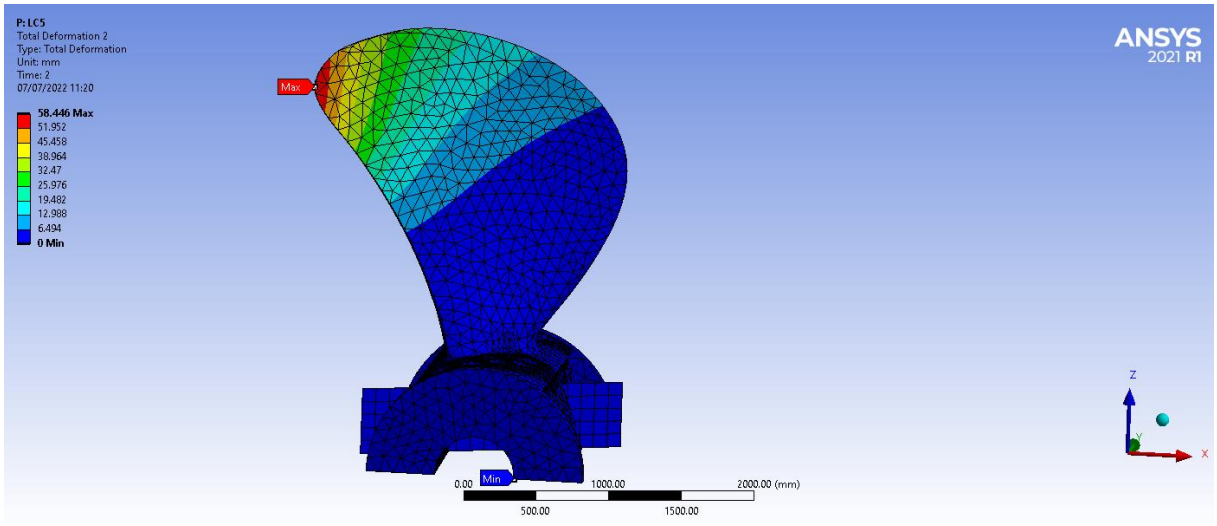

Figure 55. Maximum total deformation in load case 5

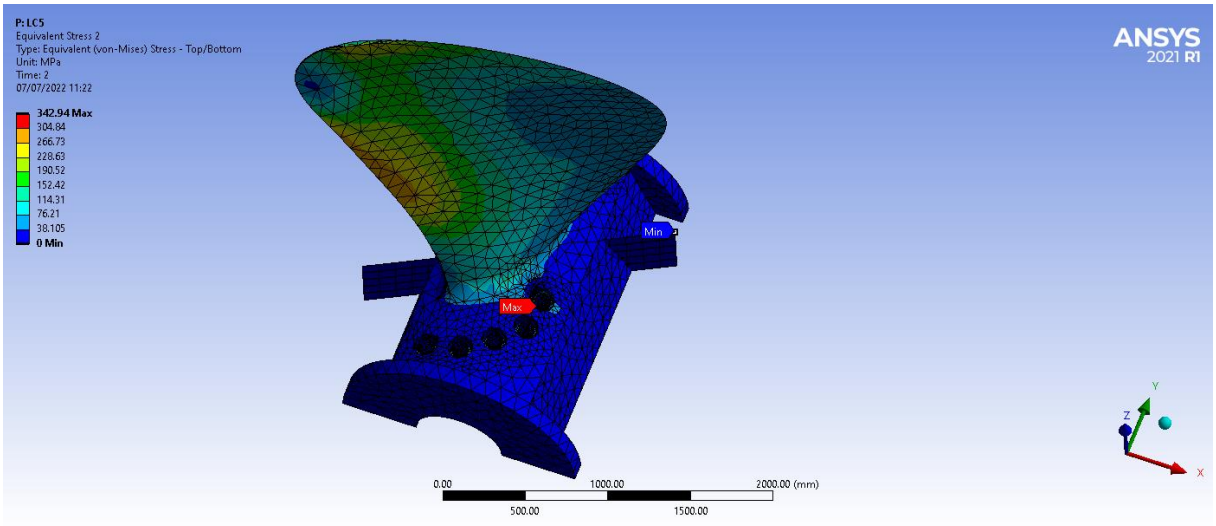

Figure 56. Maximum von Mises stress in load case 5

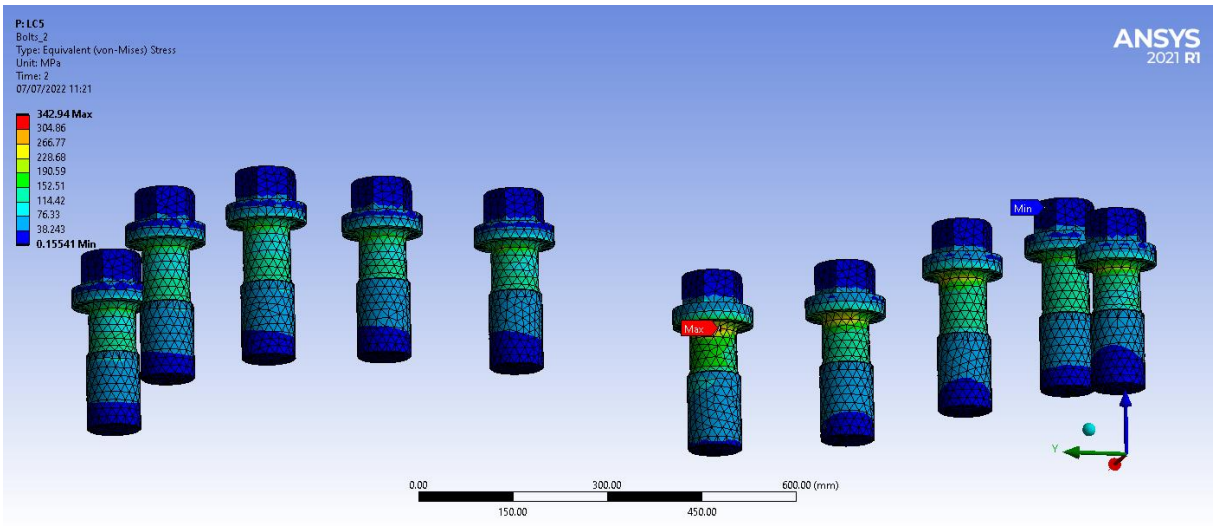

Figure 57. Maximum von Mises stress in load case 5 seeing at the bolts view

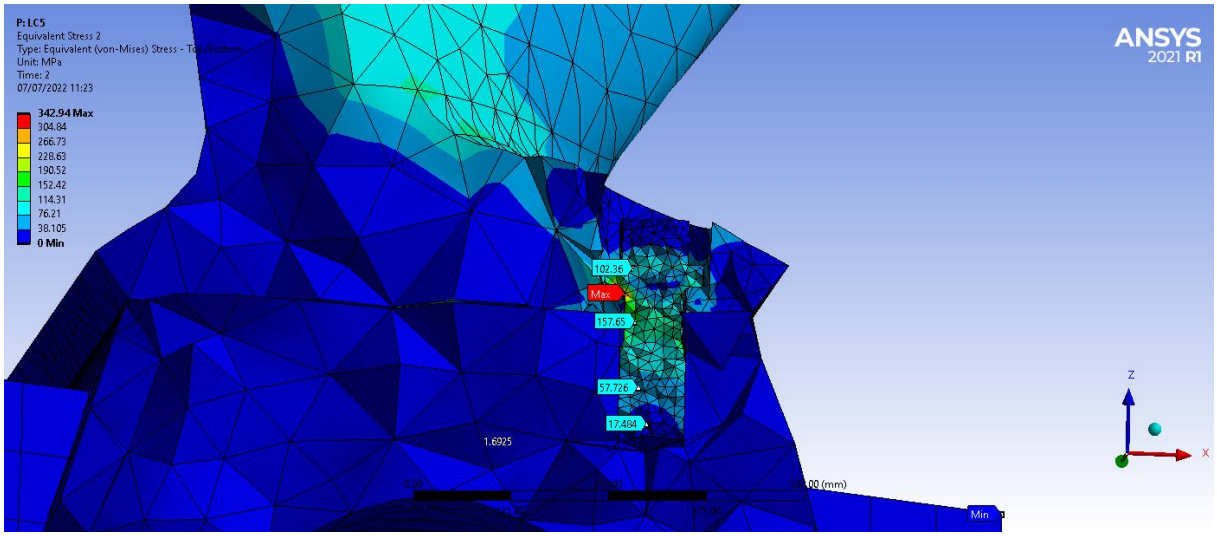

Figure 58. Maximum von Mises stress in load case 5 seeing at critical bolt's section view

From the analysis, the maximum deformation of 58.446 mm occurred at the blade tip and the maximum von Mises stress of 342.94 MPa was found at the bolt fillet between the head flange and shank. That bolt was also in the first position from the leading edge at the pressure side of the blade. However, the critical stress at the bolt was less than the allowable yield strength of the bolt. The stresses at the blade pressure side around the middle of the trailing edge where the blade force applied was were investigated high and reaching its yield strength. But the stresses at the blade foot fillet and the hub were lower than their respective yield strengths. For this load case, the bolted joints were safe.

Table 36. Summary of analysis results for ice load cases 1-5

Load cases	Max. von Mises stress (MPa)	Max. total deformation (mm)	Max. stress region	Max. def. Region
Ice load LC 1, preload at bolts, centrifugal blade force	542.69	45.893	around bolt fillet bet. shank and head flange	blade tip (middle)
Ice load LC 2, preload at bolts, centrifugal blade force	435.34	62.755	around bolt fillet bet. shank and head flange	blade tip (middle)
Ice load LC 3, preload at bolts, centrifugal blade force	502.23	38.103	around bolt fillet bet. shank and head flange	blade tip (middle)
Ice load LC 4, preload at bolts, centrifugal blade force	320.99	53.005	around bolt fillet bet. shank and head flange	blade tip
Ice load LC 5, preload at bolts, centrifugal blade force	342.94	58.446	around bolt fillet bet. shank and head flange	blade tip

5.2.7.6 Analysis of Model Class 3 with Imported Hydrodynamic Pressure Load Acting around the Blade

In this case, the analysis was carried out for the bolted joint due to the effect of hydrodynamic pressure loads acting around the blade instead of ice loads. The investigation was performed with the same model class 3, preloads on bolts, centrifugal blade force. And the hydrodynamic pressure loads for the same geometry of the propeller blade were imported. Unlike the blade force, full surfaces of suction and pressure sides of the blade were selected to apply the hydrodynamic pressure. The same boundary condition, meshing, and contact definitions were applied. The analysis results were as per the following figures.

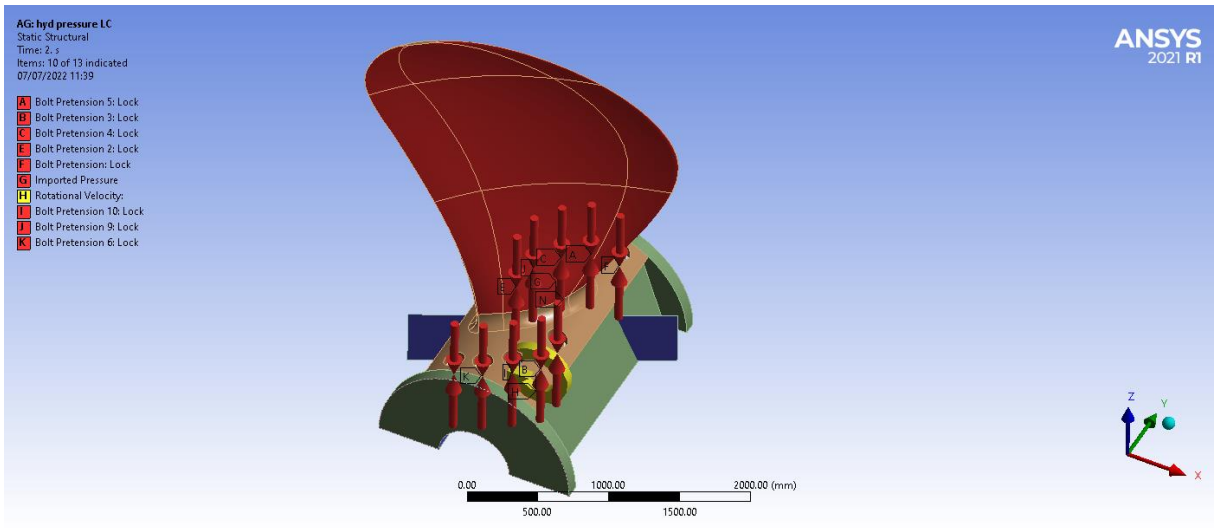

Figure 59. Application of loadings with hydrodynamic pressure load and fixed supports

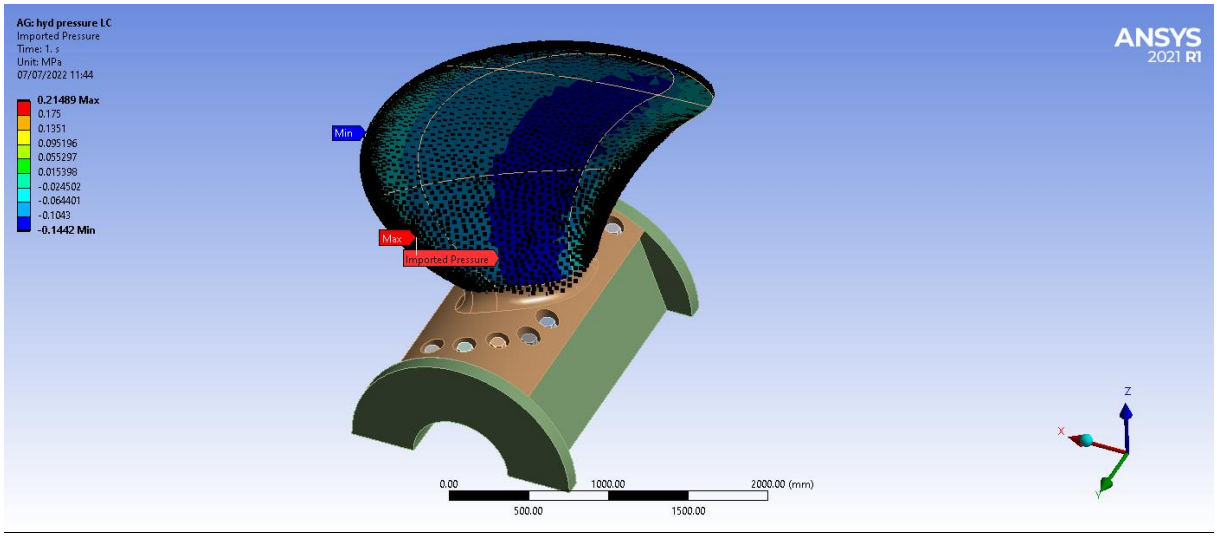

Figure 60. Imported hydrodynamic pressure load on the suction side of the blade

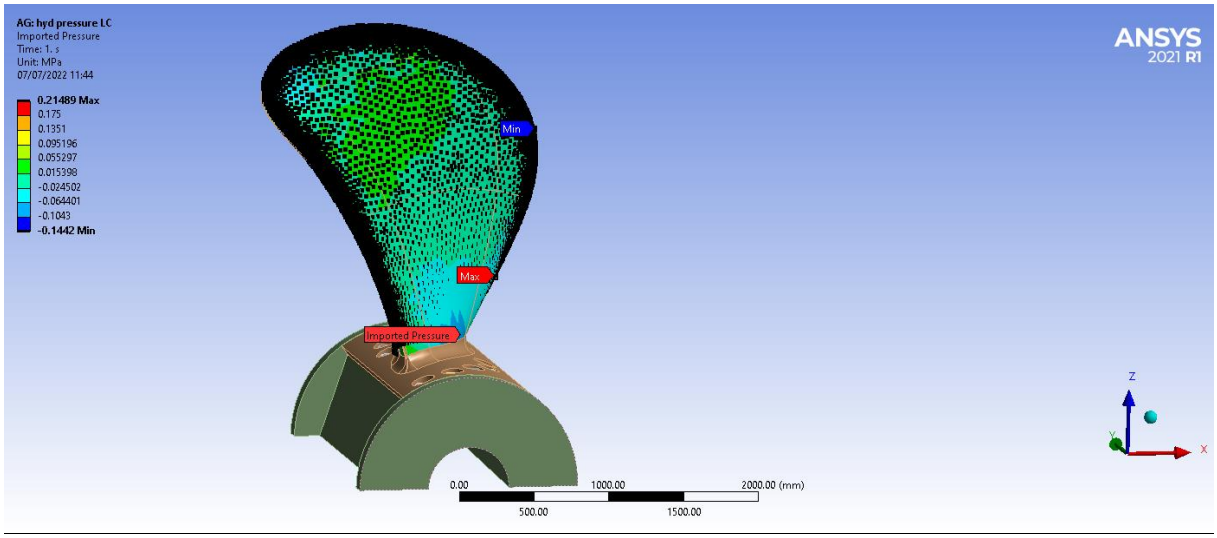

Figure 61. Imported hydrodynamic pressure load on the pressure side of the blade

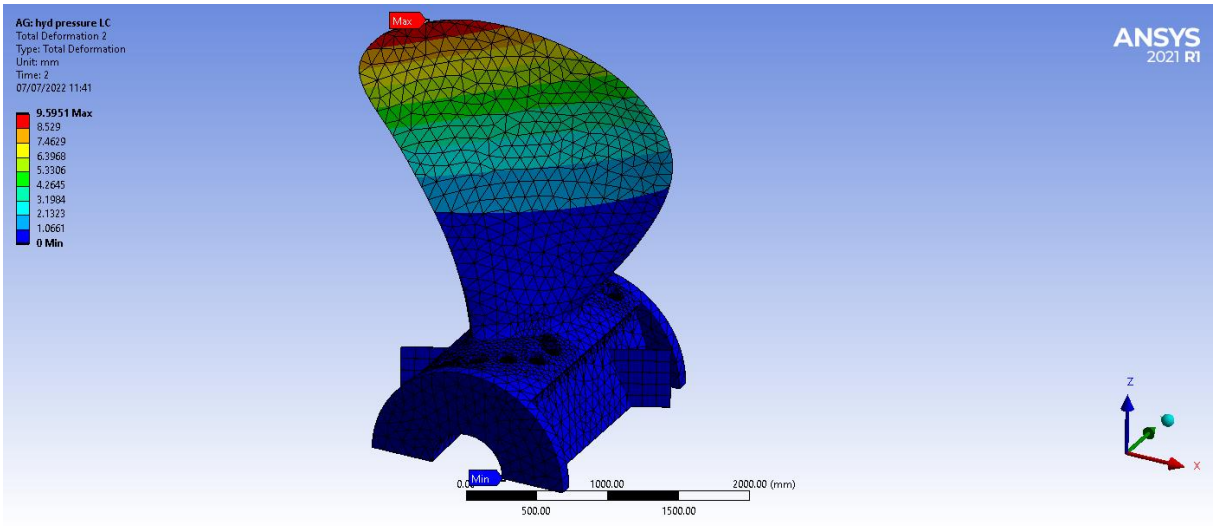

Figure 62. Maximum total deformation in imported hydrodynamic pressure load

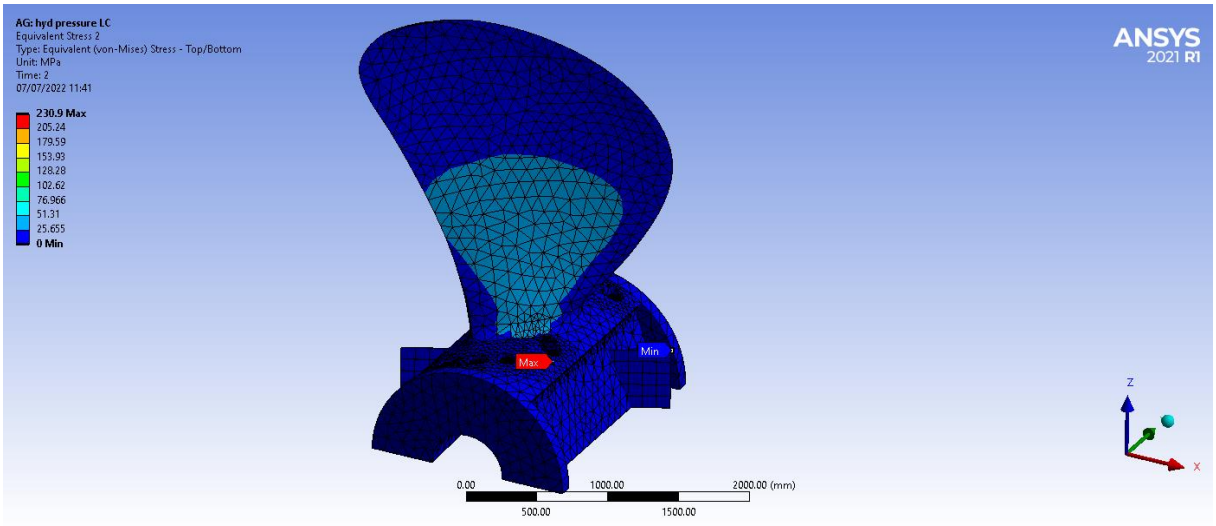

Figure 63. Maximum von Mises stress in imported hydrodynamic pressure load

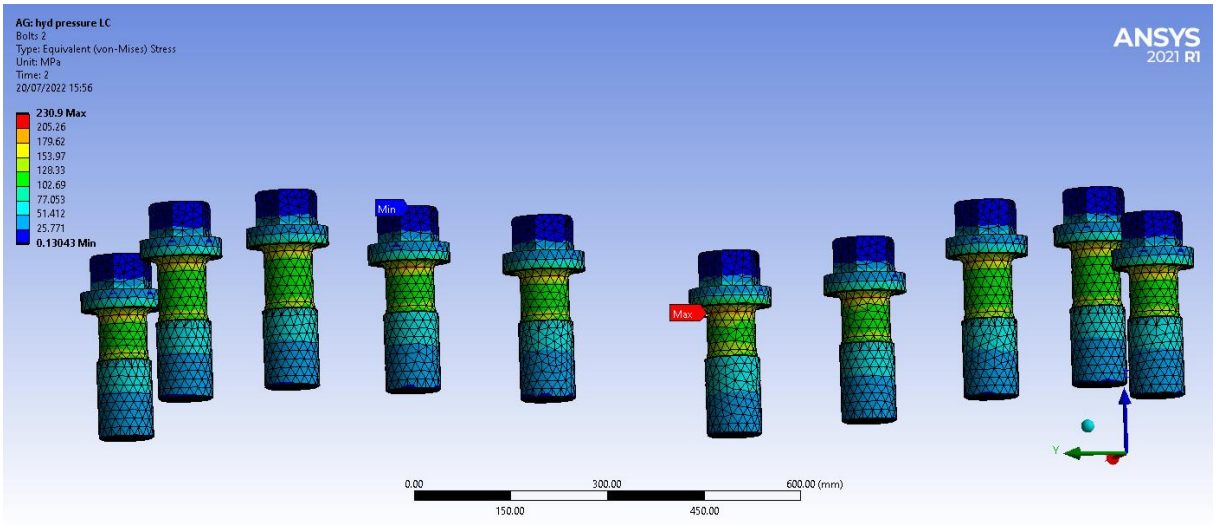

Figure 64. Maximum von Mises stress at the bolts with imported hydrodynamic pressure load

From the analysis, the maximum deformation of 9.6 mm occurred at the blade tip and the maximum von Mises stress of 230.9 MPa was found at the bolt fillet between the head flange and shank. That bolt was also in the first position from the leading edge at the pressure side of the blade. However, the critical stress at the bolt was less than the allowable yield strength of the bolt. The stresses at the blade foot fillet and the hub were lower than their respective yield strengths. For this load case, the bolted joints were safe. It could be noticed that the influence of hydrodynamic pressure load upon bolted joint had a moderate influence. Thus the results obtained from hydrodynamic pressure load case were finally lower than ice class load cases.

5.2.7.7 Analysis of Model Class 3 with Ultimate Blade Failure Load

The analysis had been done for the bolted joint when the blade failure load was exerted at the blade pressure side of the specified direction. The investigation was performed with the same model class 3, preloads on bolts, centrifugal blade force including blade failure load. The same boundary condition, meshing, and contact definitions were applied. The analysis results were as per the following figures.

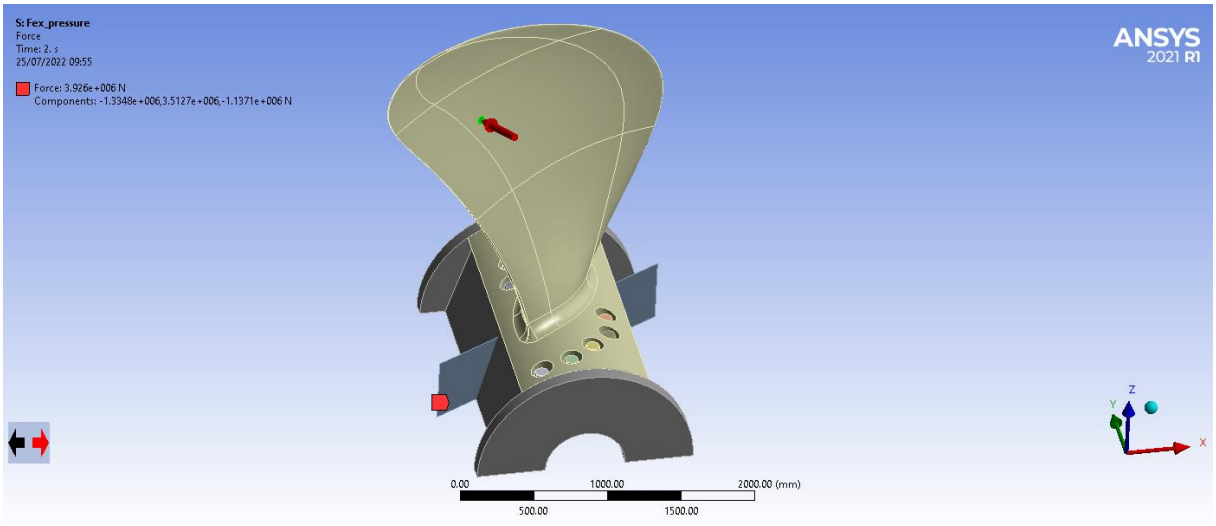

Figure 65. Application of loadings with blade failure load and fixed supports

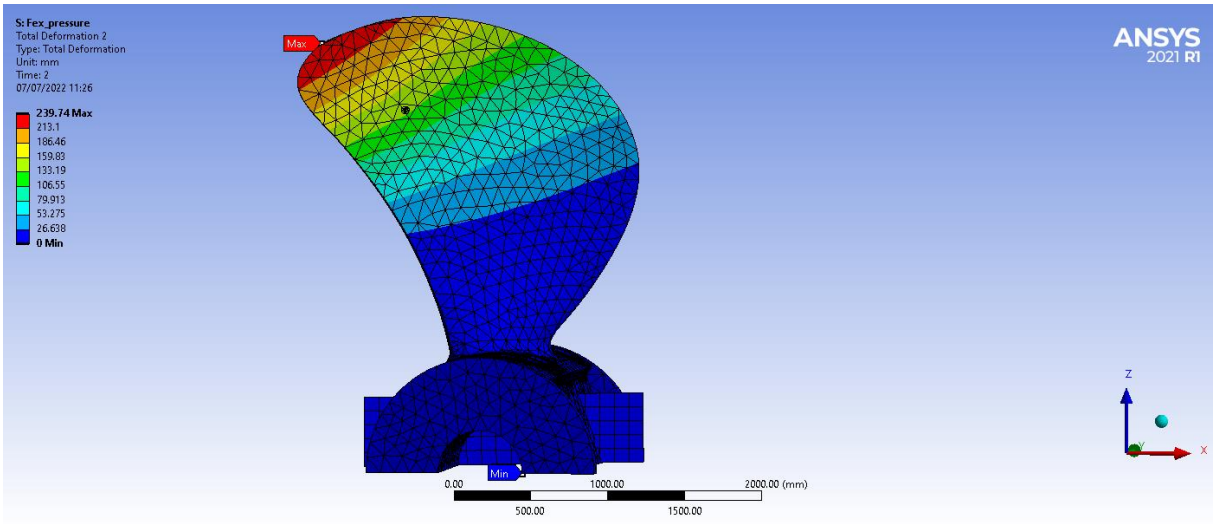

Figure 66. Maximum total deformation in blade failure load

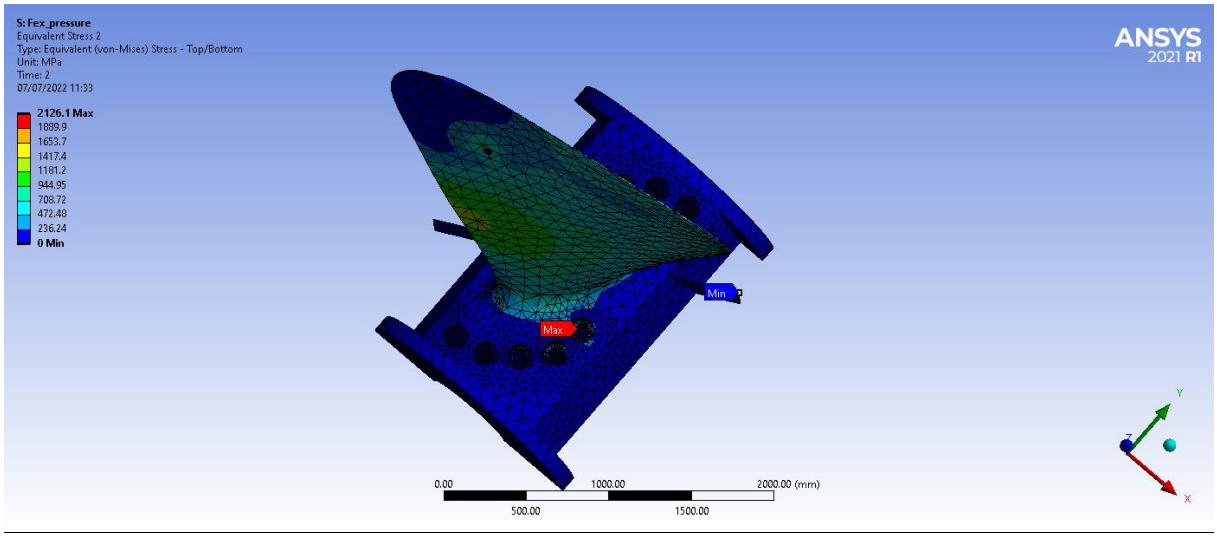

Figure 67. Maximum von Mises stress in blade failure load

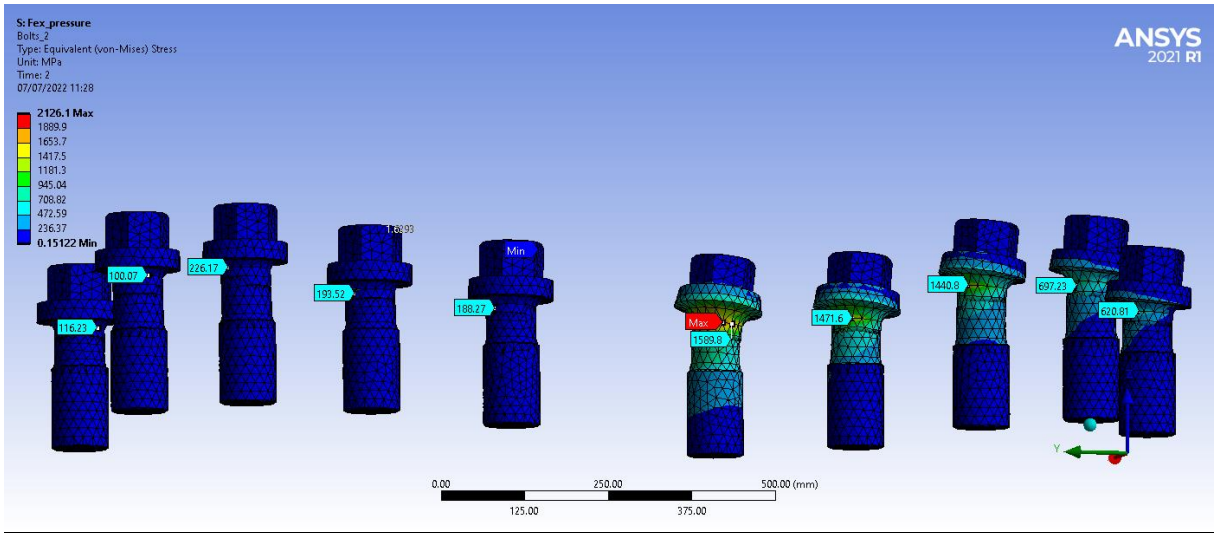

Figure 68. Maximum von Mises stress at the bolts with blade failure load

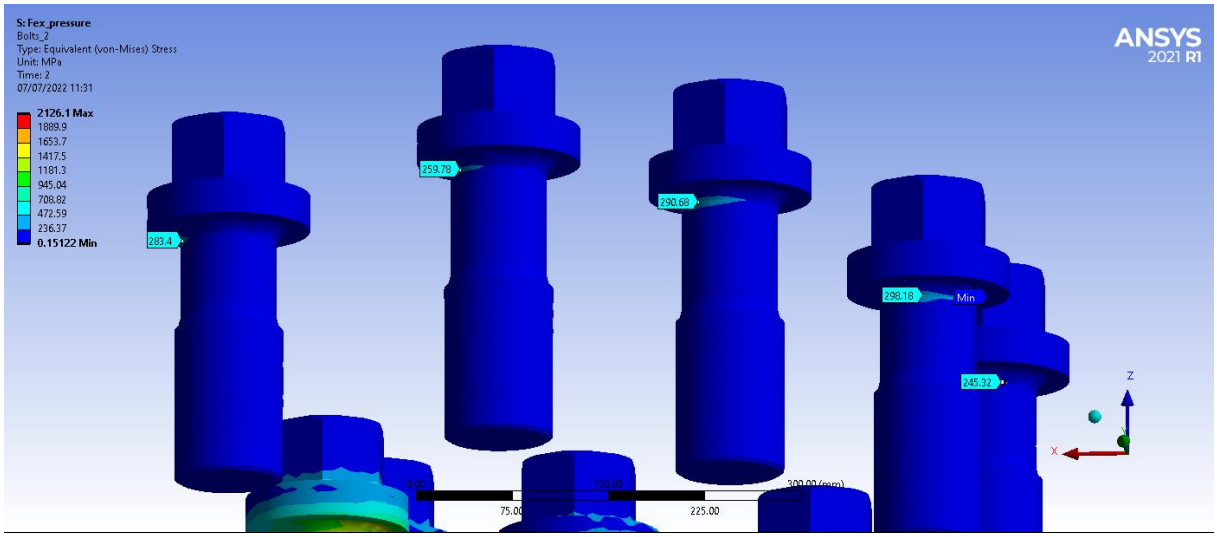

Figure 69. Maximum von Mises stress at the bolts of blade's suction side with blade failure load

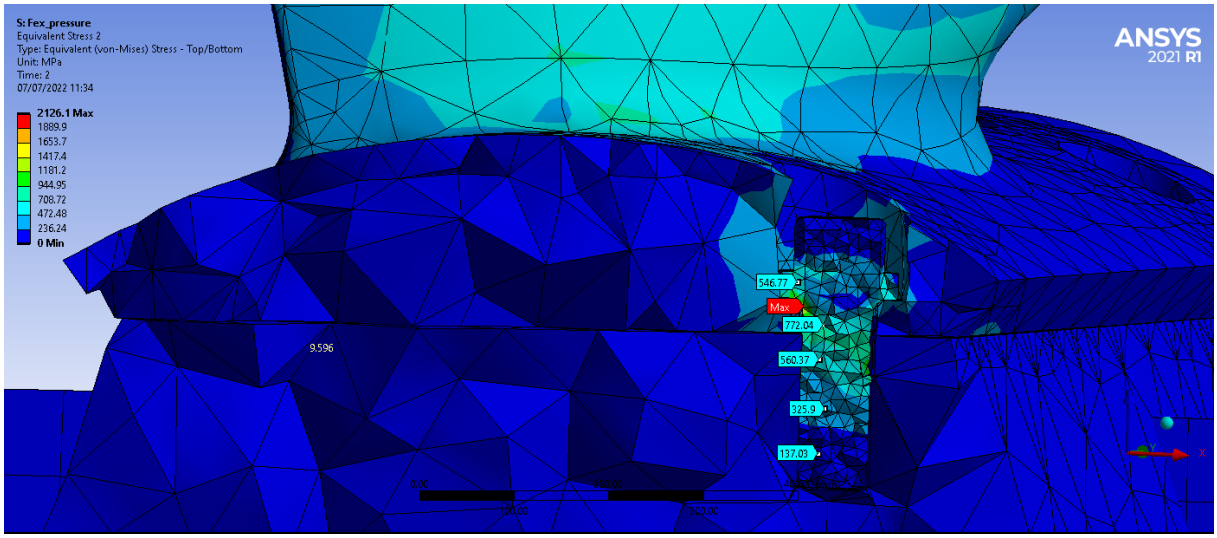

Figure 70. Maximum von Mises stress in blade failure load seeing at critical bolt's section view

This analysis was performed to observe the status of the bolted joint when the blade was destroyed by the ultimate failure load. From the results, the maximum deformation of 239.74 mm occurred at the blade tip and the maximum von Mises stress of 2126.1 MPa was found at the bolt fillet between the head flange and shank. That critical bolt was in the first position from the leading edge at the pressure side of the blade. In the section view of the joint for that bolt, stress variations around the shank and fillet were higher than yield strength. Additionally, the bolt fillets and the shanks of 5 bolts at the pressure side of the blade had higher stress concentrations than their allowable limit, and those 5 bolts would be fractured

from the shank region if blade failure load was exerted. However, the 5 bolts at the suction side of the blade had stress values less than yield strength and these bolts were safe.

These results were obtained within the scheme of static structural analysis with linear elastic behaviour in this study. To get more realistic information, non-linear analysis including full material behaviour in tensile curves can be performed. The blade shall be damaged first. Then it is possible to closely check the status of the joint whether the bolts at the blade pressure side may also be broken out or not.

In Ansys large deformation analysis can be implemented to evaluate the results within the plastic deformation region. For this the complete material descriptions of the tensile curves or stress-strain relationships for propeller and hub (Cu3 material curves), and for the bolts (martensitic steel material curves) are necessary to be applied.

The stresses at the blade and blade foot fillet were beyond the allowable limit and the blade would be damaged. But the stresses at the hub (maximum of 236.24 MPa, occurred near contacts between blade flange and hub of suction side) were lower than yield strength and the hub was safe. It could be noticed that the influence of blade failure load was significant and the analysis with more refined mesh was performed for the bolted joint to get more accurate results.

5.2.8 Sub-modelling Techniques for the Bolted Joint

To get the detailed results of deformation and stress, normally the refined mesh shall be used in the FE model. This may lead to high computational efforts. The objective of the sub-modelling method in this study is to be able to evaluate more precise results of structural analysis for the concerned part or submodel extracted from the global model. It is possible to perform this analysis at a very refined mesh saving the computational time significantly.

Before sub-modelling analysis, the preliminary analysis is done at a full model with coarse mesh. Then submodel is developed from the full model. The solution from the full model is transferred to the submodel. While importing the solution from the global model, the cut boundary constraint method was applied to the submodel in this study. This allowed the same loading conditions to be applied and the respective displacement values were automatically set to the submodel. To select the cut boundary on the submodel, the name selection option

was chosen. In this investigation, sub-modelling was used for critical bolted joint parts from load case 1 and from blade failure load case.

For the engineering judgement of the submodel, the stress distribution and deformation around the cut boundary were compared with that information cut from the global model, and it was observed that the distributions were similar.

5.2.8.1 Sub-modelling Analysis for Critical Bolted Joint Part from Load Case 1

The analysis had been done for the submodel of the critical bolted joint part from the suction side of the blade. Load case 1 solution from the global model was transferred to the submodel including, preloads on bolts, centrifugal blade force and ice load. The imported cut boundary constraint method was used in the analysis. For the element sizing the refined mesh of 4 mm was set to the bolts and 50 mm for the rest of the part in the submodel. The analysis results were as per the following figures.

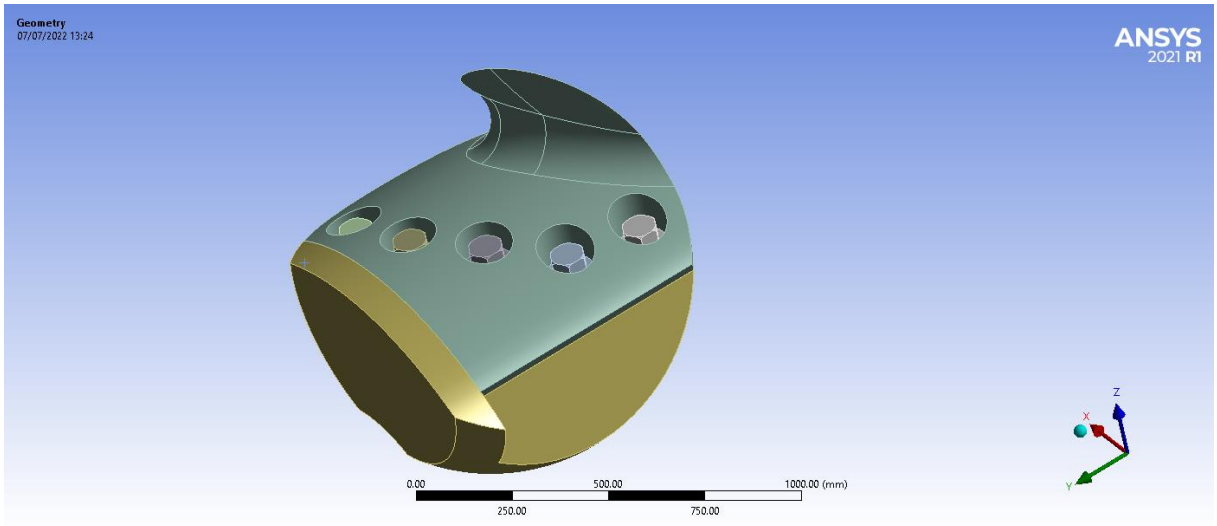

Figure 71. Sub-modelling geometry for critical bolted joint part from load case 1

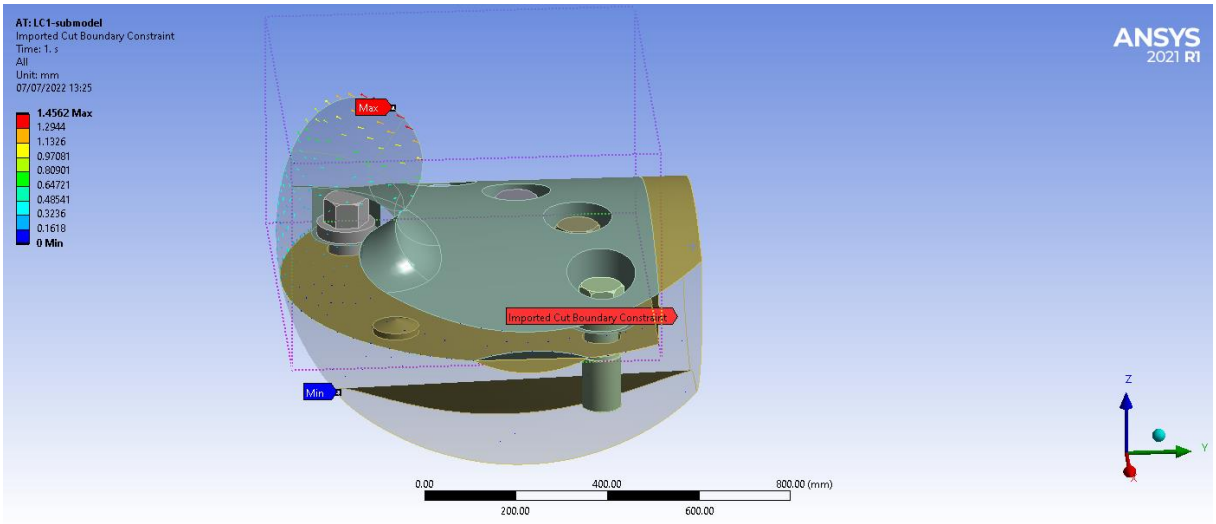

Figure 72. Imported cut boundary constraint for critical bolted joint part from load case 1

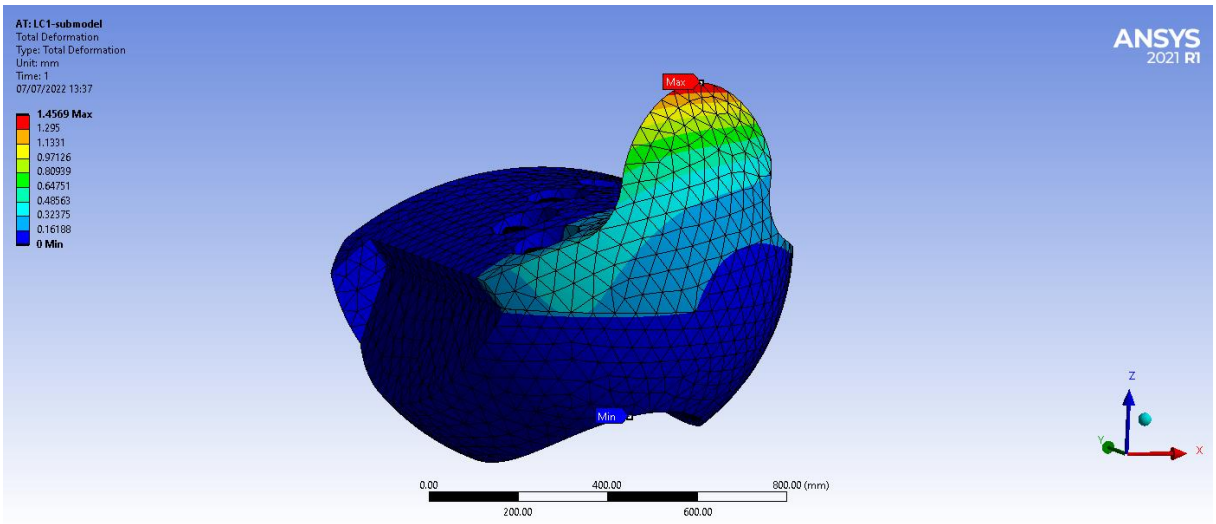

Figure 73. Total deformation in sub-modelling for critical bolted joint part from load case 1

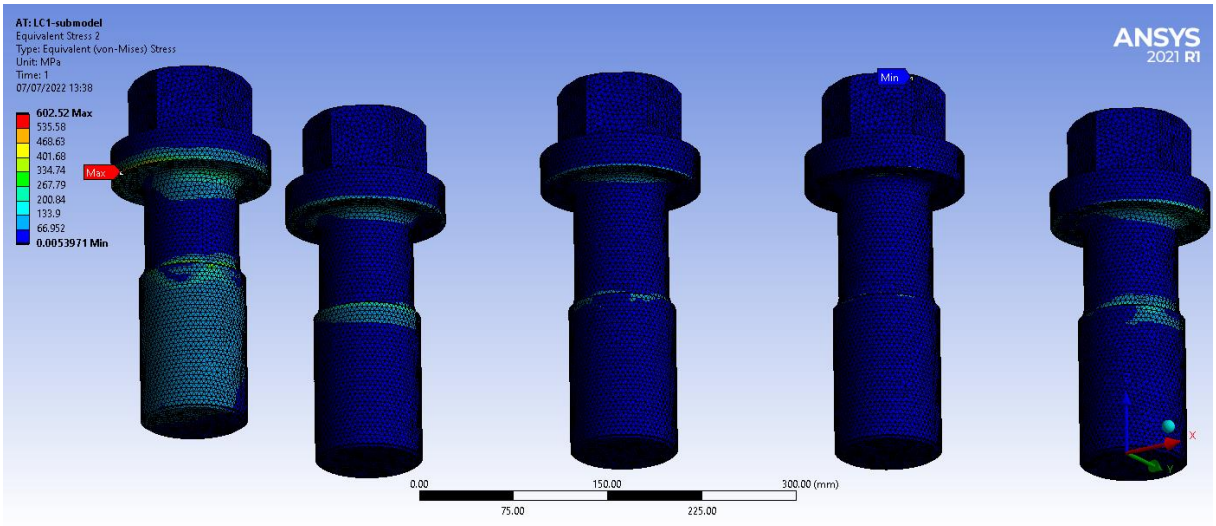

Figure 74. Von Mises stress results in the bolts of sub-modelling from load case 1

From sub-modelling analysis, the maximum von Mises stress of 602.52 MPa was found at the same bolt from load case 1 but the location was at the bottom edge of the bolt head flange and it was under allowable stress. At the head fillet, region stress variations were highly reduced. Since the critical stresses at the bolts and joint part were less than their allowable yield strengths, the bolted joints were safe.

5.2.8.2 Sub-modelling Analysis for Critical Bolted Joint Part from Blade Failure Load

The analysis had been done for the submodel of the critical bolted joint part from the pressure side of the blade. Blade failure load solution from the global model was transferred to the submodel. The imported cut boundary constraint method was used in the analysis. For the element sizing the refined mesh of 4 mm was set to the bolts and 50 mm for the rest of the part in the submodel. The analysis results were as per the following figures.

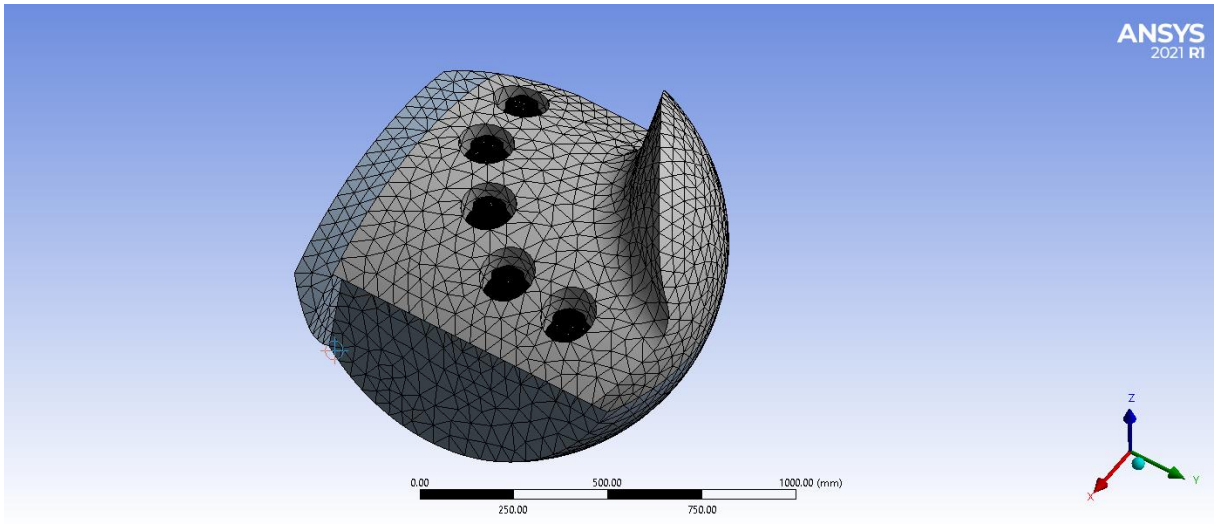

Figure 75. Sub-modelling geometry for critical bolted joint part from blade failure load

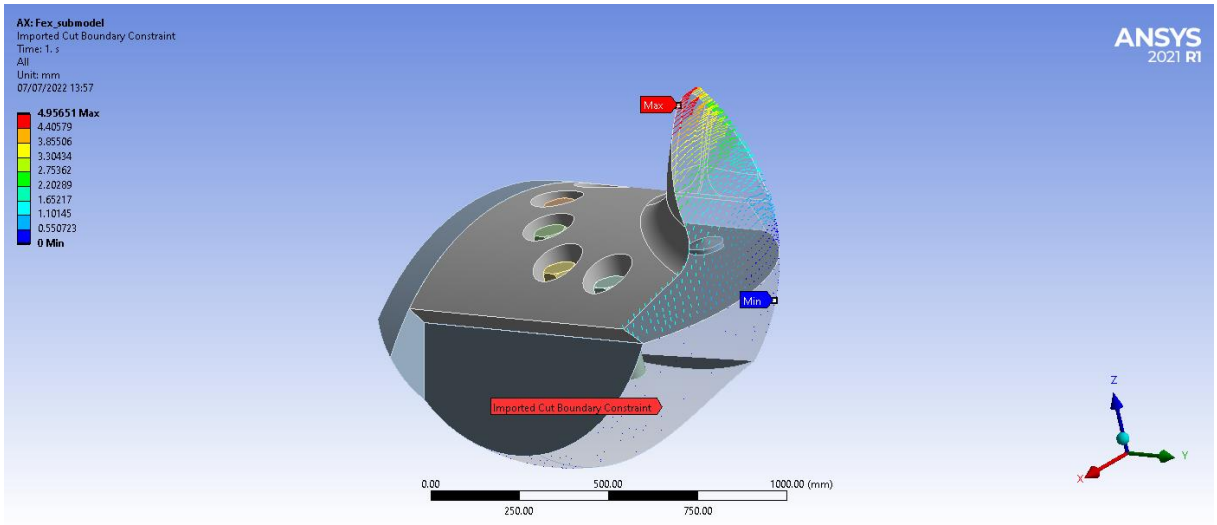

Figure 76. Imported cut boundary constraint for critical joint part from blade failure load

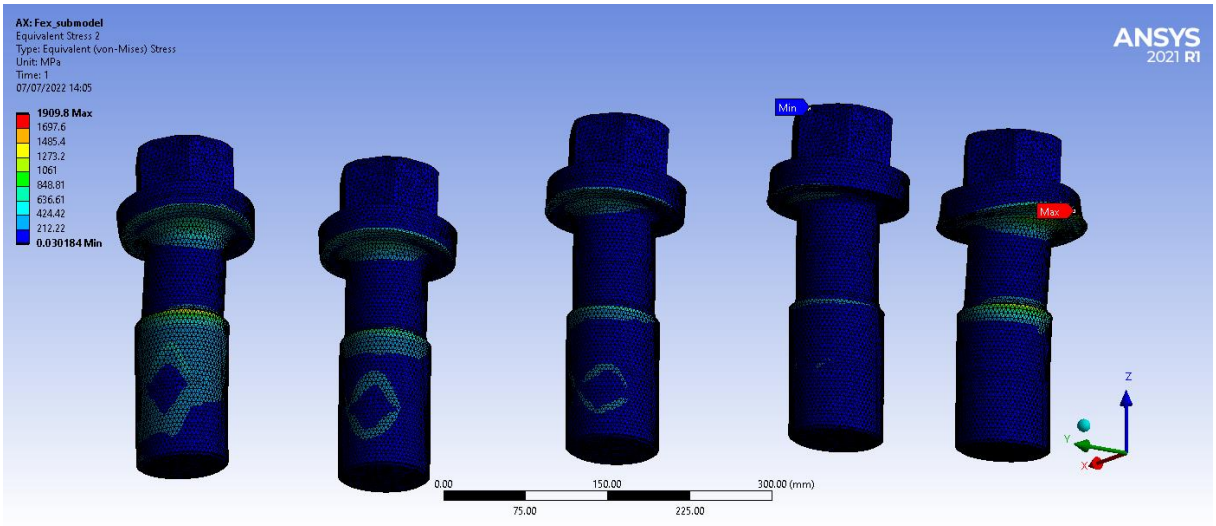

Figure 77. Von Mises stress results in the bolts of sub-modelling from blade failure load

From sub-modelling analysis, the maximum von Mises stress was slightly reduced to 1909 MPa compared to full model analysis with blade failure load. And the peak stresses were found at the bottom edges of the bolt head flange, and at the junction of the shank and threaded part in some bolts. The shanks, threaded parts and bolt head fillet areas had lower stress concentrations. Thus there might be some permanent deformations at the bottom edges of the bolt head flange and the junction of the shank and threaded part for some bolts. Thus these 5 bolts at the pressure side of the blade were not totally fractured but they might have plastic deformations in some regions when blade failure load was applied.

In order to improve the bolted joint design, some possible options are generally suggested.

- Option 1 is increasing the size of the bolt but this may need to check against the geometry and available dimensions of blade flange and hub.
- Option 2 is to increase the number of bolts possibly only at pressure side of the blade or at the loaded side.
- Option 3 is the use of a higher tensile strength material for the bolt material to get better strength at the joint for the bigger loads.
- Option 4 is the study of parameter dependency upon blade failure load, F_{ex} (refer to Eq. 5). F_{ex} is directly proportional to c and t of the blade at root section. To reduce especially thickness value, F_{ex} shall be decreased. It is inversely proportionally to the propeller diameter. But when diameter is fixed, it is less likely to alter F_{ex}. And the

propeller material also has an influence and it is adjustable to slightly degrade but should keep the minimum strength requirement.

- Option 5 shall be the use of different connection method for the blade and hub.

5.3 Comparison of Analytical and FE Results for a critical bolt

After Ansys analysis, a comparison was made between analytical and numerical FE method. Since the analytical method was simplified calculation and had limitations and could not provide results at every single point on the geometry, finite element analysis using Ansys Workbench was performed to get more detailed information and probe values of stress and deformation for the bolted joint.

In Ansys, since the probe values differ at every element or node, mean and maximum values were taken to compare with analytical results. Comparison results for ice load cases and blade failure load for the bolt shank, bearing area of head flange threaded parts of bolts and hub are attached in the APPENDIX A4.

As a summary of the appendix, von Mises stresses and deformations in analytical and FEA for specific locations of bolt shank, bolt head flange bearing area, threaded parts of bolt and hub were compared. It was noticed that stresses in the bolt shanks and threaded parts of bolt and hub had a certain amount of different percentages up to 45% for different load cases. This might be because, during analytical calculations, simplifications and assumptions were made for load distributions on the bolted joints unlike FEA which could provide detailed results and critical bolt was considered in comparison results. Additionally FEA stress values were also different for the critical bolt that suffered higher stresses as it was placed closer to the applied loads and for normal bolts with lower stresses which were located farther. But in analytical results, this differentiation would not be possible due to simplifications. Difference percentages for stresses at the bolt head flange bearing area were less. This could be that stress variations at the bolt head flange bearing area were not significant. It was also noticed that for blade failure load, stress concentrations were more than allowable strength at the head flange bearing area in both analytical and FEM cases. In FEM the compared value was taken from the critical bolt but there were also other safe bolts at the blade suction side. Difference percentages for the deformations in the bolt shanks were small. But those in the head flange

bearing area, threaded parts of bolt and hub were not closed enough because of simplifications in analytical calculations.

5.4 Issues Regarding to Corrosion Fatigue

The materials for underwater components of the built-up propeller such as blade, hub, bolts and shaft exposed to seawater shall be selected to be corrosion resistant according to class rules. Besides, the use of zinc anodes welded to the vessel hull may reduce corrosion. In Under normal operation condition with sufficient cathodic protection, negligible corrosion can be expected. However, during vessel operation with the components exposed to sea water and cyclic loading (or alternating stresses), the fatigue strength under corrosive environment shall be considered.

The propellers and shaft shall also be designed to have sufficient strength for corrosion fatigue under these alternating bending stress circumstances.

In order to mitigate corrosion fatigue, care must be taken for correct material selection and fulfiling the corrosion fatigue design criteria following the class rules. Additionally, some other treatments should also be applied including the use of surface coatings for propeller and liners for shaft during installation.

5.5 Project Template for Analytical / Simulation Model

The detailed analytical calculations and the consolidation of all the finite element analysis results of different load cases are summarized in APPENDIX A2 and APPENDIX A3. As for the project template in Ansys, it is possible to be implemented the project input information such as engineering data, geometry, analysis data into a predefined containers and then can be linked to new projects.

From the summary of the FEA results for different load cases, it was observed that an increase in fillet radius from R5 to R10 at the bolt head and shank connection could reduce stress concentration. For all load step-1 of different load cases, only with preload applied on

the bolts, maximum von Mises values were similar. In every load case, maximum stresses have occurred at the bolt head and shank fillet region, and maximum deformation was caused at the blade tip. Among the ice load cases, case 1 had the highest von Mises stress where blade force was applied at the suction side around the upper leading edge. Case 2 had the largest deformation where blade force was applied at the suction side around the tip area. It was investigated that the influences of hydrodynamic pressure load around the blade surfaces and centrifugal blade load were insignificant upon the strength of the bolted joint. The blade failure load was dominant upon blade strength and when it was applied it could also affect the bolts at the pressure side of the blade resulting in some permanent deformations on the bolts. Sub-modelling was developed to get more accurate results with refined mesh for the concerned part. In the blade failure load case, there were also permanent deformations observed in some areas on the bolts in sub-modelling.

6. DISCUSSION

6.1 Strength Pyramid of Propulsion Components regarding to the Safety of Operation

The built-up propeller assembly is composed of a propeller shaft, hub, blade and blade bolts. The strength hierarchy of the individual components can be represented by a pyramid. From top to bottom of a pyramid, the strength order has been arranged. According to the concept of the strength pyramid, the occurrence of blade failure should not influence the strength of the shafting. Alternatively, when the blade was damaged or lost by any loading or accident, the blade bolts should remain and the hub and shaft are safe. The structural failure at the assembly will happen in a sequence that the damage will happen at the blade first, then the bolts, and after that, the hub and the shaft will be in last. According to FEA results in this study, the bolted joints were safe in every ice load case. In the case of blade failure load application which was a huge amount of load, the bolted joints at the suction side of the blade were safe and those at the pressure side there were some permanent deformations at some areas of the bolts.

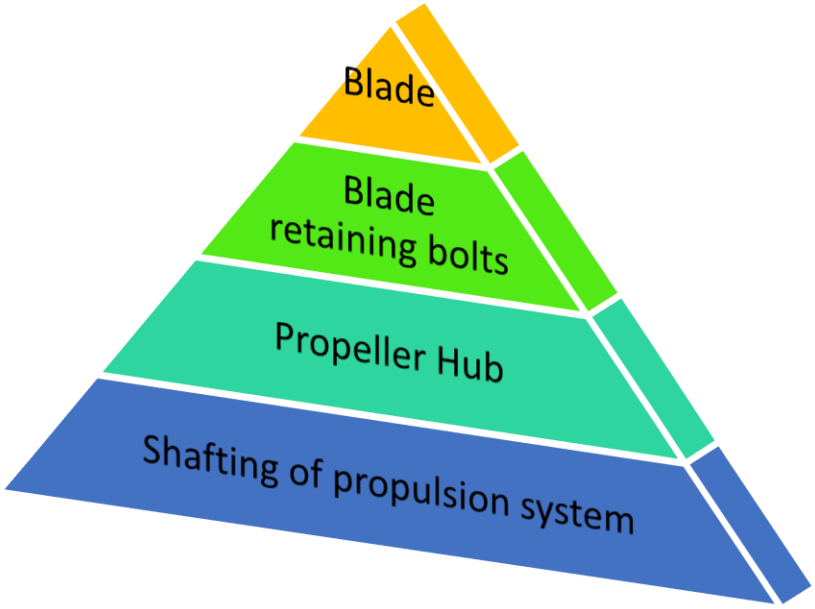

Figure 78. Strength pyramid for a built-up propeller assembly

6.2 Influence of the Different Ice Classes according to the Classification Rules on the Joint of Hub-Blade

According to the Finnish-Swedish ice class rules, there are different ice classes such as IA super, IA, IB and IC with the dependency on designed ice thickness. As per the rules, the thickness of ice influences the calculation of the blade force for respective load cases. The higher the ice class, the thicker the ice blocks. This leads to the increase of blade force which can then dominate the strength of the blade and hub joint. In this thesis, the higher ice class of IA super was selected and the bolted joint was designed accordingly with the application of blade failure load. Thus this design could cover the lower ice classes of IA, IB and IC.

7. CONCLUSION

The application and characteristics of the built-up propeller orient to the benefits of propeller maintenance, repair and blade replacing works for the ship owners and operators without delaying navigation schedules. The efficient design especially the bolted joint of blade and hub can also help the manufacturing processes easier and the installation tasks faster. Complying with the class rules, the correct materials are necessary to be selected for the propeller components and the joint to protect against corrosions and to work properly under the desired ice class and loadings.

According to the available input data including the power output of the main engine, the propeller diameter can be predicted and continuously the dimensions of the hub, propeller shaft and blade bolts can be defined based on the classification rules. Using the design blade failure load, the propeller components can also be designed in accordance with the strength of the pyramid principle. After all the dimensions of the components have been obtained, the conceptual 3D modelling shall be created to interface with other software and this may lead to efficient manufacturing and strength calculation works.

In the aspects of design safety and to be able to estimate the strength of the designed components, the analytical approach can be applied within a short time frame but this may need simplified methods and assumptions for complex geometry and sometimes results shall go to less accuracy. To compensate for this issue, the numerical approach can be integrated with finite element analysis using commercial software in the design offices, manufacturing sites and shipyards. This can support more reliable results and provide detailed and accurate outcomes for the customers, shipowners and end users.

Designing a built-up propeller also follows accordingly to a design spiral. Before the final and detailed design, design modifications shall be performed if the strength analysis results are not favourable. Since the use of commercial software is costly, computational effort should be considered. For the bolted joint design, it was observed that the fillet parts between the bolt head and shank were critical and suffered high-stress concentrations in every load case and the optimized fillet design was essential for stress reduction. During the analysis, when the FE model is tremendously huge and the use of coarse mesh is not enough to investigate the strength of a specific part of the global model, sub-modelling techniques play an important role and help the endeavours for efficient computation with refined mesh. In this study, sub-

modelling was applied in the analysis to achieve better and more reliable results for the concerned critical parts with fewer analysis efforts.

8. FUTURE ASPECTS AND PROPOSALS FOR FURTHER INVESTIGATIONS

In order to develop a more detailed design of the blade-hub joint of this built-up propeller, some aspects are proposed for further investigations.

In this study, static structural analysis of the blade-hub joint with the imported hydrodynamic pressure around the blade was observed. So CFD analysis can be performed for the propeller with the bolted joint to see how the flows around the joint behave and to evaluate how the design is efficient in terms of hydrodynamics studies.

During the operation of the propulsion machinery, the propeller is connected to the shaft, and the shaft is engaged to the propulsion engine. When propeller is directly driven by a combustion (diesel) engine, the significant torsional vibrations can be caused. Then the vibrational analysis can be done for the shaft line integrated with the propeller. The structural response of the blade and hub joint should be further studied.

In this thesis of the FEM section, due to the purpose of saving computational efforts, up to the class 3 FE model according to VDI2230 was generated. And it was a simplification model of the bolts without threads. To perform FE analysis with more detailed inputs and to expect more realistic outcomes, it is suggested to investigate the analysis with a class 4 FE model having the threads at the bolts and respective hub regions. For this sufficient computational capacity is required.

For the bolted joints, the required fillet areas at the bolts and at the joint components had been created in the model and included in the analysis. However, the different fillet shapes and sizes can also be studied by parametric analysis especially at the bolt head flange and shank connection to observe the reduction of stress concentration to get a better bolt design.

In Ansys a non-liniear analysis can be performed by setting up the condition of "high deformation". For this kind of analysis the material tensile curve data are required. This can also be observed to get more detailed results.

A dynamic analysis is not necessary because the blade failure load will considerd only under static condition.

After the built-up propeller has been designed with the best-suited materials complying with the class rules, it is also possible to study design morphology in terms of weight or volume and shape. This can be achieved by application of topology optimization in Ansys after structural analysis and this allows the weight or shape optimization without strength degrading.

Through this study, the bolted joint was designed and investigated for the blade-hub connection. Alternatively, it is suggested that a clamp-on blade connection type can also be designed for the blade and hub. This may be a challenging option for a bigger size propeller and for ice class but in this way, it can compare with bolted joint design focusing on the strength aspects.

9. ACKNOWLEDGEMENTS

I would like to convey my sincere and deepest gratitude to MMG Team, especially to my supervisor Dipl.-Ing. Jörn Klüss and M.Sc. Robert Tietze for their continuous supervision, guidance and warmest support throughout the thesis even in the middle of their busy projects and schedules. Due to their patience, clear, thorough and directive information to all my doubts, struggles and concerns about the thesis, I had overcome the challenges and difficulties whenever I faced with.

I also would like to disseminate my profound and special thanks to my supervisors, Prof. Dr.-Eng. Patrick Kaeding, Dr.-Ing. Thomas Lindemann and Dipl.-Ing. Gunnar Kistner from the University of Rostock for their consistent guidance and help in the entire thesis. Because of the selected advanced lectures and theoretical knowledge from the University of Rostock specialized in marine structural analysis integrated with the application of software tools, I could manage the structural analysis part of the thesis step by step.

Heartily I am grateful indeed to Prof. Philippe Rigo (EMShip^{+} Coordinator) for his valuable advice, guidance and support for the whole Master's Program and entire EMShip Journey. Since the beginning of joining the EMShip Program, I really appreciate how Prof. Rigo had shown and demonstrated his great care for every single student in the program. Besides, the warmest thanks are given to Ms Christine Reynders and EMShip team for their administrative aid.

Additionally, I would express my cordially thanks to every member of my family for their unconditional care and affectionate support as always and whenever I need it. Without them, I couldn't withstand and surpass these stressful years.

Moreover, I would like to acknowledge the kindness and heartfelt support from my colleagues in EMShip M120 fourth cohort. We shared our knowledge and experiences and got to learn about different cultures from different parts of the world. Memories cannot be forgettable easily.

Last but not least, I do acknowledge and thankful to individuals who provided the ways to solutions and even single support whenever I had tough times throughout this thesis and Master's program.

10. REFERENCES

[1] Prof. A.H. Techet, 2005. *2*.016 Hydrodynamics. *Marine Propellers*, version 3.0 updated 30 August, 2005, Reading#10. Available from: http://web.mit.edu/2.016/www/handouts/2005Reading10.pdf

[2] Isidoro Martinez, 1995-2022. Propellers. *Parameters and performances*, Available from: http://imartinez.etsiae.upm.es/~isidoro/bk3/c17/Propellers.pdf

[3] MAN Energy Solutions, 2018. *Basic Principles of Ship Propulsion*. Denmark: PrinfoTrekroner. Available from: https://www.man-es.com/docs/default-source/document-sync/man-alpha-fpp-eng.pdf?sfvrsn=a46da4c9_0

[4] Christopher Wojciech Dekanski, 1993. *Design and Analysis of Propeller Blade Geometry using the PDE Method*. Thesis (PhD). The University of Leeds.

[5] DNV AS, 2021. Rules for classification: Ships — DNV-RU-SHIP Pt.4 Ch.4. *Rotating machinery – power transmission*, ed. July 2021.

[6] DNV AS, 2021. Rules for classification: Ships — DNV-RU-SHIP Pt.4 Ch.5. *Rotating machinery - driven units*, ed. July 2021.

[7] DNV AS, 2021. Rules for classification: Ships — DNV-RU-SHIP Pt.6 Ch.6. *Cold climate*, ed. July 2021.

[8] DNV AS, 2021. Class guideline — DNV-CG-0038. *Calculation of shafts in marine applications*, ed. August 2021.

[9] DNV AS, 2021. Class guideline — DNV-CG-0039. *Calculation of marine propellers*, ed. July 2021.

[10] Finnish Transport Safety Agency, 2017. Act on the Ice Classes of Ships and Icebreaker Assistance (1121/2005), section 4.1. *Ice Class Regulations and the Application*, ed. November 2017.

[11] WORKSHOP INSIDER, 2021. Ship Propeller - An Overview of Types, Material, and Inspection Criteria [online]. Marine Engineering. Available from: https://workshopinsider.com/basic-principles-of-ship-propeller-and-repa [Accessed August 30, 2021].

[12] VEREIN DEUTSCHER INGENIEURE, 2015. Systematic calculation of highly stressed bolted joints-Joints with one cylindrical bolt (VDI 2230 Part 1). Düsseldorf: Fachbereich Produktentwicklung und Mechatronik.

[13] VEREIN DEUTSCHER INGENIEURE, 2014. Systematic calculation of highly stressed bolted joints-Multi bolted joints (VDI 2230 Part 2). Düsseldorf: Fachbereich Getriebe und Maschinenelemente.

[14] DIN EN ISO 3506-1, 2020. Mechanical properties of corrosion-resistant stainless steel fasteners – Part 1: Bolts, screws and studs with specified grades and property classes (ISO 3506-1:2020). Berlin: DIN Deutsches Institut für Normung e. V.

[15] J S Carlton, 2007. Marine Propellers and Propulsion. 2nd ed. Burlington: Elsevier Ltd.

[16] Germanischer Lloyd SE, 2016. Rules for Classification and Construction. *Ship Technology*, ed. July 2016.

[17] Bright Hub Engineering, 2009. Ship Propeller Shaft Mounting Explained [online]. Naval Architecture & Ship Design for Marine Engineers. Available from:

https://www.brighthubengineering.com/naval-architecture/47416-how-to-mount-a-propeller/ [Accessed 29th August, 2009].

[18] Bureau Veritas, 2022. NR467 Steel Ships. *Part C Machinery, Electricity, Automation and Fire Protection*, ed. July 2022 [online]. Available from: https://erules.veristar.com/dy/app/bootstrap.html [Accessed July, 2022].

[19] Ansys, 2020. Defining Bolt Preload. *Modeling the Bolt and Preload* [online]. Ansys Innovation Courses. Available from: https://courses.ansys.com/wp-content/uploads/2020/10/2.2.2_Defining-Bolt-Preload_new_brand.pdf [Accessed October 2020].

[20] MechaniCalc, 2022. Bolted Joint Analysis [online]. MechaniCalc, Inc. Available from: https://mechanicalc.com/reference/bolted-joint-analysis [Accessed June 2022].

[21] R E Cornwell, 2008. Computation of load factors in bolted connections, Vol. 223 Part C, pp. 795-807.

[22] DNV AS, 2021. Class guideline — DNV-CG-0041. *Ice strengthening of propulsion machinery and hull appendages*, ed. July 2020.

[23] Finnish Transport and Communications Agency, 2019. Guidelines for the application of the Finnish-Swedish Ice Class Rules. Helsinki: published on the websites of Traficom and the STA.

[24] Simon Oman1, Marko Nagode, 2017. Bolted Connection of an End-Plate Cantilever Beam. *The Distribution of Operating Force*, 63(11), 617-627.

[25] Prof. Dr.-Ing. Habil. Nikolai Kornev, 2021. Mathematical model in ship theory. *Lecture 6: Some modern propulsors*, updated 17 November, 2021. The University of Rostock.

[26] External Metric ISO Thread Table Chart Sizes M80 - M100 (engineersedge.com). Available from: https://www.engineersedge.com/hardware/metric-external-thread-sizes4.htm

[27] Bolt Preload Variation due to the Tightening Method (boltscience.com). Available from: https://www.boltscience.com/pages/basics9.htm

[28] Minimum Recommended Thread Engagement Length Calculation for Bolted Joint (mechguru.com). Available from: https://mechguru.com/machine-design/screw-or-bolt-thread-engagement-length-calculation

[29] Jaya Kishore.S, B. Siddeswara Rao, P. Kumar Babu, 2015. FEM Analysis on Submarine Propeller Blade for Improved Efficiency by using Solid Works and ANSYS-Workbench. *International Journal of Emerging Engineering Research and Technology*, 3(11), pp. 144-151.

[30] Rashtrapal B. Teltumade, Prof. Y. L. Yenarkar, 2013. Stress Analysis of Bolted Joint. International Journal of Engineering Research & Technology (IJERT), 2(9), pp. 1009-1016.

[31] Kevin H. Brown, Charles Morrow, Samuel Durbin, Allen Baca, 2008. Guideline for Bolted Joint Design and Analysis: Version 1.0. Albuquerque: Sandia National Laboratories.

[32] Wärtsilä, 2022. Built-up Propellers [online]. Wärtsilä Portals. Available from: https://www.wartsila.com/marine/build/propulsors-and-gears/propellers/wartsila-built-up-propellers-bup

[33] Practical Boat Owner, 2019. *How to measure the pitch of a propeller* [online]. Available from: https://www.safe-skipper.com/wp-content/uploads/2021/10/How-a-propeller-works2.jpg [Accessed 15 June, 2022].

[34] Marine Propellers and Propulsion (Fourth Edition), 2019. *Propeller geometry* [online]. Available from: https://ars.els-cdn.com/content/image/1-s2.0-S0003682X18300021-gr13.jpg [Accessed 16 June, 2022].

[35] Machinery Space, 2016. *A solid fixed-pitch propeller* [online]. Available from: http://www.machineryspaces.com/solid-propeller.PNG [Accessed 17 June, 2022].

[36] Semantic Scholar, 2013. *Propulsion Machinery Operating in Ice* [online]. Available from: https://d3i71xaburhd42.cloudfront.net/e181f47c3108103edb06caa27ec6a97c380c6ce7/250px/1-Figure1-1.png [Accessed 20 June, 2022].

[37] *Wärtsilä Built-up Propellers* [online]. Available from: https://www.wartsila.cn/images/default-source/products/gears-propulsors/propellers/bup/built-up-propeller.tmb-thumb425.png?sfvrsn=d4a4ec45_4 [Accessed 21 June, 2022].

[38] MAN Energy Solutions, 2018. Naval Propellers. *FPP* [online]. Available from: https://www.man-es.com/images/default-source/document-sync-images/man-alpha-fpp-manpm-00-0560-eng.png?sfvrsn=84cded41_0 [Accessed 22 June, 2022].

[39] Teignbridge, 2022. *Clamp on Blade Propellers* [online]. Available from: https://teignbridge.co.uk/wp-content/uploads/2020/11/Teignbridge-Clamp-On-prop-Exploded-View-Hi.jpg [Accessed 23 June, 2022].

[40] Wärtsilä Encyclopedia of Marine and Energy Technology, 2022. *Propeller hub (of CP propeller)* [online]. Available from: www.wartsila.com/encyclopedia/term/propeller-hub-(of-cp-propeller)

[41] Bolt Science, 2021. *Bolt Preload Variation due to the Tightening Method* [online]. Available from: https://www.boltscience.com/pages/basics9.htm

[42] Engineers EDGE, 2022. External metric ISO thread table chart sizes M80-M100 [online]. Available from: https://www.engineersedge.com/hardware/metric-external-thread-sizes4.htm

[43] Engineers EDGE, 2022. *Metric threads* [online]. Available from: https://www.engineersedge.com/hardware/image/metric-threads.gif [Accessed 20 May, 2022].

[44] The Engineer's Bible, 2021. *Clearance Hole Size for Bolts and Screws (Metric)* [online]. Available from: https://engineersbible.com/clearance-hole-metric/

[45] MechGuru, 2012. *Screw or Bolt Thread Engagement Length Calculation* [online]. Available from: https://mechguru.com/machine-design/screw-or-bolt-thread-engagement-length-calculation

APPENDICES

APPENDIX A1 : 3-D CAD model views of the Built-Up Propeller

APPENDIX A2 : Design Calculations Template and Analytical Strength Calculations for the Blade-Hub Joint

APPENDIX A3 : Consolidation of All the Finite Element Analysis Results of Different Load Cases

APPENDIX A4 : Comparison of Analytical and FE Results

APPENDIX A1: 3-D CAD MODEL VIEWS OF THE BUILT-UP PROPELLER

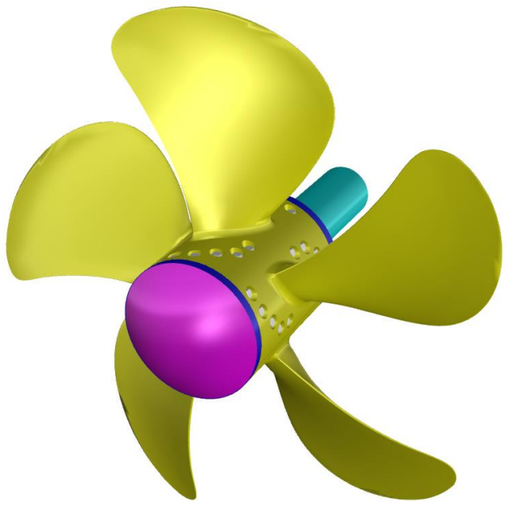

Perspective View

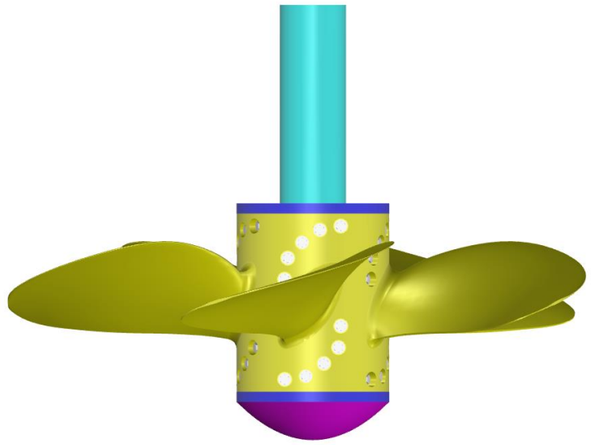

Top View

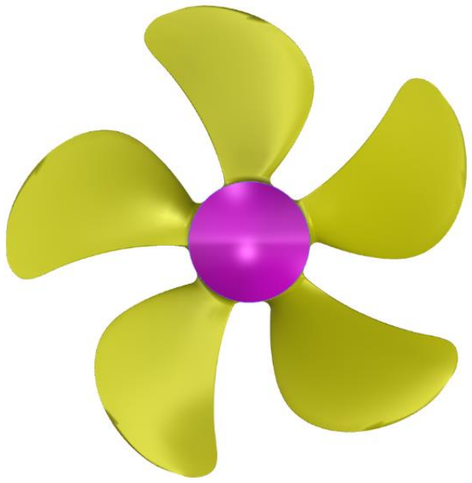

Front View

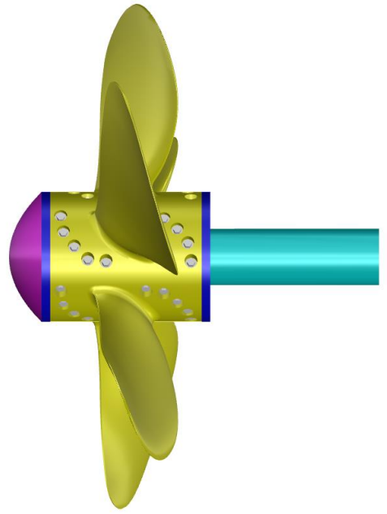

Right Side View

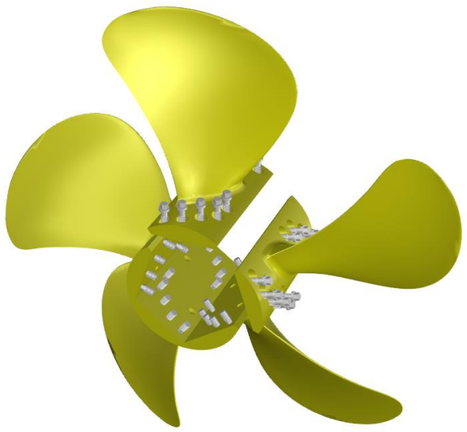

Blades and Bolts

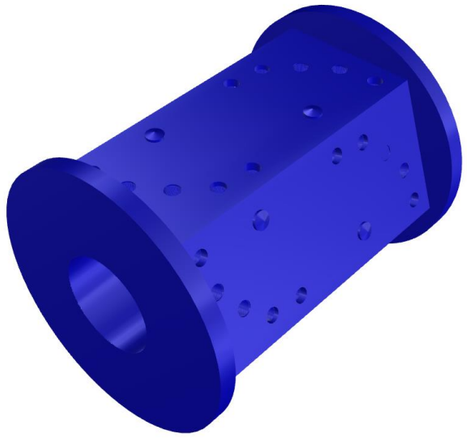

Propeller Hub

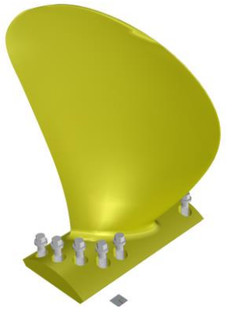

Single blade with bolts

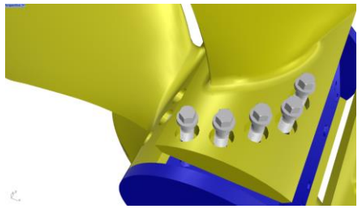

Blade-Hub Joint

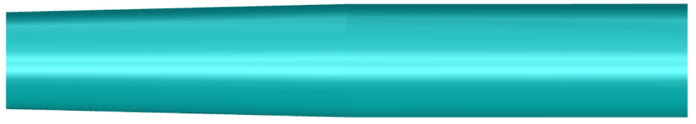

Propeller Shaft

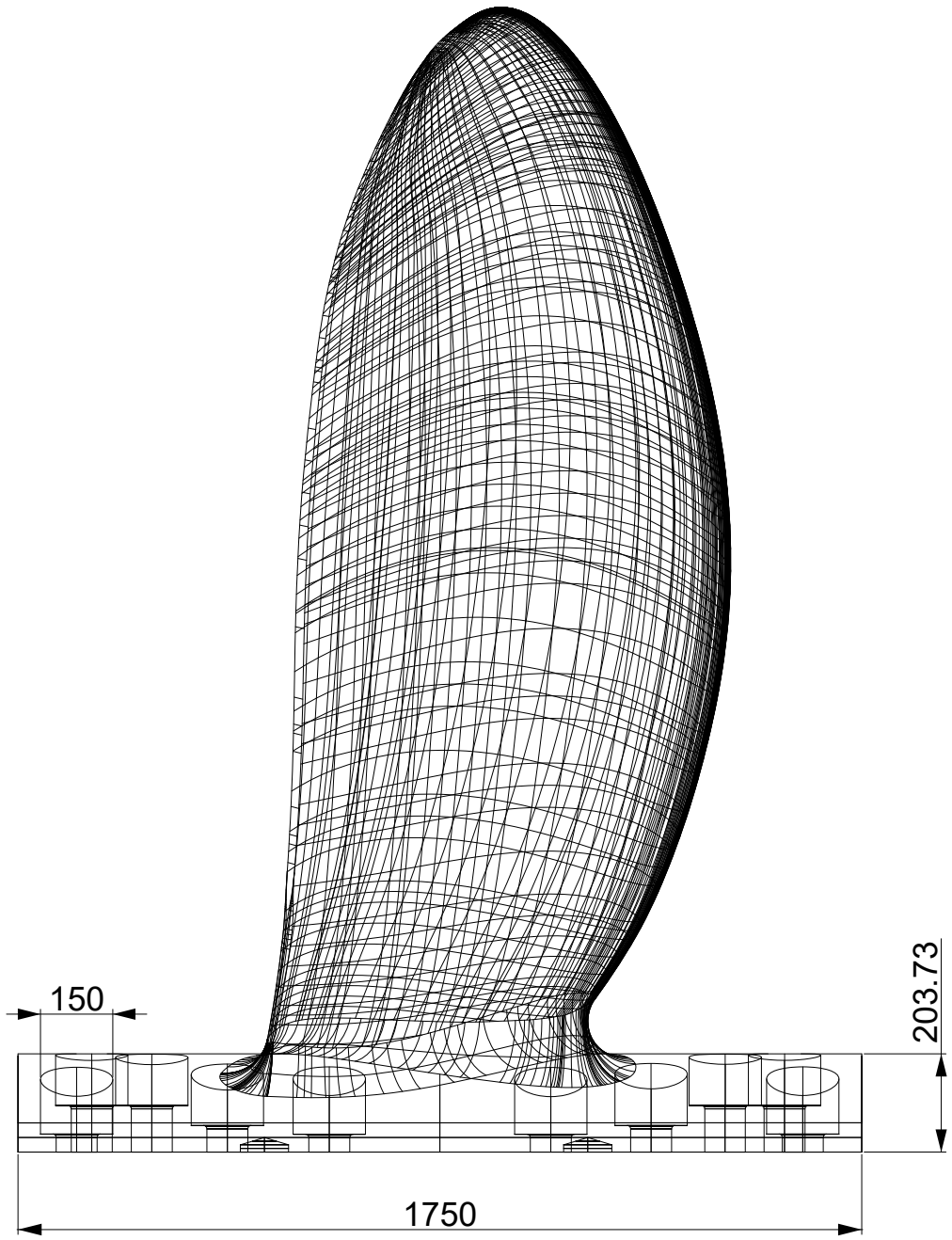

The dimensions on Blade (All dimensions are in millimeter)

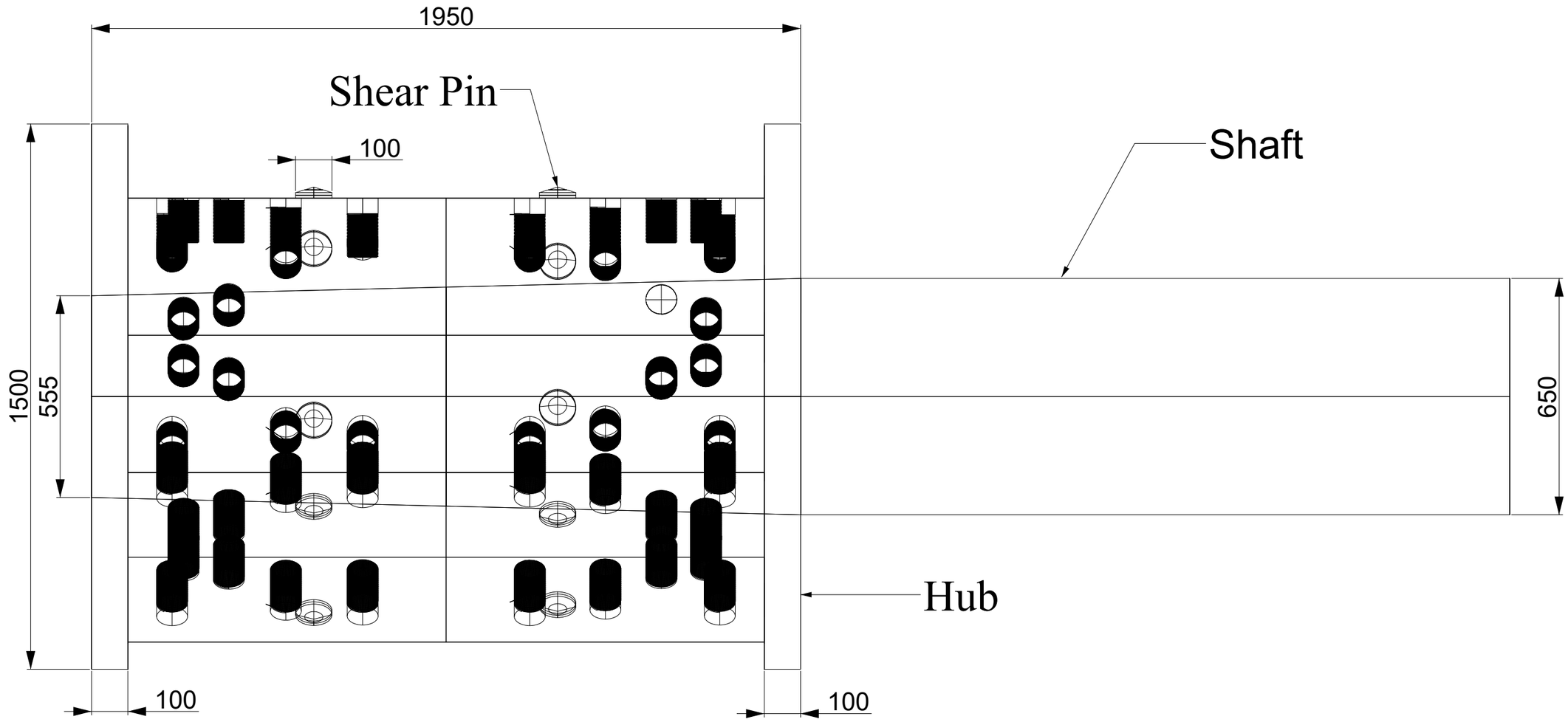

The dimensions on Hub and Shaft (All dimensions are in millimeter)

APPENDIX A2: DESIGN CALCULATIONS TEMPLATE AND ANALYTICAL STRENGTH CALCULATIONS FOR THE BLADE-HUB JOINT

Minimun propeller shaft diameter

Parameters	Value	Unit
c	0.849	m
t	0.328	m
r	0.852	m
σ_u	590	N/mm²
$\sigma_{0.2}$	270	N/mm²
σ_{ref}	398	N/mm²
D	6	m
S_Q	1.3	
S_{Fex}	1.1	
rule-based, $F_{ex,r}$	3522.563	kN
numerical FE, $F_{ex,n}$	3926.000	kN
σ_{yield}	290.000	N/mm²
P	19500	kW
n	2.217	rps
Qr	1400.085	kNm

1-(di/dps)^4	1	
$d_{PS,r}$	607.07	mm
$d_{PS,n}$	628.733	mm
Engg. SF	1.03	
d_{PS}	650	mm

Hub

hub diameter, d	1.5	m
hub length	1950	mm
Recess at the edge with 0.5R to reduce stress on shaft		

Pin at Hub projected under blade root

Qty per blade	2	
size or diameter	100	mm

shaft taper ratio	0.05	
taper diameter, d_{taper}	552.5	mm
blade fillet radius	100	mm

Blade Flange

Flange Dia. Approx., 3D	794	mm
min. flange thickness	79.4	mm
at 3D	89.8	mm

Clamped or preload at bolt shank

longer shank sectional area	4417.86	mm²
shorter shank sectional area	4417.86	mm²
safety factor for bolt	1.30	
external load on a bolt, F1	785.20	kN
external load on a bolt, F2	2.45	kN
Preload at short shank, P or F	517.32	kN
Preload at long shank, P or F_N	517.32	kN

Initial tension	384	N/mm²

Tightening torque, M_A

$\mu_{G\,min}$	0.15	
$\mu_{K\,min}$	0.22	
d2	82.341925	mm
D_{Km}	85	mm
short shank, M_A	8873.97	N-m
long shank, M_A	8873.97	N-m
OR		
short shank, M_A	8788.23	N-m
long shank, M_A	8788.23	N-m

Shear area in shank

As	4417.86467	mm²

Propeller blade mounting
thread core diameter of blade retaining bolts

Parameters	Value	Unit
PCD	0.9	m
PCD	900	mm
z_{bb}	10	
α_A	1.7	
σ_{yield}	640	MPa
d	1.5	m
d_{bb}	79.65	
	84.09	mm
M85 x 4	85	mm

blade retaining bolts dimensions

nominal dia.	85	mm
Pitch	4	mm
H	3.464	mm
Pitch diameter	82.342	mm
core dia.	80.61	mm
Hole diameter	87	mm
thread thickness	2.1650625	mm
TPI	6.35	
Le	85.70	mm
J	1.33	
Le1	114.26	mm
Taken Le1	120.00	mm
Bolt Head	**Hexagonal Flange or collar bolt**	
head+collar height	85	mm
head diameter	98.15	mm
effective head diameter	85	mm
collar/flange height	28.33	mm
collar/flange	127.5	mm
Preload (initial tension)	384	N/mm²

longer shank length	90	mm
shorter shank length	70	mm
reduced shank diameter	72.5488875	mm
shank diameter, taken	75	mm
fillet at Shank and col	5	mm
height of tapered core	10	mm
Total bolt length, L	220	mm
Total bolt length, L	200	mm
shank length/bolt leng	0.41	
shank length/bolt leng	0.35	

Blade forces on propeller, IA Super

Parameters	Value	Unit
EAR	0.581	
D	6	m
d	1.5	m
n	2.217	rps
z	5	
H_{ice}	1.75	m
back, D_{limit}	1.861	m
F_b	**969.1**	kN
face, D_{limit}	4.667	m
F_f	**813.4**	kN

Load cases

1	Fb	969.15	kN
2	50% of Fb	484.57	kN
3	Ff	813.4	kN
4	50% of Ff	406.7	kN
5	60% of Ff or Fb whichever is greater	581.49	kN

Blade Failure Load
(ultimate blade load resulting in plastic bending deformation of the blade)

rule-based, $F_{ex,r}$	3522.563	kN
numerical FE, $F_{ex,n}$	3926.000	kN

Centrifugal force on one blade

density of blade	7640	kg/m^3
volume of blade with flange	0.5557	m^3
m_blade&flange	4245.40	kg
propeller speed	2.217	rps
distance, r	1.174	m
F_centrifugal	24.496	kN

Stresses acting on Joint design

Pre-tension stress on a bolt

	σ_preload(shank)	384	N/mm²

Stress at clamped parts assembly (blade flange and hub joint) due to preload

	σ_clamped joint	-384	N/mm²

Tensile stresses on a bolt due to centrifugal loads on blade

	σ_tc	0.554	N/mm²
	σ_tc	0.554	N/mm²

Tensile stresses on a bolt due to transverse loads on blade (Fb, Ff, Fex)

LC1	σ_tt or ct	43.874	N/mm²
LC2	σ_tt or ct	21.937	N/mm²
LC3	σ_tt or ct	36.823	N/mm²
LC4	σ_tt or ct	18.412	N/mm²
LC5	σ_tt or ct	26.324	N/mm²
Fex	σ_tFex or cFex	177.73	N/mm²

Shear stresses on a bolt due to transverse loads on blade (Fb, Ff, Fex)

LC1	σ_st	21.937	N/mm²
LC2	σ_st	10.969	N/mm²
LC3	σ_st	18.412	N/mm²
LC4	σ_st	9.206	N/mm²
LC5	σ_st	13.162	N/mm²
Fex	σ_sFex	88.866	N/mm²

Von-Mises stress at bolt's shank (at a point of junction between blade flange and hub)

load factor, n	0.1994	

Shank

LC1	σ_VM	392.93	N/mm²
LC2	σ_VM	388.50	N/mm²
LC3	σ_VM	391.50	N/mm²
LC4	σ_VM	387.79	N/mm²
LC5	σ_VM	389.39	N/mm²
Fex	σ_VM	420.67	N/mm²

Young's modulus for propeller

E	125000	MPa

Total strain on a bolt

	E	215000	MPa
LC1	ε	0.00183	
LC2		0.00181	
LC3		0.00182	
LC4		0.00180	
LC5		0.00181	
Fex		0.00196	

Total deformation on a bolt shank

LC1	deformation	0.1645	mm
LC2		0.1626	mm
LC3		0.1639	mm
LC4		0.1623	mm
LC5		0.1630	mm
Fex		0.1761	mm
LC1		0.1279	mm
LC2		0.1265	mm
LC3		0.1275	mm
LC4		0.1263	mm
LC5		0.1268	mm
Fex		0.1370	mm

Compressive stresses at bearing area under bolt flange due to centrifugal and transv

	bearing area	804.25	mm²
LC1	σ_bolt bearing	244.05	N/mm²
LC2		123.55	N/mm²
LC3		205.32	N/mm²
LC4		104.18	N/mm²
LC5		147.65	N/mm²
Fex		979.36	N/mm²

Deformation at bearing area under bolt flange due to centrifugal and transverse loa

LC1	Deformation	-0.0322	mm
LC2		-0.0163	mm
LC3		-0.0271	mm
LC4		-0.0137	mm
LC5		-0.0195	mm
Fex		-0.1291	mm

External thread shear stresses at bolt thread area due to preload, transverse and cer

LC1	σ_bolt thread	36.78	N/mm²
LC2		31.79	N/mm²
LC3		35.18	N/mm²
LC4		30.98	N/mm²
LC5		32.78	N/mm²
Fex		67.26	N/mm²

Deformation at bolt thread area due to preload, transverse and centrifugal loads

LC1	Deformation	0.0205	N/mm²
LC2		0.0177	N/mm²
LC3		0.0196	N/mm²
LC4		0.0173	N/mm²
LC5		0.0183	N/mm²
Fex		0.0375	N/mm²

Internal thread shear stresses at hub thread area due to preload, transverse and cen

LC1	σ_bolt thread	30.65	N/mm²
LC2		26.49	N/mm²
LC3		29.31	N/mm²
LC4		25.82	N/mm²
LC5		27.32	N/mm²
Fex		56.05	N/mm²

Deformation at hub thread area due to preload, transverse and centrifugal loads

LC1	Deformation	0.0294	N/mm²
LC2		0.0254	N/mm²
LC3		0.0281	N/mm²
LC4		0.0248	N/mm²
LC5		0.0262	N/mm²
Fex		0.0538	N/mm²

APPENDIX A3: CONSOLIDATION OF ALL THE FINITE ELEMENT ANALYSIS RESULTS OF DIFFERENT LOAD CASES

								Load step 1_only Preload		Load step 2_preload locked & applied loads				
Description	**FE Model**	**Loading**	**BC**	**Method/Elem order**	**Blade Elem size (mm)**	**Hub mesh (mm)**	**Bolt mesh (mm)**	**max. VM stress (MPa)**	**max. total deformation (mm)**	**max. VM stress (MPa)**	**max. total deformation (mm)**	**max. stress region**	**max. def. Region**	**Total Solution time (s)**
Analysis 1	model class 3 with 5R head fillet bolts	LC 1, preload at bolts, blade forces, centrifugal blade force	fixed at inner cone surface of hub and shell plane for direction of loading reference	Tetrahedrons/ quadratic	100	100	15	272.5	0.19183	629.73	45.851	around bolt fillet bet. shank and head flange	blade tip (middle)	190
Analysis 2	model class 3 with 10R head fillet bolts, blade with flange, part of hub, bolts	LC 1, preload at bolts, blade forces, centrifugal blade force			100	100	15	213.41	0.17785	542.69	45.893	around bolt fillet bet. shank and head flange	blade tip (middle)	183
Analysis 3		LC 2, preload at bolts, blade forces, centrifugal blade force			100	100	15	233.58	0.1788	435.34	62.755	around bolt fillet bet. shank and head flange	blade tip (middle)	181
Analysis 4		LC 3, preload at bolts, blade forces, centrifugal blade force			100	100	15	257.44	0.18599	502.23	38.103	around bolt fillet bet. shank and head flange	blade tip (middle)	182
Analysis 5		LC 4, preload at bolts, blade forces, centrifugal blade force			100	100	15	233.58	0.1788	320.99	53.005	around bolt fillet bet. shank and head flange	blade tip	168
Analysis 6		LC 5, preload at bolts, blade forces, centrifugal blade force			100	100	15	233.58	0.1788	342.94	58.446	around bolt fillet bet. shank and head flange	blade tip	181
Analysis 7		hyd_pressure_load, preload at bolts, centrifugal blade force			100	100	15	213.41	0.17785	230.9	9.5951	around bolt fillet bet. shank and head flange	blade tip (middle)	157
Analysis 8		Fex_pressure, preload at bolts, centrifugal blade force			100	100	15	237.87	0.18357	2126.1	239.74	around bolt fillet bet. shank and head flange	blade tip	226
Analysis 9	submodel of critical joint part at suction side	LC 1, preload at bolts, blade forces, centrifugal blade force			50	50	4	submodel	submodel	602.52	submodel	at bolt head flange bottom	submodel	296
Analysis 10	submodel of critical joint part at pressure side	Fex_pressure, preload at bolts, centrifugal blade force			50	50	4	submodel	submodel	1909	submodel	at bolt head flange bottom	submodel	281

APPENDIX A4: COMPARISON OF ANALYTICAL AND FE RESULTS

Comparison of equivalent Von-mises stresses at specific points

	Bolt Shank			Bolt head flange bearing area			Bolt threaded part			Hub threaded part		
Analysis Case	**Analytical, simplified [MPa]**	**FEA, at critical bolt, mean value, [MPa]**	**% difference**	**Analytical, simplified [MPa]**	**FEA, at critical bolt, mean value, [MPa]**	**% difference**	**Analytical, simplified [MPa]**	**FEA, at critical bolt, mean value, [MPa]**	**% difference**	**Analytical, simplified [MPa]**	**FEA, at critical bolt, mean value, [MPa]**	**% difference**
LC1	392.93	331.69	15.59	244.05	241.26	1.15	36.78	49.52	34.64	30.65	24.42	20.34
LC2	388.50	266.11	31.51	123.55	145.22	17.54	31.79	37.66	18.47	26.49	19.57	26.12
LC3	391.50	306.97	21.59	205.32	195.40	4.83	35.18	44.81	27.40	29.31	23.23	20.76
LC4	387.79	214.04	44.81	104.18	107.08	2.78	30.98	38.68	24.8	25.82	18.91	26.76
LC5	389.39	228.68	41.27	147.65	133.47	9.61	32.78	40.52	23.59	27.32	20.96	23.28
Fex	420.67	424.42	0.89	979.36	1061.00	8.34	67.26	83.65	24.37	56.05	66.15	18.02

Comparison of deformations at specific points

	Bolt Shank			Bolt head flange bearing area		Bolt threaded part		Hub threaded part	
Analysis Case	**Analytical, simplified [mm]**	**FEA, at critical bolt, mean value, [mm]**	**% difference**	**Analytical, simplified [mm]**	**FEA, at critical bolt, mean value, [mm]**	**Analytical, simplified [mm]**	**FEA, at critical bolt, mean value, [mm]**	**Analytical, simplified [mm]**	**FEA, at critical bolt, mean value, [mm]**
LC1	0.1645	0.1853	12.63	0.0322	0.0526	0.0205	0.0790	0.0294	0.0538
LC2	0.1626	0.1700	4.532	0.0163	0.0280	0.0177	0.0124	0.0254	0.0125
LC3	0.1639	0.1826	11.40	0.0271	0.0337	0.0196	0.0242	0.0281	0.0340
LC4	0.1623	0.1811	11.53	0.0137	0.0350	0.0173	0.0230	0.0248	0.0220
LC5	0.1630	0.1793	10.01	0.0195	0.0362	0.0183	0.0230	0.0262	0.0130
Fex	0.1761	0.1616	8.248	0.1291	0.5993	0.0375	0.1200	0.0538	0.1110